Rare Semileptonic B Meson Decays Beyond The Standard Model

Muhammad Ali Paracha

Department of Physics

&

National Centre for Physics

Quaid-i-Azam University

Islamabad, Pakistan

March , 2012.

This work is submitted as a dissertation in partial fulfillment of the requirement for the degree of

DOCTOR OF PHILOSOPHY

IN PHYSICS

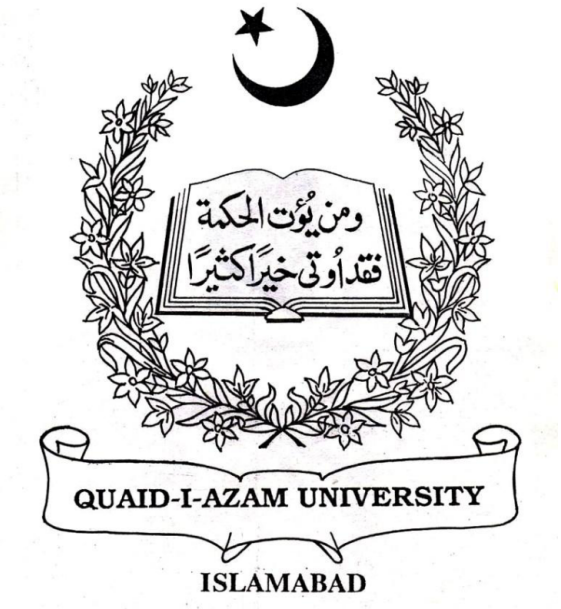

Department of Physics

&

National Centre for Physics

Quaid-i-Azam University

Islamabad, Pakistan

March, 2012.

Certificate

Certified that the work contained in this dissertation was carried out by Mr. M. Ali Paracha for his PhD degree under my supervision.

Prof. Fayyazuddin

Supervisor,

National Centre for Physics,

&

Department of Physics,

Quaid-i-Azam University, Islamabad.

Submitted through

Prof. S. K. Hasanain

Chairman,

Department of Physics,

Quaid-i-Azam University, Islamabad.

To Prof.Fayyazuddin and Prof.Riazuddin

Acknowledgements

First and foremost, I want to express my deepest gratitude to my venerable teachers and supervisiors, Prof.**Fayyazuddin** and Prof. **Riazuddin**, for their worthy kindness and invaluable favors. They guided my work with great patience, enthusiasm and a great amount of tolerance. With all my ventures, I could always rely on their remarkable ability to quickly distill any problem to its essence. Their reverential personalities and exclusive vision, as a tower of light, guide new researchers not only in Physics but also in other aspects of life. I am inspired from their working style, fatherly attitude. I feel comfortable to talk to them. I am also immensely grateful to Prof. **Nello Paver** who critically read this thesis and gave positive and useful suggestions which improved the quality of this thesis.

I wish to thank all my teachers in Physics department, especially to Prof. Pervez Hoodbhoy who taught me many courses and I gained much knowledge from him. Cooperation of the Chairman, Physics Department is also appreciated.

My heartiest thanks to all members of High Energy Theory Group at National Centre for Physics, for many fruitful discussions. I highly value advices from my collaborators, Ishtiaq Ahmed and M.Jamil Aslam. They always encouraged me when the load was heavy. Special thanks to Ishtiaq Ahmed for being such a terrific fellow throughout this work. He never failed to show concern when things got stressful. Away from work, I wish to thank all my friends, seniors and juniors, for their love, humor and tolerance.

This work is supported by the World Federation of Scientists and National Centre for Physics, Islamabad. I appreciate the research facilities provided by the centre and especially Dr. Hamid Saleem for providing a good research atmosphere.

I can never thank enough my parents for everything they have done for me. Even then, I wish to record my deepest obligations to my father who always loves me and my mother for her endless contribution to make me stay on track. No one tolerates me more than they do. Finally a great thank you to my fiance Hamana Shahid for unconditional support, belief in me and for keeping me grounded.

M. Ali Paracha

Contents

Abstract

In this thesis the exclusive rare semileptonic decays of B-mesons have been studied beyond the Standard Model. In particular the decays $B \to K_1(1270, 1400)\ell^+\ell^-$ and $B_c \to D_s^*\ell^+\ell^-$ are considered. These decays are induced by flavor changing neutral current (FCNC) transitions which at quark level arises as $b \to s\ell^+\ell^-$. In the Standard model these FCNC decays are not allowed at tree level but are allowed at loop level through Glashow-Iliopoulos-Maiani (GIM) mechanism. In addition they are also suppressed in the Standard Model due to their dependence on weak mixing angles of the quark flavor rotation matrix- the Cabibo Kobayashi Maskawa (CKM) matrix. These two circumstances make the FCNC decays relatively rare and hence are important to study physics beyond the Standard Model, commonly known as new physics. The main points of this thesis are:

- The implications of the fourth generation quarks in the decay $B \to K_1(1270, 1400)\ell^+\ell^-$ with $\ell = \mu, \tau$ are studied, where the mass eigenstates $K_1(1270)$ and $K_1(1400)$ are mixture of $^1P_1$ and $^3P_1$ states with the mixing angle θ_K. In this context, we have studied various observables like branching ratio ($\mathcal{BR}$), forward-backward asymmetry ($\mathcal{A}_{\mathcal{FB}}$) and longitudinal and transverse helicity fractions ($f_{L,T}$) of K_1 meson in $B \to K_1\ell^+\ell^-$ decays. To study these observables, we have used the Light Cone QCD sum rules form factors and set the mixing angle $\theta_K = -34°$. It is noticed that the $\mathcal{BR}$ is suppressed for $K_1(1400)$ as a final state meson compared to that of $K_1(1270)$. Same is the case when the final state leptons are tauons rather than muons. In both the channels all of the above mentioned observables are quite sensitive to the fourth generation effects. Hence the measurements of these observables at LHC, for the above mentioned processes can serve as a good tool to investigate the indirect manifestations of the fourth generation quarks.

- The same decay $B \to K_1(1270, 1400)\ell^+\ell^-$ is also studied in the standard model (SM) and in universal extra dimension (UED) model. In this work we first relate the form factors through Ward identities and then express their normalization at$q^2 = 0$ in terms of a single constant $g_+(0)$ which is extracted from the decays $B \to K_1(1270, 1400)\gamma$. These form factors are then used to analyze the physical observables such as the branching ratio and the forward-backward asymmetry in the SM. This analysis is then extended to the UED model where the dependency of the above mentioned physical observables on the compactification radius R, the only unknown parameter in the UED model. It is shown that the zero position of the forward-backward asymmetry for the decay $B \to K_1(1270, 1400)\mu^+\mu^-$ is sensitive to the UED model, therefore the zero position of the forward-backward asymmetry can serve as a handy tool to establish new physics predicted by the UED model.

- The semileptonic $B_c \to D_s^* \ell^+ \ell^-$ ($\ell = \mu, \tau$) decays have been studied in the Standard Model (SM) and in the Universal Extra Dimension (UED) model. In addition to the contribution from the Flavor Changing Neutral Current (FCNC) transitions the weak annihilation (WA) contribution is also important for this decay. It is found that the WA gives 6.7 times larger branching ratio than the penguin contribution for the decay $B_c \to D_s^* \mu^+ \mu^-$. The contribution from the WA and FCNC transitions are parameterized in terms of the form factors. In this work we first relate the form factors through Ward identities and then express them in terms of $g_+(0)$ which is extracted from the decay $B_c \to D_s^* \gamma$ through QCD sum rules approach. These form factors are then used to analyze the physical observables like branching ratio and helicity fractions of the final state D_s^* meson in the SM. This analysis is then extended to the UED model where the dependency of above mentioned physical observables depend on the compactification radius R. It is shown that the helicity fractions of D_s^* are sensitive to the UED model especially when we have muons as the final state lepton. This sensitivity is marked up at low q^2 region, irrespective of the choice of the form factors. It is hoped that in the next couple of years LHC will provide enough data on the $B_c \to D_s^* \ell^+ \ell^-$ channel, and then , these helicity fractions would serve as a useful tool to establish new physics predicted by the UED model.

Chapter 1

Introduction

The Standard Model (SM) of particle physics was proposed by Glashow, Salam and Weinberg to unify electromagnetism and weak nuclear forces. The SM is one of the successful theories of the 20th century and has been tested with great precision.

Despite its many successes, it has some theoretical limitations which impedes its status as a fundamental theory. These limitations are as follows:

- Why is the electroweak unification scale so small (hierarchy problem)?
- What is the origin of the mass patterns among the fermions?
- Why only the three generations of quarks and leptons ?
- Neutrinos are massless but the experiments have shown that neutrinos have non-zero mass.

These problems indicate that there might be some new physics (NP) beyond the SM. Various extensions of the SM are motivated to understand some of the above mentioned problems. The models proposed are the two Higgs doublet model (2HDM), Minimal supersymmetric Standard Model (MSSM), Universal extra dimension (UED) model, Standard Model with fourth generation (SM4) etc.

In this thesis we work exclusively in and beyond the SM, specifically in flavor sector. In flavor physics the ideal laboratory system is B meson, which provides a window pan to study the physics in and beyond the Standard Model. B-physics started in 1977 with the observation of a dimuon resonance at 9.5 GeV in 400 GeV proton-nucleon collision at Fermilab [1] and was named Υ resonances, its quark content is $\bar{b}b$. The dedicated B-factories Babar [2] and Belle [3] started working in 1999 and added a large amount of data to the results of CLEO [4],CERN [5]and Fermi lab experiments [6]. The recent experiment such as Large Hadron collider (LHC) will not only provide a good testing ground to investigate the Standard Model with great precision but also to study the new physics (NP) effects through the deviations of measured observables from SM values.

In general, there are two ways to search for the NP: one is the direct search where we can produce the new particles by raising the energy of colliders, and the other one is the indirect search, i.e. to increase the experimental data of different Standard Model processes where the NP effects can manifest themselves. The processes that are suitable for indirect searches of NP are those which are rare in the Standard Model and can be measured precisely. In this context the flavor physics plays an important role in order to look for physics within and beyond the Standard model. In the Standard Model the flavor symmetry is exact at tree level and its violation at loop level are very small. Thus the flavor changing processes are important to study the physics within and beyond the Standard model. Such processes in the flavor sector are rare B-meson decays. Rare B decays are mediated through Flavor changing neutral current transitions (FCNC), which are induced only at loop level through Glashow-Iliopoulos-Maiani (GIM) mechanism[7] in the Standard model. These FCNC transitions will provide a suitable tool to investigate the physics within and beyond the Standard model.

The experimental observation of inclusive [8] and exclusive [9] decays has prompted a lot of theoretical interest on rare B meson decays. Though the inclusive decays are theoretically better understood but are difficult to study experimentally. In contrast, the exclusive decays are easier to detect experimentally but are challenging to calculate theoretically; and the difficulty lies in describing the hadronic structure, which involves non-perturbative physics and provides the main uncertainty in the predictions of exclusive rare decays. In exclusive decays the long-distance effects in the meson transition amplitude of the effective Hamiltonian are encoded in the meson transition form factors which are the functions of square of momentum transfer and are model dependent quantities. In literature, some of the rare radiative and rare semileptonic decays of B-meson such as $B \to \gamma\ell^+\ell^-$ [10, **?**, 11], $B \to (K, K^*)\ell^+\ell^-$ [12, 13, 14, 15, 16, 17, 18, 19] and $B \to \phi\ell^+\ell^-$ [20] have been studied using the framework of the constituent quark model, Light cone sum rules(LCSR), QCD sum rules to describe the transition form factors of initial and final state mesons.

The exploration of Physics beyond the SM through various inclusive B meson decays like $B \to X_{s,d}\ell^+\ell^-$ and their corresponding exclusive processes, $B \to M\ell^+\ell^-$ with $M = K, K^*, K_1, \rho$ etc have been done in literature [21, 22]. These studies showed that the above mentioned inclusive and exclusive decays of B meson are very sensitive to the flavor structure of the Standard Model and provide a windowpane for any NP model. There are two different ways to incorporate the NP effects in the rare decays, one through the modification of Wilson coefficients and the other through new operators which are absent in the Standard Model. It is necessary to mention, the FCNC decay modes like $B \to X_s\ell^+\ell^-$, $B \to K^*\ell^+\ell^-$ and $B \to K\ell^+\ell^-$ which are useful not only in the determination of precise values of Wilson coefficients C_7^{eff}, C_9^{eff} and C_{10}^{eff} but also the sign of C_7^{eff}. In particular these decay modes involved observables which can distinguish between the various extensions of the Standard Model.

The observables like branching ratio, forward-backward asymmetry and helicity fractions of final

state mesons for the semileptonic B decays are greatly influenced by the different scenarios beyond the Standard Model. Therefore, the precise measurement of these observables will play an important role in the indirect searches of NP. The purpose of this thesis is to investigate the possibility of searching NP related to the Universal extra dimension model (UED) and to Standard Model with a fourth generation (SM4) in $B \to K_1(1270, 1400)\ell^+\ell^-$ and $B_c \to D_s^*\ell^+\ell^-$ decays using the above mentioned physical observables. The study of these physical observables will provide a precision test of standard model and NP when more data will be available at LHC.

The organization of this thesis is as follows. In Chapter 2 we discuss the theoretical framework needed to study the said processes both in standard model and NP models. In section 2.1 we give the expression of the effective Hamiltonian, the explicit form of the quark level operators and the amplitude for the said processes, which at the quark level arises from $b \to s\ell^+\ell^-$. In sections 2.2 and 2.3 we give a brief introduction to the fourth generation standard model and UED model which was proposed by Appelquist, Cheng and Dobrescu.

In chapter 3 we present the Exclusive $B \to K_1(1270, 1400)\ell^+\ell^-$ beyond the third generation. In section 3.1 we discuss how the NP effects arises in SM4. In section 3.2. we present the mixing of $K_1(1270)$ and $K_1(1400)$ and the form factors used in this study. In section 3.3, we discuss the observables of $B \to K_1\ell^+\ell^-$ in detail. In section 3.4, we give the numerical analysis of the physical observables and discuss their sensitivity to the fourth generation SM scenario. We conclude our findings in section 3.5.

In chapter 4 we present the same decay as in chapter 3 in universal extra dimension model. Section 4.2 presents the matrix element for the decay $B \to K_1\ell^+\ell^-$, Ward identities and develop the relations between the form factors which results in reducing the number of unknown quantities. In section 4.3, pole contribution of various form factors are discussed and relations among different coupling constants are obtained with the help of Ward identities. In Section 4.4, we discuss the sensitivity of the physical observables in UED model. Section 4.5, summarizes the main points of our study.

In Chapter 5 we present the semileptonic charm B-meson decays in universal extra dimension model. In section 5.1 we give the introduction of charm B-meson decays and its importance in phenomenology. In section 5.2 we present the matrix element and form factors for the decay $B_c \to D_s^*\ell^+\ell^-$ and we also discuss the weak annihilation form factors for the said decay. Section 5.3 the pole contribution for the said decay is discussed. In section 5.4 we give the formulas for the physical observables such as branching ratio and helicity fractions of D_s^*-meson for the decay $B_c \to D_s^*\ell^+\ell^-$. In section 5.5 we present the numerical analysis of the above physical observables and also compare our form factors with QCD sum rules for the same observables. Finally, we summarize the main points of our study in section 5.6.

This Ph.D. thesis is based upon the following publications.

1. $K_1(1270) - K_1(1400)$ mixing and the fourth generation SM effects in $B \to K_1\ell^+\ell^-$ decays, Aqeel Ahmed, Ishtiaq Ahmed, M. Ali Paracha, Abdur Rehman , Phys.Rev.D 84:033010, 2011.

2. Form factors, branching ratio and forward-backward asymmetry in $B \to K_1 \ell^+ \ell^-$ decays, M. Ali Paracha, Ishtiaq Ahmed and M. Jamil Aslam, Eur.Phys.J.C52:967-973,2007.

3. Exclusive $B \to K_1 \ell^+ \ell^-$ decay in model with single universal extra dimension, Ishtiaq Ahmed, M. Ali Paracha and M. Jamil Aslam, Eur.Phys.J.C54:591-599,2008.

4. Semileptonic charmed B meson decays in Universal Extra Dimension Model, M.Ali Paracha, Ishtiaq Ahmed and M.Jamil Aslam, Phys.Rev.D 84: 035003, 2011.

Chapter 2

Theoretical Framework

In this chapter we present the theoretical framework appropriate to study the processes $B \to K_1(1270, 1400)\ell^+\ell^-$ and $B_c \to D_s^*\ell^+\ell^-$ both in Standard Model and in NP models. We also include a brief introduction to NP models such as Standard Model with fourth generation (SM4) and universal extra dimension model (UED). The phenomenological implications of these models will be discussed in next chapters.

2.1 Effective Hamiltonian

The basic starting point to do phenomenology of weak decays of hadrons is the effective Hamiltonian which has the following generic structure

$$\mathcal{H}_{eff} = \frac{G_F}{\sqrt{2}} \sum_i V_{CKM} C_i(\mu) O_i(\mu) \tag{2.1}$$

Here G_F is the Fermi coupling constant, V_{CKM} are the Cabibo-Kobayashi and Maskawa(CKM) matrix elements, $O_i(\mu)$ are the four-quark operators and $C_i(\mu)$ are the corresponding Wilson coefficients at the energy scale μ [23]. Now the amplitude for the decay of meson M to a final state meson F can be written as

$$\begin{aligned} A(M \to F) &= \langle F | H_{eff} | M \rangle \\ &= \frac{G_F}{\sqrt{2}} \sum_i V_{CKM}^i C_i(\mu) \langle F | O_i(\mu) | M \rangle \end{aligned} \tag{2.2}$$

Wilson coefficients give the short distance effects where as the long distance effects involve the matrix elements of the operators in Eq.(2.2) between initial and final state mesons. The explicit form of the operators which are sandwiched between the initial and final state meson can be written as [24]

Current Current Operators

$$O_1 = (\bar{c}_\alpha b_\beta)_{V-A}(\bar{s}_\beta c_\alpha)_{V-A} \tag{2.3}$$

$$O_2 = (\bar{c}b)_{V-A}(\bar{s}c)_{V-A} \tag{2.4}$$

QCD-Penguins

$$O_3 = (\bar{s}b)_{V-A}\sum_{q=u,d,s,c,b}(\bar{q}q)_{V-A} \tag{2.5}$$

$$O_4 = (\bar{s}_\alpha b_\beta)_{V-A}\sum_{q=u,d,s,c,b}(\bar{q}_\beta q_\alpha)_{V-A} \tag{2.6}$$

$$O_5 = (\bar{s}b)_{V-A}\sum_{q=u,d,s,c,b}(\bar{q}q)_{V+A} \tag{2.7}$$

$$O_6 = (\bar{s}_\alpha b_\beta)_{V-A}\sum_{q=u,d,s,c,b}(\bar{q}_\beta q_\alpha)_{V+A} \tag{2.8}$$

Electroweak penguins

$$O_7 = \frac{3}{2}(\bar{s}b)_{V-A}\sum_{q=u,d,s,c,b}e_q\,(\bar{q}q)_{V+A} \tag{2.9}$$

$$O_8 = \frac{3}{2}(\bar{s}_\alpha b_\beta)_{V-A}\sum_{q=u,d,s,c,b}(\bar{q}_\beta q_\alpha)_{V+A} \tag{2.10}$$

$$O_9 = \frac{3}{2}(\bar{s}b)_{V-A}\sum_{q=u,d,s,c,b}e_q\,(\bar{q}q)_{V-A} \tag{2.11}$$

$$O_{10} = \frac{3}{2}(\bar{s}_\alpha b_\beta)_{V-A}\sum_{q=u,d,s,c,b}(\bar{q}_\beta q_\alpha)_{V-A} \tag{2.12}$$

Magnetic Penguins

$$O_{7\gamma} = \frac{e}{8\pi^2}m_b\bar{s}_\alpha\sigma^{\mu\nu}(1+\gamma^5)b_\alpha F_{\mu\nu} \tag{2.13}$$

$$O_{8G} = \frac{g}{8\pi^2}m_b\bar{s}_\alpha\sigma^{\mu\nu}(1+\gamma^5)T^a_{\alpha\beta}b_\beta G^a_{\mu\nu} \tag{2.14}$$

Semileptonic Operators

$$O_9 = (\bar{s}b)_{V-A}\left(\bar{\ell}\ell\right)_V \qquad O_{10} = (\bar{s}b)_{V-A}\left(\bar{\ell}\ell\right)_A \tag{2.15}$$

$$O_{\nu\bar{\nu}} = (\bar{s}b)_{V-A}(\bar{\nu}\nu)_{V-A} \qquad O_{\ell\bar{\ell}} = (\bar{s}b)_{V-A}\left(\bar{\ell}\ell\right)_{V-A}$$

The above set of operators characterize the interplay of QCD and electroweak effects. As already mentioned earlier, this thesis deals with rare decays of B mesons into a final state hadron with lepton-antilepton pair so the operators responsible for these decays are electromagnetic penguin operator $O_{7\gamma}$ given in Eq.(2.12) and the semileptonic operators given in Eq.(2.15).

At the quark level the said processes are induced by the transition $b \to s\ell^+\ell^-$, which in the Standard Model is described by the following effective Hamiltonian

$$\mathcal{H}_{eff} = -\frac{4G_F}{\sqrt{2}} V_{tb}V_{ts}^* \Big[\sum_{i=1}^{10} C_i(\mu) O_i(\mu)\Big], \tag{2.16}$$

In terms of the above Hamiltonian, the amplitude for $b \to s\ell^+\ell^-$ can be written as:

$$\begin{aligned}\mathcal{M}_{SM}(b \to s\ell^+\ell^-) = -\frac{G_F\alpha}{\sqrt{2}\pi} V_{tb}V_{ts}^* \Big\{ & C_9^{eff}(\bar{s}\gamma_\mu Lb)(\bar{\ell}\gamma^\mu \ell) \\ & + C_{10}(\bar{s}\gamma_\mu Lb)(\bar{\ell}\gamma^\mu\gamma_5\ell) - 2m_b C_7^{eff}(\bar{s}i\sigma_{\mu\nu}\frac{q^\nu}{q^2} Rb)(\bar{\ell}\gamma^\mu\ell)\Big\}\end{aligned} \tag{2.17}$$

where $R, L = (1 \pm \gamma_5)/2$ and q is the momentum transfer. The semileptonic operator O_{10} can not be induced by the insertion of four-quark operators because of the absence of the neutral Z boson in the effective theory. Hence, the Wilson coefficient C_{10} is not renormalized under QCD corrections and therefore it is independent of the energy scale. In addition to this, the above quark level decay amplitude can take contributions from the matrix-elements of four-quark operators, $\sum_{i=1}^{6} \langle l^+l^- s\,|O_i|\,b\rangle$, which are usually absorbed into the effective Wilson coefficient $C_9^{eff}(\mu)$, which can be decomposed into the following three parts [22, 25]

$$C_9^{SM} = C_9^{eff}(\mu) = C_9(\mu) + Y_{SD}(z,s') + Y_{LD}(z,s'),$$

where the parameters z and s' are defined as $z = m_c/m_b$, $s' = q^2/m_b^2$. $Y_{SD}(z,s')$ describes the short-distance contributions from four-quark operators far away from the $c\bar{c}$ resonance regions, which can be calculated reliably in the perturbative theory. The long-distance contributions $Y_{LD}(z,s')$ from four-quark operators near the $c\bar{c}$ resonance cannot be calculated from first principles of QCD and are usually parameterized in the form of a phenomenological Breit-Wigner formula making use of the vacuum saturation approximation and quark-hadron duality. The expressions for $Y_{SD}(z,s')$ and $Y_{LD}(z,s')$ can be written as

$$\begin{aligned} Y_{SD}(z,s') = & \; h(z,s')(3C_1(\mu) + C_2(\mu) + 3C_3(\mu) + C_4(\mu) + 3C_5(\mu) + C_6(\mu)) \\ & -\frac{1}{2}h(1,s')(4C_3(\mu) + 4C_4(\mu) + 3C_5(\mu) + C_6(\mu)) \\ & -\frac{1}{2}h(0,s')(C_3(\mu) + 3C_4(\mu)) + \frac{2}{9}(3C_3(\mu) + C_4(\mu) + 3C_5(\mu) + C_6(\mu)) \end{aligned} \tag{2.18}$$

with

$$h(z,s') = -\frac{8}{9}\ln z + \frac{8}{27} + \frac{4}{9}x - \frac{2}{9}(2+x)|1-x|^{1/2} \begin{cases} \ln\left|\frac{\sqrt{1-x}+1}{\sqrt{1-x}-1}\right| - i\pi & \text{for } x \equiv 4z^2/s' < 1 \\ 2\arctan\frac{1}{\sqrt{x-1}} & \text{for } x \equiv 4z^2/s' > 1 \end{cases},$$

$$h(0,s') = \frac{8}{27} - \frac{8}{9}\ln\frac{m_b}{\mu} - \frac{4}{9}\ln s' + \frac{4}{9}i\pi \ . \tag{2.19}$$

and

$$Y_{LD}(z,s') = \frac{3\pi}{\alpha^2}C^{(0)} \sum_{V_i=\psi_i} \kappa_i \frac{m_{V_i}\Gamma(V_i \to l^+l^-)}{m_{V_i}^2 - s'm_b^2 - im_{V_i}\Gamma_{V_i}} \tag{2.20}$$

where $C^{(0)} = 3C_1 + C_2 + 3C_3 + C_4 + 3C_5 + C_6$.

Irrespective of this, the non-factorizable effects [26] from the charm loop can bring about further corrections to the radiative $b \to s\gamma$ transition, which can be absorbed into the effective Wilson coefficient C_7^{eff}. Specifically, the Wilson coefficient C_7^{eff} takes the form [27]

$$C_7^{eff}(\mu) = C_7(\mu) + C_{b\to s\gamma}(\mu),$$

with

$$C_{b\to s\gamma}(\mu) = i\alpha_s\left[\frac{2}{9}\eta^{14/23}(G_1(x_t) - 0.1687) - 0.03C_2(\mu)\right], \tag{2.21}$$

$$G_1(x) = \frac{x(x^2-5x-2)}{8(x-1)^3} + \frac{3x^2\ln^2 x}{4(x-1)^4}, \tag{2.22}$$

where $\eta = \alpha_s(m_W)/\alpha_s(\mu)$, $x = m_t^2/m_W^2$. $C_{b\to s\gamma}$ is the absorptive part for the $b \to sc\bar{c} \to s\gamma$ re-scattering and we have dropped out the small contributions proportional to CKM sector $V_{ub}V_{us}^*$. In the above mentioned NP physics models, the NP effects only modify the Wilson coefficients.

2.2 Fourth Generation Standard Model

It is well known that the SM includes three generations of fermions, but it does not prohibit the fourth generation. The restrictions on the number of fermion generations come from the QCD asymptotic freedom which constraint them to nine. Therefore, shortly after the measurement of the third generation, a fourth generation was an obvious extension.

Interest in the fourth generation Standard Model (SM4) was fairly high in the 1980s until the electroweak precision data seemed to rule it out. The other reason which stimulates the interest in the fourth generation was the measurement of the number of light neutrinos at the Z pole that showed only three light neutrinos could exist. However, the discovery of neutrino oscillations suggested the possibility of a mass scale beyond the SM, and the models with the sufficiently massive neutrino became acceptable [28].Though the early study of the EW precision measurements ruled out a fourth generation [29], however it was subsequently pointed out [30] that if the fourth generation masses are not degenerate, then the EW precision data do not prohibit the fourth generation [31]. Therefore, the SM can be simply extended with a sequential repetition as four quark and four lepton left handed doublets and corresponding right

handed singlets.

The possible sequential fourth generation may play an important role in understanding the well known problem of CP violation and flavor structure of standard theory [32, 33, 34, 35, 36], electroweak symmetry breaking [37, 38, 39, 40], hierarchies of fermion mass and mixing angle in quark/lepton sectors[41, 42]. A thorough discussion on the theoretical and experimental aspects of the fourth generation can be found in ref [43].

On the experimental side, recent searches by the CDF collaboration for direct production of fourth generation up-type quark (t') and down-type quark (b') found $m_{t'} > 335$ GeV [44] and $m_{b'} > 385$ GeV [45], assuming $Br(t' \to Wq, (q = d, s, b)) = 100\%$ and $Br(b' \to Wt) = 100\%$ respectively. This indeed suggests that the fourth generation fermion must be heavy, which supports the scenario of compositeness. The underlying assumption to perform these searches is that $m_{t'} - m_{b'} < M_W$ and negligible mixing of the (t', b') states with the two lightest quark generations. To account for EW precision data such conditions are generally required for the SM4 with the one Higgs doublet [46]. Moreover, when a fourth generation of fermions is embedded in theories beyond the SM, the large splitting case ($m_{t'} - m_{b'} > M_W$) and the inverted scenario ($m_{t'} < m_{b'}$) have not been excluded. Recently, it has also been shown [47] that the precision EW data can accommodate ($m_{t'} - m_{b'} > M_W$) if there are two Higgs doublets. Thus there is no uniquely interesting set of assumptions under which experimental data must be interpreted [48] and the determination of the allowed parameter space of fourth generation fermions will be an important goal of the LHC era. The large values of the masses of fourth generation would provide special room to new interactions originating at a higher scale and the precise determination of the fourth generation quark properties may present the existence of physics beyond the SM.

The sequential fourth generation model with an additional up-type quark t' and down-type quark b' , a heavy charged lepton τ' and an associated neutrino ν' is a simple and non-supersymmetric extension of the SM, and as such does not add any new dynamics to the SM. Being the simplest extension of the SM, it retains all the properties of the SM where the new top quark t' like the other up-type quarks, contributes to $b \to s$ transition at the loop level. Therefore, the effect of the fourth generation shows up by changing the values of Wilson coefficients $C_7(\mu)$, $C_9(\mu)$ and C_{10} via the virtual exchange of fourth generation up-type quark t', which then take the form:

$$\lambda_t C_i \to \lambda_t C_i^{SM} + \lambda_{t'} C_i^{new}, \tag{2.23}$$

Here, $\lambda_f = V_{fb}^* V_{fs}$ and the explicit forms of the C_i's can be obtained from the corresponding expressions for the Wilson coefficients in the SM by substituting $m_t \to m_{t'}$. By adding the extra family of quarks, the CKM matrix of the SM is extended by an extra row and column, which now becomes 4×4 unitary matrix which requires six real parameters and three phases. These two extra phases imply the possibility

of extra sources of CP-violation. The unitarity of the CKM matrix now leads to

$$\lambda_u + \lambda_c + \lambda_t + \lambda_{t'} = 0.$$

Since $\lambda_u = V_{ub}^* V_{us}$ has a very small value compared to the others, we will neglect it. Then, $\lambda_t \approx -\lambda_c - \lambda_{t'}$ and from Eq. (2.23) we have

$$\lambda_t C_i^{SM} + \lambda_{t'} C_i^{new} = -\lambda_c C_i^{SM} + \lambda_{t'} \left(C_i^{new} - C_i^{SM} \right). \tag{2.24}$$

One can clearly see that in the limits $\lambda_{t'} \to 0$ or $m_{t'} \to m_t$ the term $\lambda_{t'} \left(C_i^{new} - C_i^{SM} \right)$ vanishes, which is the requirement of the GIM mechanism. Including the contribution of the t' quark in the penguin loop, the Wilson coefficients C_i's can be written in the following form

$$\begin{aligned} C_7^{tot}(\mu) &= C_7^{SM}(\mu) + \frac{\lambda_{t'}}{\lambda_t} C_7^{new}(\mu), \\ C_9^{tot}(\mu) &= C_9^{SM}(\mu) + \frac{\lambda_{t'}}{\lambda_t} C_9^{new}(\mu), \\ C_{10}^{tot} &= C_{10}^{SM} + \frac{\lambda_{t'}}{\lambda_t} C_{10}^{new}, \end{aligned} \tag{2.25}$$

where we factored out the $\lambda_t = V_{tb}^* V_{ts}$ term in the effective Hamiltonian given in Eq. (2.16) and the last term in these expressions corresponds to the contribution of the t' quark to the Wilson coefficients. $\lambda_{t'}$ can be parameterized as:

$$\lambda_{t'} = |V_{t'b}^* V_{t's}| \, e^{i\phi_{sb}} \tag{2.26}$$

where ϕ_{sb} is the new CP odd phase. The free quark decay amplitude in SM4 is exactly the same as given in Eq.(2.17).

2.3 Appelquist Cheng and Dobrescu Model

In our usual universe we have 3 spatial +1 temporal dimensions and if an extra dimension exists and is compactified, fields living in all dimensions would manifest themselves in the 3+1 space by the appearance of Kaluza-Klein excitations. The most pertinent question is whether ordinary fields propagate or not in all extra dimensions. One obvious possibility is the propagation of gravity in whole ordinary plus extra dimensional universe, the "bulk". Contrary to this there are the models with universal extra dimensions (UED) in which all the fields propagate in all available dimensions [49] and the Appelquist, Cheng and Dobrescu (ACD) model belongs to one of UED scenarios [50].

This model is the minimal extension of the SM in $4 + \delta$ dimensions, and in literature a simple case $\delta = 1$ is considered [50]. The topology for this extra dimension is orbifold S^1/Z_2, and the coordinate

$x_5 = y$ runs from 0 to $2\pi R$, where R is the the compactification radius. The Kaluza-Klein (KK) mode expansion of the fields are determined from the boundary conditions at two fixed points $y = 0$ and $y = \pi R$ on the orbifold. Under parity transformation $P_5 : y \to -y$ the fields may be even or odd. Even fields have their correspondent in the 4 dimensional SM and their zero mode in the KK mode expansion can be interpreted as the ordinary SM field. The odd fields do not have their correspondent in the SM and therefore do not have zero mode in the KK expansion.

The significant features of the ACD model are:

i) the compactification radius R is the only free parameter with respect to SM

ii) no tree level contribution of KK modes in low energy processes (at scale $\mu \ll 1/R$) and no production of single KK excitation in ordinary particle interactions is a consequence of conservation of KK parity.

The detailed description of ACD model is provided in [51]; here we summarize main features of its construction from [50].

Gauge group

As the ACD model is the minimal extension of SM therefore the gauge bosons associated with the gauge group $SU(2)_L \times U(1)_Y$ are W_i^a ($a = 1, 2, 3$, $i = 0, 1, 2, 3, 5$) and B_i, and the gauge couplings are $\hat{g}_2 = g_2\sqrt{2\pi R}$ and $\hat{g}' = g'\sqrt{2\pi R}$ (the hat on the coupling constant refers to the extra dimension). The charged bosons are $W_i^{\pm} = \frac{1}{\sqrt{2}}\left(W_i^1 \mp W_i^2\right)$ and the mixing of W_i^3 and B_i give rise to the fields Z_i and A_i as they do in the SM. The relations for the mixing angles are:

$$c_W = \cos\theta_W = \frac{\hat{g}_2}{\sqrt{\hat{g}_2^2 + \hat{g}'^2}} \qquad c_W = \sin\theta_W = \frac{\hat{g}'}{\sqrt{\hat{g}_2^2 + \hat{g}'^2}} \tag{2.27}$$

The Weinberg angle remains the same as in the SM, due to the relationship between five and four dimensional constants. The gluons which are the gauge bosons associated to $SU(3)_C$ are $G_i^a(x, y)$ ($a = 1, \ldots, 8$).

Higgs sector and mixing between Higgs fields and gauge bosons

The Higgs doublet can be written as:

$$\phi = \begin{pmatrix} i\chi^+ \\ \frac{1}{\sqrt{2}}\left(\psi - i\chi^3\right) \end{pmatrix} \tag{2.28}$$

with $\chi^{\pm} = \frac{1}{\sqrt{2}}\left(\chi^1 \mp \chi^2\right)$. Now only field ψ has a zero mode, and we assign the vacuum expectation value $\hat{v}$ to such mode, so that $\psi \to \hat{v} + H$. H is the the SM Higgs field, and the relation between the expectation values in five and four dimension is: $\hat{v} = v/\sqrt{2\pi R}$.

The Goldstone fields $G_{(n)}^0$, $G_{(n)}^{\pm}$ arises due to the mixing of charged $W_{5(n)}^{\pm}$ and $\chi_{(n)}^{\pm}$, as well as neutral

fields $Z_{5(n)}$. These Goldstone modes are then used to give masses to the $W^{\pm\mu}_{(n)}$ and $Z^{\mu}_{(n)}$, and $a^{0}_{(n)}$, $a^{\pm}_{(n)}$, new physical scalars.

Yukawa terms

In the SM, Yukawa coupling of the Higgs field to the fermion provides the fermion mass terms. The diagonalization of such terms leads to the introduction of the CKM matrix. In order to have chiral fermions in ACD model, the left and right-handed components of the given spinor cannot be simultaneously even under the parity operator of fifth dimension P_5. This makes the ACD model to be the minimal flavor violation model, since there are no new operators beyond those present in the SM and no new phase beyond the CKM phase and the unitarity triangle remains the same as in SM [51]. In order to have 4-d mass eigenstates of higher KK levels, a further mixing is introduced among the left-handed doublet and right-handed singlet of each flavor f. The mixing angle is such that $\tan\left(2\alpha_{f(n)}\right) = \frac{m_f}{n/R}$ $(n \geq 1)$ giving mass $m_{f(n)} = \sqrt{m_f^2 + \frac{n^2}{R^2}}$, hence the mixing angle is negligible for all flavors except the top [50].

Integrating over the fifth-dimension y gives the four-dimensional Lagrangian:

$$\mathcal{L}_4(x) = \int_0^{2\pi R} \mathcal{L}_5(x, y) \tag{2.29}$$

which describes: (i) zero modes corresponding to the SM fields, (ii) their massive KK excitations, (iii) KK excitations without zero modes which do not corresponds to any field in SM. Feynman rules used in the further calculation are given in Ref. [51].

In the ACD model the NP comes through the Wilson coefficients. Buras et al. have computed the above coefficients at NLO in ACD model including the effects of KK modes [51, 52]; we use these results to study $B \to K_1(1270, 1400)\ell^+\ell^-$ and $B_c \to D_s^*\ell^+\ell^-$ decays. As it has already been mentioned that ACD model is the minimal extension of SM with only one extra dimension and it has no extra operator other than the SM. Thus the whole contribution from all the KK states is in the Wilson coefficients, i.e. now they depend on the additional ACD parameter, the inverse of compactification radius R. At large value of $1/R$ the SM phenomenology should be recovered, since the new states, being more and more massive, decoupled from the low-energy theory.

In the ACD model, the Wilson coefficients are modified and they contain the contribution from KK-excitations which are not present in the SM, which comes as an intermediate state in penguin and box diagrams. Thus, these coefficients can be expressed in terms of the functions $F(x_t, 1/R)$, $x_t = \frac{m_t^2}{M_W^2}$, which generalize the corresponding SM function $F_0(x_t)$ according to:

$$F(x_t, 1/R) = F_0(x_t) + \sum_{n=1}^{\infty} F_n(x_t, x_n) \tag{2.30}$$

with $x_n = \frac{m_n^2}{M_W^2}$ and $m_n = \frac{n}{R}$ [50]. The relevant diagrams are Z^0 penguins, γ penguins, gluon penguins, γ magnetic penguins, Chormomagnetic penguins and the corresponding functions are $C\,(x_t, 1/R)$, $D\,(x_t, 1/R)$, $E\,(x_t, 1/R)$, $D'\,(x_t, 1/R)$ and $E'\,(x_t, 1/R)$ respectively. These functions can be found in [51, 52] and to make the thesis self contained, we collect here the formulae needed for our analysis.

•C_7

In place of C_7, one defines an effective coefficient $C_7^{(0)eff}$ which is renormalization scheme independent [53]:

$$C_7^{(0)eff}(\mu_b) = \eta^{\frac{16}{23}} C_7^{(0)}(\mu_w) + \frac{8}{3}(\eta^{\frac{14}{23}} - \eta^{\frac{16}{23}}) C_8^{(0)}(\mu_w) + C_2^{(0)}(\mu_w) \sum_{i=1}^{8} h_i \eta^{\alpha_i} \tag{2.31}$$

where $\eta = \frac{\alpha s(\mu_w)}{\alpha_s(\mu_b)}$, and

$$C_2^{(0)}(\mu_w) = 1,\ C_7^{(0)}(\mu_w) = -\frac{1}{2} D'(x_t, \frac{1}{R}),\ C_8^{(0)}(\mu_w) = -\frac{1}{2} E'(x_t, \frac{1}{R}); \tag{2.32}$$

the superscript (0) stays for leading log approximation. Furthermore:

$$\begin{aligned}
\alpha_1 &= \frac{14}{23} \quad \alpha_2 = \frac{16}{23} \quad \alpha_3 = \frac{6}{23} \quad \alpha_4 = -\frac{12}{23} \\
\alpha_5 &= 0.4086 \quad \alpha_6 = -0.4230 \quad \alpha_7 = -0.8994 \quad \alpha_8 = -0.1456 \\
h_1 &= 2.996 \quad h_2 = -1.0880 \quad h_3 = -\frac{3}{7} \quad h_4 = -\frac{1}{14} \\
h_5 &= -0.649 \quad h_6 = -0.0380 \quad h_7 = -0.0185 \quad h_8 = -0.0057.
\end{aligned} \tag{2.33}$$

The functions D' and E' are given in Eq. (2.33) with

$$D_0'(x_t) = -\frac{(8x_t^3 + 5x_t^2 - 7x_t)}{12(1-x_t)^3} + \frac{x_t^2(2-3x_t)}{2(1-x_t)^4} \ln x_t \tag{2.34}$$

$$E_0'(x_t) = -\frac{x_t(x_t^2 - 5x_t - 2)}{4(1-x_t)^3} + \frac{3x_t^2}{2(1-x_t)^4} \ln x_t \tag{2.35}$$

$$\begin{aligned}
D_n'(x_t, x_n) = {} & \frac{x_t(-37 + 44x_t + 17x_t^2 + 6x_n^2(10 - 9x_t + 3x_t^2) - 3x_n(21 - 54x_t + 17x_t^2))}{36(x_t-1)^3} \\
& + \frac{x_n(2 - 7x_n + 3x_n^2)}{6} \ln \frac{x_n}{1+x_n} \\
& - \frac{(-2 + x_n + 3x_t)(x_t + 3x_t^2 + x_n^2(3 + x_t) - x_n)(1 + (-10 + x_t)x_t))}{6(x_t-1)^4} \ln \frac{x_n + x_t}{1+x_n}
\end{aligned} \tag{2.36}$$

$$\begin{aligned}
E_n'(x_t, x_n) = {} & \frac{x_t(-17 - 8x_t + x_t^2 + 3x_n(21 - 6x_t + x_t^2) - 6x_n^2(10 - 9x_t + 3x_t^2))}{12(x_t-1)^3} \\
& + -\frac{1}{2} x_n(1+x_n)(-1+3x_n) \ln \frac{x_n}{1+x_n} \\
& + \frac{(1+x_n)(x_t + 3x_t^2 + x_n^2(3+x_t) - x_n(1 + (-10 + x_t)x_t))}{2(x_t-1)^4} \ln \frac{x_n + x_t}{1+x_n}
\end{aligned} \tag{2.37}$$

Following [52] one gets the expressions for the sum over n :

$$\begin{aligned}\sum_{n=1}^{\infty} D'_n(x_t,x_n) &= -\frac{x_t(-37+x_t(44+17x_t))}{72(x_t-1)^3} \\ &+\frac{\pi M_w R}{2}[\int_0^1 dy \frac{2y^{\frac{1}{2}}+7y^{\frac{3}{2}}+3y^{\frac{5}{2}}}{6}]\coth(\pi M_w R\sqrt{y}) \\ &+\frac{(-2+x_t)x_t(1+3x_t)}{6(x_t-1)^4}J(R,-\frac{1}{2}) \\ &-\frac{1}{6(x_t-1)^4}[x_t(1+3x_t)-(-2+3x_t)(1+(-10+x_t)x_t)]J(R,\frac{1}{2}) \\ &+\frac{1}{6(x_t-1)^4}[(-2+3x_t)(3+x_t)-(1+(-10+x_t)x_t)]J(R,\frac{3}{2}) \\ &-\frac{(3+x_t)}{6(x_t-1)^4}J(R,\frac{5}{2})] \end{aligned} \tag{2.38}$$

$$\begin{aligned}\sum_{n=1}^{\infty} E'_n(x_t,x_n) &= -\frac{x_t(-17+(-8+x_t)x_t)}{24(x_t-1)^3} \\ &+\frac{\pi M_w R}{2}[\int_0^1 dy(y^{\frac{1}{2}}+2y^{\frac{3}{2}}-3y^{\frac{5}{2}})\coth(\pi M_w R\sqrt{y})] \\ &-\frac{x_t(1+3x_t)}{(x_t-1)^4}J(R,-\frac{1}{2}) \\ &+\frac{1}{(x_t-1)^4}[x_t(1+3x_t)-(1+(-10+x_t)x_t)]J(R,\frac{1}{2}) \\ &-\frac{1}{(x_t-1)^4}[(3+x_t)-(1+(-10+x_t)x_t)]J(R,\frac{3}{2}) \\ &+\frac{(3+x_t)}{(x_t-1)^4}J(R,\frac{5}{2})] \end{aligned} \tag{2.39}$$

where

$$J(R,\alpha)=\int_0^1 dy y^{\alpha}[\coth(\pi M_w R\sqrt{y})-x_t^{1+\alpha}\coth(\pi m_t R\sqrt{y})]. \tag{2.40}$$

•C_9

In the ACD model and in the Naive dimensional regularization(NDR) scheme one has

$$C_9(\mu)=P_0^{NDR}+\frac{Y(x_t,\frac{1}{R})}{\sin^2\theta_W}-4Z(x_t,\frac{1}{R})+P_E E(x_t,\frac{1}{R}) \tag{2.41}$$

where $P_0^{NDR}=2.60\pm0.25$ [54] and the last term is numerically negligible. Besides

$$\begin{aligned} Y(x_t,\frac{1}{R}) &= Y_0(x_t)+\sum_{n=1}^{\infty}C_n(x_t,x_n) \\ Z(x_t,\frac{1}{R}) &= Z_0(x_t)+\sum_{n=1}^{\infty}C_n(x_t,x_n) \end{aligned} \tag{2.42}$$

$$Y_0(x_t) = \frac{x_t}{8}[\frac{x_t-4}{x_t-1}+\frac{3x_t}{(x_t-1)^2}\ln x_t]$$

$$Z_0(x_t) = \frac{18x_t^4 - 163x_t^3 + 259x_t^2 - 108x_t}{144(x_t-1)^3} + [\frac{32x_t^4 - 38x_t^3 + 15x_t^2 - 18x_t}{72(x_t-1)^4} - \frac{1}{9}] \ln x_t \tag{2.43}$$

$$C_n(x_t, x_n) = \frac{x_t}{8(x_t-1)^2}[x_t^2 - 8x_t + 7 + (3 + 3x_t + 7x_n - x_t x_n) \ln \frac{x_t + x_n}{1 + x_n}] \tag{2.44}$$

and

$$\sum_{n=1}^{\infty} C_n(x_t, x_n) = \frac{x_t(7-x_t)}{16(x_t-1)} - \frac{\pi M_w R x_t}{16(x_t-1)^2}[3(1+x_t)J(R, -\frac{1}{2}) + (x_t - 7)J(R, \frac{1}{2})] \tag{2.45}$$

•C_{10}

C_{10} is μ independent and is given by

$$C_{10} = -\frac{Y(x_t, \frac{1}{R})}{\sin^2 \theta_w}. \tag{2.46}$$

The normalization scale is fixed to $\mu = \mu_b \simeq 5$ GeV.

We use these values of Wilson coefficients in the processes $B \to K_1(1270, 1400)\ell^+\ell^-$ and $B_c \to D_s^* \ell^+ \ell^-$ and will be discussed in Chapter 4 and Chapter 5.

Chapter 3

Exclusive $B \to K_1(1270, 1400)\ell^+\ell^-$ beyond the third generation

3.1 Introduction

As discussed in Chapter 1, there are several possible extensions of the SM. Among them the Standard Model with fourth generation (SM4) seems to be the most economical one in the number of additional particles and simpler in the sense that it does not introduce any new operators. It thus provides a natural extension of the SM which has been searched for previously at the LEP and Tevatron and now will be investigated at the LHC [55]. If a fourth family is discovered, it is likely to have consequences at least as profound as those that have emerged from the discovery of the third family. The fourth-generation SM not only provides a simple explanation of some of the experimental results which are difficult to reconcile with SM including the CP violation anomaly seen in $B_s - B_s$ mixing [56, 57] but also gives enough CP-asymmetries to facilitate baryogenesis [58]. In addition, the fact that the heavier quarks (t', b') and leptons (ν', τ') of the fourth generation can play a crucial role in dynamical electroweak symmetry breaking (DEWSB) [59] as an economical way to address the hierarchy puzzle in the SM. Furthermore, the LHC will provide a suitable amount of data which enlighten these puzzles more clearly as well as decide the belief in the extra generation and help us to enhance our theoretical understanding of these puzzles.

In the past few years, a number of analysis showed: (a)the SM with fourth generation is consistent with the electroweak precision tests (EWPT) [60, 61]. It is pointed out [62, 63, 64] that in the presence of a fourth generation a heavy Higgs boson does not contradict with EWPT, (b) SU(5) gauge couplings unification could be achieved without supersymmetry [65], (c) Electroweak baryogensis can be accommodated [66] and (d) the DEWSB might be actuated by the presence of the extra generation. Moreover, the

fourth-generation SM, in principle, could resolve certain anomalies present in flavor changing processes [67]. Furthermore the mismatch in the CP-asymmetry in $B \to K\pi$ data [68] with the SM [69] as well as CP violation in $B \to \phi K_s$ decay may also provide some hint of NP [70]. Henceforth the measurement of different observables in the rare B decays can be very helpful to put or to check the constraints on the 4th generation parameters.

The study of inclusive and exclusive processes of B-meson are very sensitive to flavor structure of the SM and provides a windowpane for any NP including the fourth-generation SM. Since it is expected that $m_{t'} > m_t$, the fourth generation quark can manifest their indirect existence in the penguin loop diagrams. Due to this reason FCNC transitions are at the forefront and one of the main research direction of all operating B factories including CLEO, Belle, Tevatron and LHCb [55]. However, the studies that involve the direct searches of the fourth generation quarks or their indirect searches via FCNC processes require the values of the quark masses and mixing elements which are not free parameters but rather they are constrained by experiments [71]. In the fourth generation SM the NP arises due to the modified Wilson coefficients C_7^{eff} ,C_9^{eff} and C_{10}^{eff} as the fourth generation quark (t') contributes in $b \to s(d)$ transition at the loop level along with other quarks u, c and t of SM.

The complementary information from the rare B decays is necessary for the indirect searches of NP including fourth generation. This complementary investigation improve the precision of SM parameters which are helpful in discovery of the NP. In this connection, like the rare semileptonic decays involving $B \to (X_s, K^*, K)\ell^+\ell^-$, the $B \to K_1(1270, 1400)\ell^+\ell^-$ decays are also rich in phenomenology for the NP [76]. The physical states $K_1(1270)$ and $K_1(1400)$ are mixture of $^3P_1$ and $^1P_1$ states K_{1A} and K_{1B}.

$$|K_1(1270)\rangle = |K_{1A}\rangle \sin\theta_K + |K_{1B}\rangle \cos\theta_K, \tag{3.1a}$$

$$|K_1(1400)\rangle = |K_{1A}\rangle \cos\theta_K - |K_{1B}\rangle \sin\theta_K, \tag{3.1b}$$

where the magnitude of mixing angle θ_K has been estimated to be $34^\circ \leq |\theta_K| \leq 58^\circ$ in Ref. [77]. Recently, from the study of $B \to K_1(1270)\gamma$ and $\tau \to K_1(1270)\nu_\tau$, the value of θ_K has been estimated to be $\theta_K = -(34 \pm 13)^\circ$, where the minus sign of θ_K is related to the chosen phase of $|K_{1A}\rangle$ and $|K_{1B}\rangle$ [78].

Many studies have shown [76] that the observables like branching ratio ($\mathcal{BR}$), forward-backward asymmetry ($\mathcal{A}_{FB}$) and helicity fractions $f_{L,T}$ for semileptonic B decays are greatly influenced by the different scenarios beyond the SM. Therefore, the precise measurement of these observables will play an important role in the indirect searches of NP. In this respect, it is natural to ask how these observables are influenced by the fourth generation parameters. The purpose of present study is to address this question i.e. investigate the possibility of searching NP due to the fourth generation SM in $B \to K_1(1270, 1400)\ell^+\ell^-$ decays with $\ell = \mu, \tau$ using the above mentioned observables.

3.2 Form Factors and Mixing of $K_1(1270) - K_1(1400)$

The exclusive $B \to K_1(1270, 1400)\ell^+\ell^-$ decays involve the hadronic matrix elements of quark operators given in Eq. (2.17) which can be parameterized in terms of the form factors as:

$$\begin{aligned}\langle K_1(k,\varepsilon)\,|V_\mu|\,B(p)\rangle &= \varepsilon_\mu^*\,(M_B + M_{K_1})\,V_1(q^2) \\ &- (p+k)_\mu\,(\varepsilon^*\cdot q)\,\frac{V_2(q^2)}{M_B + M_{K_1}} \\ &- q_\mu\,(\varepsilon\cdot q)\,\frac{2M_{K_1}}{q^2}\,\left[V_3(q^2) - V_0(q^2)\right]\end{aligned} \tag{3.2}$$

$$\langle K_1(k,\varepsilon)\,|A_\mu|\,B(p)\rangle = \frac{2i\epsilon_{\mu\nu\alpha\beta}}{M_B + M_{K_1}}\varepsilon^{*\nu}p^\alpha k^\beta A(q^2) \tag{3.3}$$

where $V_\mu = \bar{s}\gamma_\mu b$ and $A_\mu = \bar{s}\gamma_\mu\gamma_5 b$ are the vectors and axial vector currents, involved in the transition matrix, respectively. Also $p(k)$ are the momenta of the $B(K_1)$ mesons and ε_μ correspond to the polarization of the final state axial vector K_1 meson. In Eq.(3.2) we have

$$V_3(q^2) = \frac{M_B + M_{K_1}}{2M_{K_1}}V_1(q^2) - \frac{M_B - M_{K_1}}{2M_{K_1}}V_2(q^2) \tag{3.4}$$

with

$$V_3(0) = V_0(0)$$

In addition, there is also a contribution from the Penguin form factors which can be written as

$$\begin{aligned}&\langle K_1(k,\varepsilon)\,|\bar{s}i\sigma_{\mu\nu}q^\nu b|\,B(p)\rangle \\ &= \left[\left(M_B^2 - M_{K_1}^2\right)\varepsilon_\mu - (\varepsilon\cdot q)(p+k)_\mu\right]F_2(q^2) \\ &+ (\varepsilon^*\cdot q)\left[q_\mu - \frac{q^2}{M_B^2 - M_{K_1}^2}(p+k)_\mu\right]F_3(q^2)\end{aligned} \tag{3.5}$$

$$\langle K_1(k,\varepsilon)\,|\bar{s}i\sigma_{\mu\nu}q^\nu\gamma_5 b|\,B(p)\rangle = -i\epsilon_{\mu\nu\alpha\beta}\varepsilon^{*\nu}p^\alpha k^\beta F_1(q^2) \tag{3.6}$$

with $F_1(0) = 2F_2(0)$.

As the physical states $K_1(1270)$ and $K_1(1400)$ are mixed states of the K_{1A} and K_{1B} with mixing angle θ_K defined in Eqs. (3.1a-3.1b), the $B \to K_1$ form factors can be parameterized as

$$\begin{pmatrix} \langle K_1(1270)|\bar{s}\gamma_\mu(1-\gamma_5)b|B\rangle \\ \langle K_1(1400)|\bar{s}\gamma_\mu(1-\gamma_5)b|B\rangle \end{pmatrix} = M \begin{pmatrix} \langle K_{1A}|\bar{s}\gamma_\mu(1-\gamma_5)b|B\rangle \\ \langle K_{1B}|\bar{s}\gamma_\mu(1-\gamma_5)b|B\rangle \end{pmatrix}, \tag{3.7}$$

$$\begin{pmatrix} \langle K_1(1270)|\bar{s}\sigma_{\mu\nu}q^\mu(1+\gamma_5)b|B\rangle \\ \langle K_1(1400)|\bar{s}\sigma_{\mu\nu}q^\mu(1+\gamma_5)b|B\rangle \end{pmatrix} = M \begin{pmatrix} \langle K_{1A}|\bar{s}\sigma_{\mu\nu}q^\mu(1+\gamma_5)b|B\rangle \\ \langle K_{1B}|\bar{s}\sigma_{\mu\nu}q^\mu(1+\gamma_5)b|B\rangle \end{pmatrix}, \tag{3.8}$$

where the mixing matrix M is

$$M = \begin{pmatrix} \sin\theta_K & \cos\theta_K \\ \cos\theta_K & -\sin\theta_K \end{pmatrix}. \tag{3.9}$$

So the form factors A^{K_1}, $V_{0,1,2}^{K_1}$ and $F_{0,1,2}^{K_1}$ satisfy the following relation

$$\begin{pmatrix} \frac{A^{K_1(1270)}}{m_B+m_{K_1(1270)}} \\ \frac{A^{K_1(1400)}}{m_B+m_{K_1(1400)}} \end{pmatrix} = M \begin{pmatrix} \frac{A^{K_{1A}}}{m_B+m_{K_{1A}}} \\ \frac{A^{K_{1B}}}{m_B+m_{K_{1B}}} \end{pmatrix}, \tag{3.10}$$

$$\begin{pmatrix} (m_B+m_{K_1(1270)})V_1^{K_1(1270)} \\ (m_B+m_{K_1(1400)})V_1^{K_1(1400)} \end{pmatrix} = M \begin{pmatrix} (m_B+m_{K_{1A}})V_1^{K_{1A}} \\ (m_B+m_{K_{1B}})V_1^{K_{1B}} \end{pmatrix}, \tag{3.11}$$

$$\begin{pmatrix} \frac{V_2^{K_1(1270)}}{m_B+m_{K_1(1270)}} \\ \frac{V_2^{K_1(1400)}}{m_B+m_{K_1(1400)}} \end{pmatrix} = M \begin{pmatrix} \frac{V_2^{K_{1A}}}{m_B+m_{K_{1A}}} \\ \frac{V_2^{K_{1B}}}{m_B+m_{K_{1B}}} \end{pmatrix}, \tag{3.12}$$

$$\begin{pmatrix} m_{K_1(1270)}V_0^{K_1(1270)} \\ m_{K_1(1400)}V_0^{K_1(1400)} \end{pmatrix} = M \begin{pmatrix} m_{K_{1A}}V_0^{K_{1A}} \\ m_{K_{1B}}V_0^{K_{1B}} \end{pmatrix}, \tag{3.13}$$

$$\begin{pmatrix} F_1^{K_1(1270)} \\ F_1^{K_1(1400)} \end{pmatrix} = M \begin{pmatrix} F_1^{K_{1A}} \\ F_1^{K_{1B}} \end{pmatrix}, \tag{3.14}$$

$$\begin{pmatrix} (m_B^2-m_{K_1(1270)}^2)F_2^{K_1(1270)} \\ (m_B^2+m_{K_1(1400)}^2)F_2^{K_1(1400)} \end{pmatrix} = M \begin{pmatrix} (m_B^2+m_{K_{1A}}^2)F_2^{K_{1A}} \\ (m_B^2+m_{K_{1B}}^2)F_2^{K_{1B}} \end{pmatrix}, \tag{3.15}$$

$$\begin{pmatrix} F_3^{K_1(1270)} \\ F_3^{K_1(1400)} \end{pmatrix} = M \begin{pmatrix} F_3^{K_{1A}} \\ F_3^{K_{1B}} \end{pmatrix}, \tag{3.16}$$

For the numerical analysis we have used the light-cone QCD sum rules for the form factors [78], summarized in Table 3.1, where the momentum dependence dipole parametrization is:

$$\mathcal{T}_i^X(q^2) = \frac{\mathcal{T}_i^X(0)}{1-a_i^X\,(q^2/m_B^2)+b_i^X\,(q^2/m_B^2)^2}. \tag{3.17}$$

where $\mathcal{T}$ is A, V or F form factors and the subscript i can take a value 0, 1, 2 or 3 the superscript X belongs to K_{1A} or K_{1B} state.

$\mathcal{T}_i^X(q^2)$	$\mathcal{T}(0)$	a	b	$\mathcal{T}_i^X(q^2)$	$\mathcal{T}(0)$	a	b
$V_1^{K_{1A}}$	0.34	0.635	0.211	$V_1^{K_{1B}}$	-0.29	0.729	0.074
$V_2^{K_{1A}}$	0.41	1.51	1.18	$V_1^{K_{1B}}$	-0.17	0.919	0.855
$V_0^{K_{1A}}$	0.22	2.40	1.78	$V_0^{K_{1B}}$	-0.45	1.34	0.690
$A^{K_{1A}}$	0.45	1.60	0.974	$A^{K_{1B}}$	-0.37	1.72	0.912
$F_1^{K_{1A}}$	0.31	2.01	1.50	$F_1^{K_{1B}}$	-0.25	1.59	0.790
$F_2^{K_{1A}}$	0.31	0.629	0.387	$F_2^{K_{1B}}$	-0.25	0.378	-0.755
$F_3^{K_{1A}}$	0.28	1.36	0.720	$F_3^{K_{1B}}$	-0.11	1.61	10.2

Table 3.1: $B \to K_{1A,1B}$ form factors [78], where a and b are the parameters of the form factors in dipole parametrization.

3.3 Physical Observables

In this section, we calculate some interesting observables like the branching ratio ($\mathcal{BR}$), forward-backward asymmetry ($\mathcal{A}_{FB}$) as well as the helicity fractions of the final state K_1 meson and their sensitivity for the NP due to fourth generation SM,. From Eq. (2.17), one can get the decay amplitudes for $B \to K_1(1270)\ell^+\ell^-$ and $B \to K_1(1400)\ell^+\ell^-$ as

$$\mathcal{M}(B \to K_1\ell^+\ell^-) = -\frac{G_F\alpha}{2\sqrt{2}\pi}V_{tb}V_{ts}^*\left[T_V^\mu\bar{\ell}\gamma_\mu\ell + T_A^\mu\bar{\ell}\gamma_\mu\gamma_5\ell\right] \tag{3.18}$$

where the matrix elements T_A^μ and T_V^μ can be written in terms of auxiliary functions, as

$$T_A^\mu = C_{10}^{tot}\left\langle K_1(k,\epsilon)\left|\bar{s}\gamma^\mu\left(1-\gamma^5\right)b\right|B(p)\right\rangle = \Big\{f_4\epsilon^{\mu\nu\rho\sigma}\varepsilon_\mu^* p_\rho k_\sigma + if_5\varepsilon^{*\mu} - if_6(q\cdot\varepsilon)(p^\mu+k^\mu) + if_0(q\cdot\varepsilon)q^\mu\Big\} \tag{3.19}$$

$$T_V^\mu = C_9^{tot}\left\langle K_1(k,\epsilon)\left|\bar{s}\gamma^\mu\left(1-\gamma^5\right)b\right|B(p)\right\rangle - C_7^{tot}\frac{2im_b}{q^2}\langle K_1(k,\epsilon)\left|\bar{s}\sigma^{\mu\nu}\left(1+\gamma^5\right)q_\nu b\right|B(p)\rangle = f_1\epsilon^{\mu\nu\rho\sigma}\varepsilon_\nu^* p_\rho k_\sigma - if_2\varepsilon^{*\mu} - f_3(q\cdot\varepsilon)(p^\mu+k^\mu) \tag{3.20}$$

The auxiliary functions appearing in Eqs. (3.20) and (3.19) are defined as:

$$f_1 = 4(m_b+m_s)\frac{C_7^{eff}}{q^2}\left\{F_1^{K_{1A}}\sin\theta_K + F_1^{K_{1B}}\cos\theta_K\right\} + 2C_9^{eff}\left\{\frac{A_1^{K_{1A}}\sin\theta_K}{m_B+m_{K_{1A}}} + \frac{A_1^{K_{1B}}\cos\theta_K}{m_B+m_{K_{1B}}}\right\} \tag{3.21}$$

$$f_2 = 2(m_b+m_s)\frac{C_7^{eff}}{q^2}\left\{(m_B^2-m_{K_{1A}}^2)F_2^{K_{1A}}\sin\theta_K + (m_B^2-m_{K_{1B}}^2)F_2^{K_{1B}}\cos\theta_K\right\} + C_9^{eff}\left\{(m_B+m_{K_{1A}})V_1^{K_{1A}}\sin\theta_K + (m_B+m_{K_{1B}})V_1^{K_{1B}}\cos\theta_K\right\} \tag{3.22}$$

$$f_3 = 2(m_b+m_s)\frac{C_7^{eff}}{q^2}\left\{\left(F_2^{K_{1A}} + \frac{q^2F_3^{K_{1A}}}{m_B^2-m_{K_{1A}}^2}\right)\sin\theta_K + \left(F_2^{K_{1B}} + \frac{q^2F_3^{K_{1B}}}{m_B^2-m_{K_{1B}}^2}\right)\cos\theta_K\right\} + C_9^{eff}\left(\frac{V_2^{K_{1A}}\sin\theta_K}{m_B+m_{K_{1A}}} + \frac{V_2^{K_{1B}}\cos\theta_K}{m_B+m_{K_{1B}}}\right) \tag{3.23}$$

$$f_4 = 2C_{10}^{eff}\left(\frac{A^{K_{1A}}\sin\theta_K}{m_B+m_{K_{1A}}} + \frac{A^{K_{1B}}\cos\theta_K}{m_B+m_{K_{1B}}}\right) \tag{3.24}$$

$$f_5 = C_{10}^{eff}\left\{(m_B+m_{K_{1A}})V_1^{K_{1A}}\sin\theta_K + (m_B+m_{K_{1B}})V_1^{K_{1B}}\cos\theta_K\right\} \quad (3.25)$$

$$f_6 = C_{10}^{eff}\left(\frac{V_2^{K_{1A}}\sin\theta_K}{m_B+m_{K_{1A}}} + \frac{V_2^{K_{1B}}\cos\theta_K}{m_B+m_{K_{1B}}}\right) \quad (3.26)$$

$$f_0 = 2\frac{C_{10}^{eff}}{q^2}\left\{m_{K_{1A}}\left(V_3^{K_{1A}} - V_0^{K_{1A}}\right)\sin\theta_K + m_{K_{1B}}\left(V_3^{K_{1B}} - V_0^{K_{1B}}\right)\cos\theta_K\right\} \quad (3.27)$$

3.3.1 Branching ratio

The double differential decay rate for $B \to K_1\ell^+\ell^-$ can be written as [50, 78]

$$\frac{d\Gamma}{dq^2 d\cos\theta} = \frac{G_F^2\alpha^2}{2^{11}\pi^5 m_B^3}\left|V_{tb}V_{ts}^*\right|^2 u(q^2)\times\left|\mathcal{M}\right|^2 \quad (3.28)$$

with

$$\left|\mathcal{M}\right|^2 = \mathcal{A}(q^2)\cos^2\theta + \mathcal{B}(q^2)\cos\theta + \mathcal{C}(q^2) \quad (3.29)$$

and

$$u(q^2) \equiv \sqrt{\lambda\left(1-\frac{4m_\ell^2}{q^2}\right)}, \quad (3.30)$$

where

$$\begin{aligned}\lambda &\equiv \lambda\left(m_B^2, m_{K_1}^2, q^2\right)\\ &= m_B^4 + m_{K_1}^4 + q^4 - 2m_{K_1}^2m_B^2 - 2q^2m_B^2 - 2q^2m_{K_1}^2.\end{aligned} \quad (3.31)$$

By performing the integration on $\cos\theta$ in Eq. (3.28), one gets the differential decay rate so

$$\frac{d\Gamma}{dq^2} = \frac{G_F^2\alpha^2}{2^{11}\pi^5 m_B^3}\left|V_{tb}V_{ts}^*\right|^2\frac{1}{3}[2\mathcal{A}(q^2)+6\mathcal{B}(q^2)] \quad (3.32)$$

where

$$\begin{aligned}\mathcal{A}(q^2) &= \frac{1}{2}\lambda(q^2-4m_\ell^2)\left[|f_1|^2+|f_4|^2\right] - \frac{1}{m_{K_1}^2q^2}\left[|f_2|^2+|f_5|^2\right] - \frac{\lambda}{m_{K_1}^2q^2}\left[|f_3|^2+|f_6|^2\right]\\ &+ \frac{2\left(m_B^2-m_{K_1}^2-q^2\right)}{m_{K_1}^2q^2}\left\{\lambda\Re\left[f_2f_3^*\right]+\Re\left[f_5f_6^*\right]\right\} \quad (3.33)\\ \mathcal{B}(q^2) &= 4\Re\left[f_1f_5^*+f_2f_4^*\right]\sqrt{q^2(q^2-4m_\ell^2)\lambda} \quad (3.34)\\ \mathcal{C}(q^2) &= \frac{1}{2}(q^2-4m_\ell^2)\lambda\left[|f_1|^2+|f_4|^2+8|f_5|^2\right] + 4|f_2|^2(2m_\ell^2+q^2) + \frac{\lambda}{m_{K_1}^2q^2}\left[|f_2+|f_5|^2+\lambda(|f_3|^2+|f_6|^2)\right]\\ &- 2\Re(f_2f_3^*) + |f_0|^2 4m_\ell^2q^2 + 2\Re(f_5f_6^*)\left[m_B^2 - M_{K_1}^2 - (4m_\ell^2-q^2)\right]\\ &- 8m^2\Re(f_5f_6^*) - \Re(f_0f_6^*(m_B^2+m_{K_1}^2)) + \frac{1}{m_{K_1}^2}\left[|f_6|^2 2m_\ell^2(2(m_B^2+m_{K_1}^2-q^2))\right] \quad (3.35)\end{aligned}$$

The kinematical variables used in the above equations are defined as $u = (p - p_{l^-})^2 - (p - p_{l^+})^2$, $u = -u(q^2)\cos\theta$. Here λ is defined in Eq. (3.31) and θ is the angle between the moving direction of ℓ^+ and B meson in the centre of mass frame of the $\ell^+\ell^-$ pair.

3.3.2 Forward-backward asymmetry

In this section we investigate the forward-backward asymmetry ($\mathcal{A}_{FB}$) of leptons. The measurement of the $\mathcal{A}_{FB}$ is significant due to the minimal dependence upon the form factors [80], hence this observable has great importance to check the more clear signals of any NP than the other observables such as branching ratio etc. The differential $\mathcal{A}_{FB}$ of the final state lepton for the said decays can be written as

$$\frac{d\mathcal{A}_{FB}(q^2)}{dq^2} = \frac{\int_0^1 \frac{d^2\Gamma}{dq^2 d\cos\theta} d\cos\theta - \int_{-1}^0 \frac{d^2\Gamma}{dq^2 d\cos\theta} d\cos\theta}{\int_{-1}^1 \frac{d^2\Gamma}{dq^2 d\cos\theta} d\cos\theta} \tag{3.36}$$

The differential $\mathcal{A}_{FB}$ for $B \to K_1\ell^+\ell^-$ decays can be obtained from Eq. (3.28), as

$$\begin{aligned} \frac{d\mathcal{A}_{FB}(q^2)}{dq^2} &= -\frac{G_F^2\alpha^2}{2^{11}\pi^5 m_B^3} |V_{tb}V_{ts}^*|^2 \, u\left(q^2\right) \\ &\quad \times \frac{3\mathcal{B}(q^2)}{2\mathcal{A}(q^2) + 6\mathcal{C}(q^2)} \end{aligned} \tag{3.37}$$

where $\mathcal{A}(q^2)$, $\mathcal{B}(q^2)$ and $\mathcal{C}(q^2)$ are defined in Eqs. (3.33, 3.34, 3.35).

3.3.3 Helicity Fractions of K_1 meson

We now discuss helicity fractions of $K_1(1270, 1400)$ meson in $B \to K_1\ell^+\ell^-$ which are interesting observables and are insensitive to the uncertainties arising due to form factors and other input parameters. Thus the helicity fractions can be a good tool to test the NP beyond the SM. The final state meson helicity fractions were already discussed in the literature for $B \to K^*\,(K_1)\,\ell^+\ell^-$ decays [50].

The explicit expression of the longitudinal (f_L) and the transverse(f_T) helicity fractions for $B \to K_1\ell^+\ell^-$ decay can be obtained by trading $|\mathcal{M}|$ to $|\mathcal{M}_L|$ and $|\mathcal{M}_\pm|$, respectively, in Eq. (3.28). Here

$$|\mathcal{M}_L|^2 = \mathcal{D}_L \cos^2\theta + \mathcal{E}_L \tag{3.38}$$

$$|\mathcal{M}_\pm|^2 = \mathcal{D}_\pm \cos^2\theta + \mathcal{E}_\pm \tag{3.39}$$

By performing the integration on $\cos\theta$ in Eq. (3.28), we get

$$\frac{d\Gamma_L}{dq^2} = \frac{G_F^2\alpha^2}{2^{11}\pi^5} \frac{|V_{tb}V_{ts}^*|^2}{m_B^3} u(q^2) \frac{2}{3} \left[\mathcal{D}_L(q^2) + 3\mathcal{E}_L(q^2)\right] \tag{3.40}$$

$$\frac{d\Gamma_\pm}{dq^2} = \frac{G_F^2\alpha^2}{2^{11}\pi^5} \frac{|V_{tb}V_{ts}^*|^2}{m_B^3} u(q^2) \frac{2}{3} [\mathcal{D}_\pm(q^2) + 3\mathcal{E}_\pm(q^2)] \tag{3.41}$$

where $\mathcal{D}_L(q^2)$, $\mathcal{D}_\pm(q^2)$, $\mathcal{E}_L(q^2)$ and $\mathcal{E}_\pm(q^2)$ can be parameterized in terms of the auxiliary functions [c.f. Eqs. $(3.21-3.27)$] as

$$\begin{aligned}\mathcal{D}_L(q^2) &= \frac{1}{2m_{K_1}^2}\Big\{|f_5|^2\left[\left(m_B^2-m_{K_1}^2-q^2\right)^2-16m^2m_{K_1}^2\right]+|f_2|^2\left(2m_{K_1}^2q^2+\lambda\right)\\ &+\lambda^2|f_3|^2-8m^2\lambda|f_5|^2+4m^2q^2\lambda|f_0|^2-2\Re(f_5f_6^*)\left(m_B^2-m_{K_1}^2-q^2\right)\lambda\\ &-4\lambda\Re(f2f_3^*)\left(m_B^2-m_{K_1}^2-q^2\right)+\lambda|f_6|^2\left[8\left(m_B^2+m_{K_1}^2-4q^2\right)m^2+\lambda\right]\Big\} \qquad (3.42)\\ \mathcal{D}_+(q^2) &= \frac{1}{4}\Big\{\left(q^2+4m^2\right)\left[\lambda|f_4|^2+4|f_5|^2+4\sqrt{\lambda}\left(\Im(f_1^*f_2)+\Im(f_4^*f_5)\right)\right]\\ &+(q^2-4m^2)\left(\lambda|f_1|^2+4|f_2|^2\right)\Big\} \qquad (3.43)\\ \mathcal{D}_-(q^2) &= \frac{1}{4}\Big\{\left(q^2+4m^2\right)\left[\lambda|f_1|^2+|f_2|^2\right]+(q^2-4m^2)\left[\lambda|f_4|^2+4\sqrt{\lambda}\left(\Im(f_1f_2^*)+\Im(f_4f_5^*)\right)\right]\Big\} \qquad (3.44)\\ \mathcal{E}_L(q^2) &= \frac{1}{2m_{K_1}^2}\Big\{\left(4m^2-q^2\right)\Big[|f_5|^2\left(m_B^4-(m_{K_1}^2+q^2)m_B^2\right)+|f_2|^2\left(m_B^2-m_{K_1}^2-q^2\right)^2\\ &+2\lambda^2\left(|f_3|^2+|f_6|^2\right)-4\lambda\left(m_B^2-m_{K_1}^2-q^2\right)\Re(f_2f_3^*)\Big]+q^2\lambda\Re(f_5f_6^*)\left[\left(m_B^2-m_{K_1}^2\right)+4m^2-q^2\right]\\ &-4m^2\lambda\Im(f5f_6^*)\left(m_B^2-m_{K_1}^2\right)+\left(m_{K_1}^2+q^2\right)|f_5|^2\left[q^2\left(4m^2-m_{K_1}^2-q^2\right)+4m^2\left(m_{K_1}^2+q^2\right)\right]\Big\} \qquad (3.45)\\ \mathcal{E}_+(q^2) &= \frac{1}{4}\left(q^2-4m^2\right)\Big\{\lambda\left(|f_1|^2+|f_4|^2\right)+\left(|f_2|^2+|f_5|^2\right)+4\sqrt{\lambda}\left(\Im(f_1^*f_2)+\Im(f_4^*f_5)\right)\Big\} \qquad (3.46)\\ \mathcal{E}_-(q^2) &= \frac{1}{4}\left(q^2-4m^2\right)\Big\{\lambda\left(|f_1|^2+|f_4|^2\right)+\left(|f_2|^2+|f_5|^2\right)+4\sqrt{\lambda}\left(\Im(f_1f_2^*)+\Im(f_4f_5^*)\right)\Big\} \qquad (3.47)\end{aligned}$$

Finally the longitudinal and transverse helicity fractions become

$$\begin{aligned}f_L(q^2) &= \frac{d\Gamma_L(q^2)/dq^2}{d\Gamma(q^2)/dq^2} \qquad (3.48)\\ f_\pm(q^2) &= \frac{d\Gamma_\pm(q^2)/dq^2}{d\Gamma(q^2)/dq^2} \qquad (3.49)\\ f_T(q^2) &= f_+(q^2)+f_-(q^2) \qquad (3.50)\end{aligned}$$

so that the sum of the longitudinal and transverse helicity amplitudes is equal to one i.e. $f_L(q^2)+f_T(q^2)=1$ for each value of q^2 [50].

3.4 Numerical Results and Discussion

In this section we shall calculate the physical observables like the branching ratio ($\mathcal{BR}$), the forward-backward asymmetry ($\mathcal{A}_{FB}$) and helicity fractions ($f_{L,T}$) of $K_1(1270,1400)$ meson for the $B\to K_1(1270,1400)\ell^+\ell^-$ decays with $\ell=\mu,\tau$, as well as see their sensitivities to the SM4 effects. As $K_1(1270)$ and $K_1(1400)$ are mixed states of $|K_{1A}\rangle$ and $|K_{1B}\rangle$ with mixing angle θ_K defined in Eq.(3.1b),many attempts had been made in literature to constrain the value of θ_K. Recently from the studies of $B\to K_1(1270)\gamma$ and

$\tau \to K_1(1270)\nu_\tau$, the values of θ_K was obtained to be $\theta_K = (-34 \pm 13)^\circ$ [78]. Here we have taken the central values of all the input parameters, the numerical values of which used in our numerical calculations are given below

$m_B = 5.28$ GeV, $m_b = 4.28$ GeV, $m_\mu = 0.105$ GeV,
$m_\tau = 1.77$ GeV, $f_B = 0.25$ GeV, $|V_{tb}V_{ts}^*| = 45 \times 10^{-3}$,
$\alpha^{-1} = 137$, $G_F = 1.17 \times 10^{-5}$ GeV^{-2},
$\tau_B = 1.54 \times 10^{-12}$ sec, $m_{K_1(1270)} = 1.270$ GeV,
$m_{K_1(1400)} = 1.403$ GeV, $m_{K_{1A}} = 1.31$ GeV,
$m_{K_{1B}} = 1.34$ GeV , $\theta_K = -34^\circ$, $\phi_{sb} = 90^\circ$.

First we discuss the ($\mathcal{BR}s$) of $B \to K_1(1270)\mu^+\mu^-(\tau^+\tau^-)$ decays which we have plotted as a function of q^2 (GeV^2), shown in figs 3.1 and 3.2, both in SM and in the fourth generation scenario. Fig 3.1 and 3.2 shows the $\mathcal{BR}s$ of $B \to K_1(1270)$ with $\mu^+\mu^-$ and $\tau^+\tau^-$ respectively and figs (3.3,3.4) represents the same for $B \to K_1(1400)$. These figures show that the values of the $\mathcal{BR}$ strongly depend on the fourth generation effects which come mainly through the Wilson coefficients with $m_{t'}$ instead of m_t as well as from $V_{t'b}V_{t's}$ which are encapsulated in Eq.(2.25). One can see clearly from these curves that an increment in the values of fourth generation parameters increase the value of the branching ratio accordingly, i.e. the $\mathcal{BR}$ is an increasing function of both $m_{t'}$ and $V_{t'b}V_{t's}$.

As an exclusive decay, the new physics effects in the branching ratios are usually masked by the uncertainties involved in different input parameters where the form factors are major contributors. However,for the present case the new physics effects are well prominent and lie well separated from the SM values error bounds. Furthermore the constructive characteristic of the fourth generation effects to the $\mathcal{BR}$, manifests throughout the whole q^2 region, particularly for the case of decays $B \to K_1(1270)\ell^+\ell^-$ with $\ell = \mu, \tau$. However for the decays $B \to K_1(1400)\ell^+\ell^-$ with $\ell = \mu, \tau$ the SM4 effects are mitigated by the uncertainties in the form factors. Additionally, one can also extract the constructive characteristic of the fourth generation effects to the $\mathcal{BR}$ from Table 3.2. Also, the quantitative analysis of the $\mathcal{BR}$ shows that the NP effects due to the fourth generation are comparatively more sensitive to the case of $B \to K_1(1270)\ell^+\ell^-$ than the case of $B \to K_1(1400)\ell^+\ell^-$.

It is also important to emphasis here that the experimental and the statistical errors should be less than the predictions of NP, otherwise these uncertainties precludes the NP. Similarly, the NP comes through the different models are close to each other. Therefore it is hard to distinguish the results of various NP models, unless the precise experimental data are available. It is expected that in the current collider, the number of events will be large and statistical error will be small to test the predictions of various physical observables considered in this thesis.

Moreover, Table 3.2 shows that the maximum deviation (when we set $m_{t'} = 600$ GeV, $V_{t'b}V_{t's} = 1.5 \times 10^{-3}$) from the SM value due to the fourth generation effects: for the case of $B \to K_1(1270)\mu^+\mu^-$

is approximately 6 times, for the case of $B \to K_1(1270)\tau^+\tau^-$ is about 3.3 times, for $B \to K_1(1400)\mu^+\mu^-$ is approximately 5.9 time and for $B \to K_1(1400)\tau^+\tau^-$ is about 2.9 times than that of SM values. Furthermore it is difficult to measure the decay $B \to K_1\tau^+\tau^-$ experimentally, but if the technical difficulties are overcome, then this decay channel can be used as a handy tool to investigate the NP.

	$\mathcal{BR}(B \to K_1(1270)\mu^+\mu^-)$, SM value: 1.97×10^{-6}		
$\lvert V_{t'b}V_{t's}\rvert$	$m_{t'} = 300$	$m_{t'} = 500$	$m_{t'} = 600$
3×10^{-3}	2.01×10^{-6}	2.18×10^{-6}	2.38×10^{-6}
1.5×10^{-2}	3.04×10^{-6}	7.43×10^{-6}	1.22×10^{-5}
	$\mathcal{BR}(B \to K_1(1400)\mu^+\mu^-)$, SM value: 5.76×10^{-8}		
$\lvert V_{t'b}V_{t's}\rvert$	$m_{t'} = 300$	$m_{t'} = 500$	$m_{t'} = 600$
3×10^{-3}	5.88×10^{-8}	6.36×10^{-8}	6.90×10^{-8}
1.5×10^{-2}	8.78×10^{-8}	2.09×10^{-7}	3.44×10^{-7}
	$\mathcal{BR}(B \to K_1(1270)\tau^+\tau^-)$, SM value: 6.06×10^{-8}		
$\lvert V_{t'b}V_{t's}\rvert$	$m_{t'} = 300$	$m_{t'} = 500$	$m_{t'} = 600$
3×10^{-3}	6.14×10^{-8}	6.38×10^{-8}	6.62×10^{-8}
1.5×10^{-2}	8.12×10^{-8}	1.39×10^{-7}	2.01×10^{-7}
	$\mathcal{BR}(B \to K_1(1400)\tau^+\tau^-)$, SM value: 9.39×10^{-10}		
$\lvert V_{t'b}V_{t's}\rvert$	$m_{t'} = 300$	$m_{t'} = 500$	$m_{t'} = 600$
3×10^{-3}	9.51×10^{-10}	9.80×10^{-10}	1.01×10^{-9}
1.5×10^{-2}	1.24×10^{-9}	1.98×10^{-9}	2.74×10^{-9}

Table 3.2: The values of branching ratio of $B \to K_1(1270, 1400)\ell^+\ell^-$ with $\ell = \mu,\ \tau$ for different values of $m_{t'}$ and $|V^*_{t'b}V_{t's}|$.

	$\mathcal{R}_\mu = \frac{\mathcal{BR}(B\to K_1(1400)\mu^+\mu^-)}{\mathcal{BR}(B\to K_1(1270)\mu^+\mu^-)}$, SM value: 2.92×10^{-2}		
$\lvert V_{t'b}V_{t's}\rvert$	$m_{t'} = 300$	$m_{t'} = 500$	$m_{t'} = 600$
3×10^{-3}	2.92×10^{-2}	2.91×10^{-2}	2.90×10^{-2}
1.5×10^{-2}	2.88×10^{-2}	2.81×10^{-2}	2.81×10^{-2}
	$\mathcal{R}_\tau = \frac{\mathcal{BR}(B\to K_1(1400)\tau^+\tau^-)}{\mathcal{BR}(B\to K_1(1270)\tau^+\tau^-)}$, SM value: 1.54×10^{-2}		
$\lvert V_{t'b}V_{t's}\rvert$	$m_{t'} = 300$	$m_{t'} = 500$	$m_{t'} = 600$
3×10^{-3}	1.54×10^{-2}	1.53×10^{-2}	1.52×10^{-2}
1.5×10^{-2}	1.52×10^{-2}	1.42×10^{-2}	1.36×10^{-2}

Table 3.3: The values of branching fractions $\mathcal{R}_\ell$, with $\ell = \mu, \tau$, for different values of $m_{t'}$ and $|V^*_{t'b}V_{t's}|$.

It is also important to emphasis here that the change in branching ratios due to the uncertainty of the mixing angle θ_K are small for the decays $B \to K_1(1270)\ell^+\ell^-$ and is shown in figs. 3.5 and 3.6. However for the decays $B_1(1400)\ell^+\ell^-$ the change due to the uncertainty in the mixing angle θ_K is large and the NP effects are hidden in it particularly when tauons are the final leptons [79]. Therefore, any dramatically increment in the measurement of the branching ratio for the decay $B \to K_1(1270)\ell^+\ell^-$ at the current experiment will be a clear indication of NP effects. So the precise measurement of branching ratio is very handy tool to extract the information about the fourth generation parameters.

To observe sensitivity on the fourth generation parameters, it is instructive to study the ratios of $\mathcal{BR}$ $\mathcal{R}_\ell = \mathcal{BR}(B \to K_1(1400)\ell^+\ell^-)/\mathcal{BR}(B \to K_1(1270)\ell^+\ell^-)$, with $\ell = \mu,\ \tau$, as a function of q^2 shown in Figs. 3.7 and 3.8. While $\mathcal{R}_\mu$, $\mathcal{R}_\tau$ are sensitive to θ_K as was shown in ref.[78] the present study shows that they are insensitive to the NP due to SM4. Therefore the ratios of branching ratio is a good observable

(**a**) (**b**)

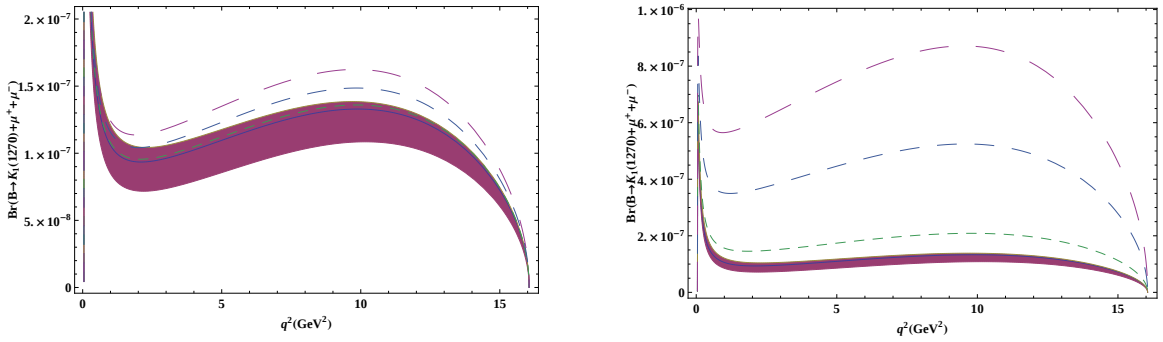

Figure 3.1: The dependence of branching ratio of $B \to K_1(1270)\mu^+\mu^-$ on q^2 for different values of $m_{t'}$ and $|V^*_{t'b}V_{t's}|$. In all the graphs, the band corresponds to the SM, small dashed , medium dashed, long dashed correspond, $m_{t'}$ = 300 GeV, 500 GeV and 600 GeV respectively. $|V^*_{t'b}V_{t's}|$ has the value 0.003 and 0.015 in (a) and (b) respectively.

to fix the value of θ_K. The numerical results of branching fractions corresponding to the values of $m_{t'}$ and $|V_{t'b}V_{t's}|$ are summarized in Table 3.3.

To illustrate the generic effects due to the fourth generation quarks on the forward-backward asymmetry $\mathcal{A}_{FB}$, we plot $\frac{d(\mathcal{A}_{FB})}{dq^2}$ as a function of q^2 in Figs. 3.9-3.13. As it is shown in Ref. [78] the zero position of the $\mathcal{A}_{FB}$ depends weakly on the value of θ_K but can be changed due to the variation of the SM4. As it is clear from Figs.(3.9) and (3.10), the uncertainty in the zero position of $\mathcal{A}_{FB}$ due to hadronic uncertainties is negligible. Therefore, the zero position of the $\mathcal{A}_{FB}$ could also provide a stringent test for the NP effects. In the present study fig. 3.9 shows that for the case of muons as final state leptons, the increment in the $|V_{t'b}V_{t's}|$ and $m_{t'}$ values shift the zero position of the $\mathcal{A}_{FB}$ towards the low q^2 region, this behavior is compatible with $B \to K^*\mu^+\mu^-$ decay [82]. Moreover, the maximum values of $|V_{t'b}V_{t's}|$ and $m_{t'}$, shift the central value of SM (2.8 GeV^2) of zero position of the $\mathcal{A}_{FB}$ for the case of $B \to K_1(1270)\mu^+\mu^-$ to the value 2.1 GeV^2 (see Fig. 3.9-b). For the case of $B \to K_1(1400)\mu^+\mu^-$ (see Fig. 3.11) the zero position of the $\mathcal{A}_{FB}$ is shifted from its SM value (3.4 GeV^2) to the value 2.4 GeV^2. Besides the zero position of $\mathcal{A}_{FB}$, the magnitude of $\mathcal{A}_{FB}$ is also an important tool (particularly, when the tauons are the final state leptons where the zero of the $\mathcal{A}_{FB}$ is absent) to investigate the NP. A closer look on the pattern of Figs. 3.9-3.10 tells us that the fourth generation parameters decrease the magnitude of $\mathcal{A}_{FB}$ from its SM value. The analysis of $\mathcal{A}_{FB}$ also demonstrate that in contrast to the $\mathcal{BR}$, the magnitude of the $\mathcal{A}_{FB}$ is decreasing function of the fourth generation parameters. It is clear from these graphs that decreasing behavior of the magnitude of $\mathcal{A}_{FB}$ is irrespective of the final state particles. It is suitable to comment here that just like the zero position of the $\mathcal{A}_{FB}$, the magnitude of

(**a**) (**b**)

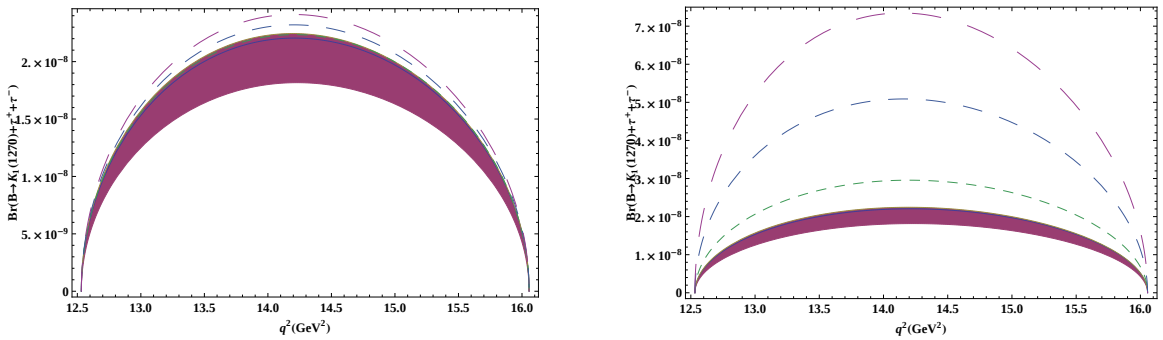

Figure 3.2: The dependence of branching ratio of $B \to K_1(1270)\tau^+\tau^-$ on q^2 for different values of $m_{t'}$ and $|V^*_{t'b}V_{t's}|$. The legends and the values of fourth generation parameters are same as in Fig. 3.1.

$\mathcal{A}_{FB}$ depends on the values of the Wilson coefficient C_7, C_9 and C_{10}. Thus the effects on the magnitude of $\mathcal{A}_{FB}$ are almost insensitive due to the uncertainties in the form factors. We have noticed that the uncertainty due to the mixing angle θ_K, magnitude of $\mathcal{A}_{FB}$ for the decay $B \to K_1(1270)\tau^+\tau^-$ is mildly effected and is shown in fig 3.13. On the other hand the change in the magnitude of $\mathcal{A}_{FB}$ due to the fourth generation are very prominent and easy to measure experimentally and are insensitive to mixing angle θ_K. In the last, precise measurement of the zero position and the magnitude of $\mathcal{A}_{FB}$ for the decay $B \to K_1(1270)\mu^+\mu^-$ are very good observables to yield any indirect imprints of NP including fourth generation.

We now discuss another interesting observable to get the complementary information about NP in $B \to K_1(1270, 1400)\ell^+\ell^-$ transitions i.e. the helicity fractions of $K_1(1270, 1400)$ produced in the final state. The measurement of longitudinal K^* helicity fractions (f_L) in the decay modes $B \to K^*\ell^+\ell^-$ by the BABAR collaboration [83] put enormous interest in this observable. Therefore it is important to study, the helicity fractions of final state meson, just like $\mathcal{BR}$ and $\mathcal{A}_{FB}$, are also very sensitive observables the NP [50]. Current and future B factories will accumulate more data on this observable which will be helpful not only to reduce the experimental errors but also get any possible hint of NP from this observable. In this regard, it is natural to study the helicity fractions for the FCNC processes like $B \to K_1(1270, 1400)\ell^+\ell^-$ in and beyond the SM. For this purpose, we have plotted the longitudinal (f_L) and transverse (f_T) helicity fractions of $K_1(1270, 1400)$ for SM and with different values of fourth generation parameters in Figs.(3.14-3.17). In these figures the values of the longitudinal (f_L) and transverse (f_T) helicity fractions of $K_1(1270, 1400)$ are plotted against q^2 and one can clearly see that at each value of q^2 the sum of f_L and f_T is equal to one.

Fig.3.14 shows that for the case of muons as final state leptons, the effects of the fourth generation

(**a**) (**b**)

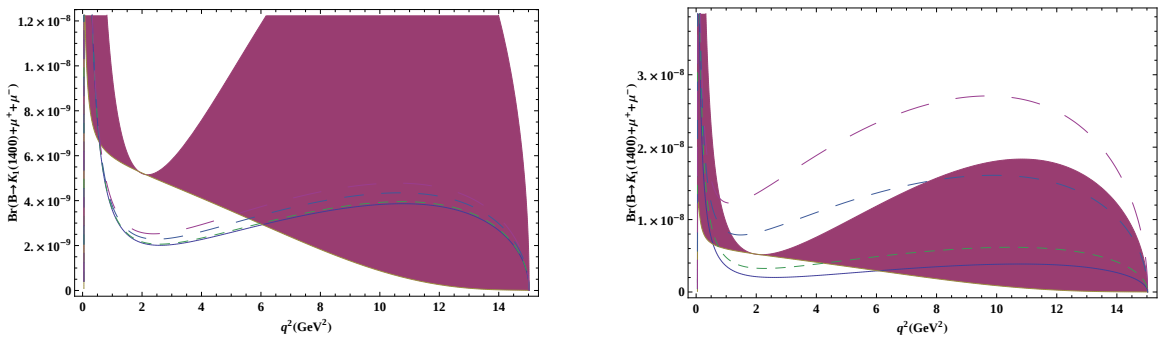

Figure 3.3: The dependence of branching ratio of $B \to K_1(1400)\mu^+\mu^-$ on q^2 for different values of $m_{t'}$ and $|V_{t'b}^* V_{t's}|$. The legends and the values of fourth generation parameters are same as in Fig. 3.1.

on the longitudinal (transverse) helicity fractions of $K_1(1270)$ are marked up in the $0 < q^2 \leq 12$ GeV^2 region. On the other hand, for $K_1(1400)$ the physical region is $0 < q^2 \leq 6$ GeV^2. However we didn't mention here the curves of helicity fractions for the decays $B \to K_1(1400)\ell^+\ell^-$ as like other observables the SM4 effects are mitigated by both the hadronic uncertainties and the uncertainties in the mixing angle θ_K. It is clear from the figure 3.15 that although the influence of the fourth generation parameters on the maximum (minimum) values of the $K_1(1270)$ helicity fractions are not very much effected (One can see from Fig. 3.14 that for the case of $B \to K_1(1270)\mu^+\mu^-$, the difference in the extremum values of helicity fractions , even at the maximum values of fourth generation parameters, is negligible to the SM value) but there is a reasonable shift in the position of these values which lies roughly at $q^2 \simeq 1.8$ GeV^2 for SM. Fig. 3.14 also show that how the position of the maximum (minimum) values of f_L (f_T) varies with the change in $m_{t'}$ and $|V_{t'b}V_{t's}|$ values. Furthermore, the position of these extremum values are shifted towards the low q^2 region and on setting the maximum values of the fourth generation parameters this shift in the position is approximately 0.9 GeV^2. Now we turn our attention to the case, where tauons are the final state leptons and for this case the helicity fractions of $K_1(1270)$ are plotted in Fig. 3.17. One can easily see that in contrast to the case of muons, there is no shift in the position of the extremum values of the helicity fractions, and are fixed at $q^2 = 12.5$ GeV^2. However, the change in the maximum (minimum) value of longitudinal (transverse) is more prominent as compared to the previous case where the muons are the final state leptons. These figures have also highlighted the variation in the extremum values of helicity fractions from the SM due to the change in the fourth generation parameters. The change in extremum values are very well marked up as compared to the uncertainties due to the mixing angle θ_K which is shown in figs.3.16 and 3.17, and uncertainties due to the hadronic matrix element. For $B \to K_1(1270)\tau^+\tau^-$, the maximum setting of the fourth generation

(a) (b)

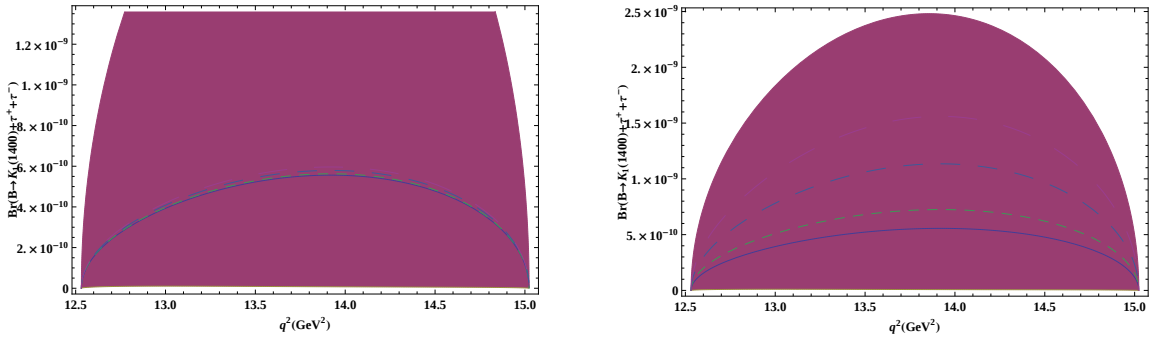

Figure 3.4: The dependence of branching ratio of $B \to K_1(1400)\tau^+\tau^-$ on q^2 for different values of $m_{t'}$ and $|V^*_{t'b}V_{t's}|$. The legends and the values of fourth generation parameters are same as in Fig. 3.1.

parameters the maximum (minimum) value of longitudinal (transverse) helicity fraction is changed from its SM value 0.51(0.49) to 0.72(0.28) which is suitable amount of change to measure.

The numerical analysis of helicity fractions shows that the measurement of the maximum (minimum) values of f_L and f_T and its position in the case of $B \to K_1(1270)\tau^+\tau^-$ and $B \to K_1(1270)\mu^+\mu^-$ respectively can be used as a good tool in studying the NP beyond the SM and the existence of the fourth generation quarks.

3.5 Conclusion

In our study on the rare $B \to K_1(1270, 1400)\ell^+\ell^-$ decays with $\ell = \mu$, τ, we have calculated branching ratio ($\mathcal{BR}$), the forward backward asymmetry $\mathcal{A}_{FB}$ and helicity fractions $f_{L,T}$ of the final state mesons and analyzed the implications of the fourth generation effects on these observable for the said decays.

We have found a strong dependency of the $\mathcal{BR}$ on the fourth generation parameters $V_{t'b}V_{t's}$ and $m_{t'}$ particularly for the decay $B \to K_1(1270)\ell^+\ell^-$. The study has shown that the $\mathcal{BR}$ is an increasing function of these parameters. At maximum values of these parameters, i.e. $|V_{t'b}V_{t's}| = 0.015$ and $m_{t'} = 600$ GeV, the values of $\mathcal{BR}$ increases approximately 6 to 7 times larger than that of SM values when the final leptons are muons and for the case of of tauns these values are enhanced 3 to 4 times to the SM value. Hence the accurate measurement of the $\mathcal{BR}s$ for these decays is an important tool to reveal some signals of physics beyond the three generations of SM.

Besides the $\mathcal{BR}$, our analysis shows that $\mathcal{A}_{FB}$ is a very good observable to test the existence of the fourth generation quarks, especially the zero position of the $\mathcal{A}_{FB}$. We have found that the value of the $\mathcal{A}_{FB}$ decreases with increasing values of $V_{t'b}V_{t's}$ and $m_{t'}$. Thus the decrement in the values of the $\mathcal{A}_{FB}$

(a) (b)

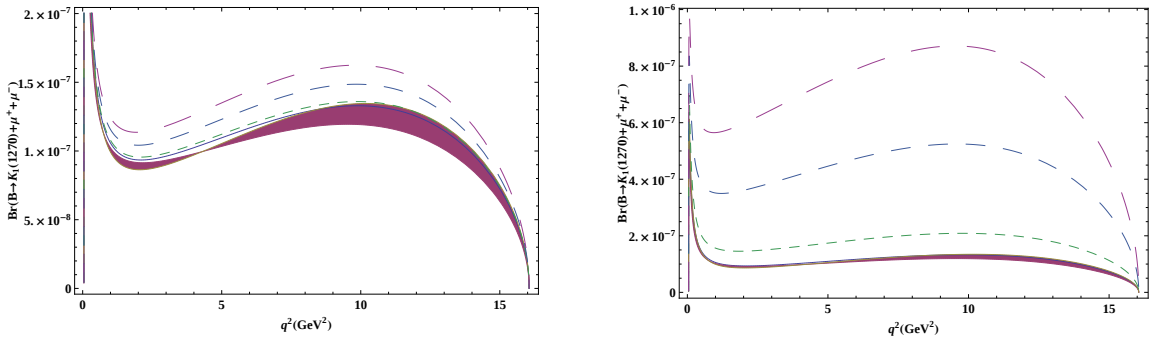

Figure 3.5: The dependence of branching ratio of $B \to K_1(1270)\mu^+\mu^-$ on q^2 for different values of $m_{t'}$ and $|V^*_{t'b}V_{t's}|$. The band represents the uncertainty in mixing angle $\theta_K = -34°, -47°, -21°$. The other legends are exactly the same as that of Fig.3.1.

from the SM values is important imprint of NP, and also the shift in the zero position of $\mathcal{A}_{FB}$ (which is towards low q^2 region) provides a prominent signature of the NP fourth generation quarks.

To further comprehend the fourth generation effects on these decays, we have calculated the helicity fractions $f_{L,T}$ of final state mesons. We have first calculated the helicity fractions of final state mesons in the SM and then analyzed their extension to the fourth generation scenario. The study has shown that the deviation from the SM values of the helicity fractions are quite large when we consider tauons as final state of leptons. It is also shown that there is a noticeable change due to fourth generation in the position of the extremum values of the longitudinal and transverse helicity fractions of $K_1(1270)$ meson for the case of muons as a final state leptons. Therefore, the helicity fraction of $K_1(1270)$ meson can be a stringent test in finding the status of the fourth generation quarks.

It is also important to mention here that because we do not know the exact form of the NP, therefore to determine the form of NP we need complimentary observables for process which are based on the $b \to s\ell^+\ell^-$ [84]. In this context the decay channel $B \to K_1\ell^+\ell^-$ is relevant to get the complimentary information about the parameters of fourth generation SM to that of the information obtained from other experiments such as the inclusive $B \to X_s\ell^+\ell^-$ and the exclusive $B \to M(K, K^*)\ell^+\ell^-$ decays. It is also worth mentioning here that the information obtained about the fourth generation parameters from the other experiments can be used to fix the mixing angle θ_K between the K_1 states in our process. Therefore, the fourth generation SM information obtained from the other experiments will not only compliment our results but can be useful to understand the mixing nature of $K_1(1270)$ and $K_1(1400)$ mesons.

To summarize, the more data to be available from Tevatron and LHCb will provide a powerful

(a) (b)

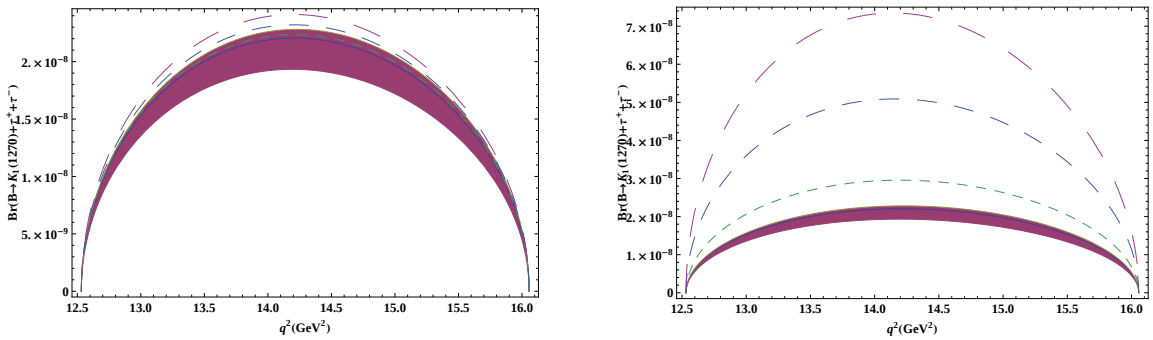

Figure 3.6: The dependence of branching ratio of $B \to K_1(1270)\mu^+\mu^-$ on q^2 for different values of $m_{t'}$ and $|V^*_{t'b}V_{t's}|$. The band represents the uncertainty in mixing angle $\theta_K = -34°, -47°, -21°$. The other legends are exactly the same as that of Fig.3.1.

(a) (b)

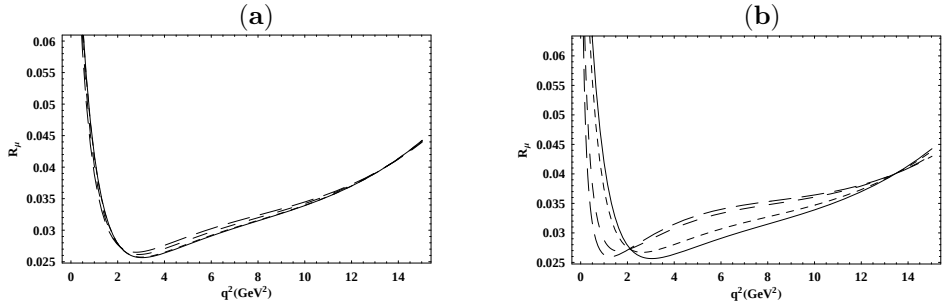

Figure 3.7: The dependence of branching fraction $\mathcal{R}_\mu = \mathcal{BR}(B \to K_1(1400)\mu^+\mu^-)/\mathcal{BR}(B \to K_1(1270)\mu^+\mu^-)$ on q^2 for different values of $m_{t'}$ and $|V^*_{t'b}V_{t's}|$. The legends and the values of fourth generation parameters are same as in Fig. 3.1.

testing ground for the SM and the possible existence of the fourth generation quarks and also put some constraints on the fourth generation parameters such as $V_{t'b}V_{t's}$ and $m_{t'}$. Our analysis of the fourth generation on the observables for $B \to K_1\ell^+\ell^-$ decays are useful for probing or refuting the existence of fourth family of quarks.

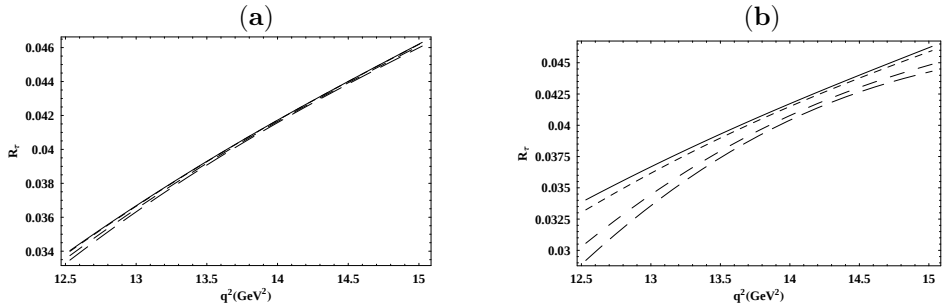

Figure 3.8: The dependence of branching fraction $\mathcal{R}_\tau = \mathcal{BR}(B \to K_1(1400)\tau^+\tau^-)/\mathcal{BR}(B \to K_1(1270)\tau^+\tau^-)$ on q^2 for different values of $m_{t'}$ and $|V^*_{t'b}V_{t's}|$. The legends and the values of fourth generation parameters are same as in Fig. 3.1.

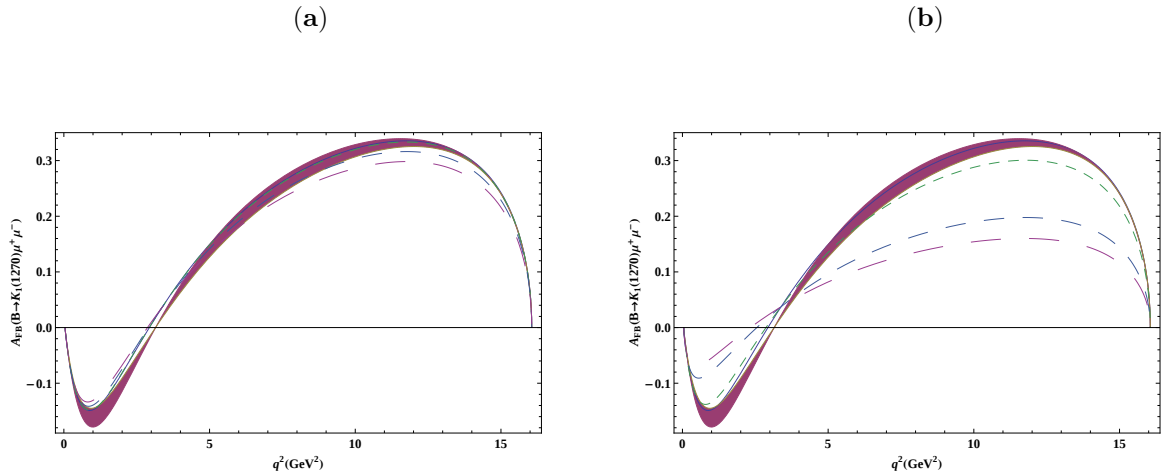

Figure 3.9: The dependence of forward backward asymmetry of $B \to K_1(1270)\mu^+\mu^-$ on q^2 for different values of $m_{t'}$ and $|V^*_{t'b}V_{t's}|$. The legends and the values of fourth generation parameters are same as in Fig. 3.1.

(**a**) (**b**)

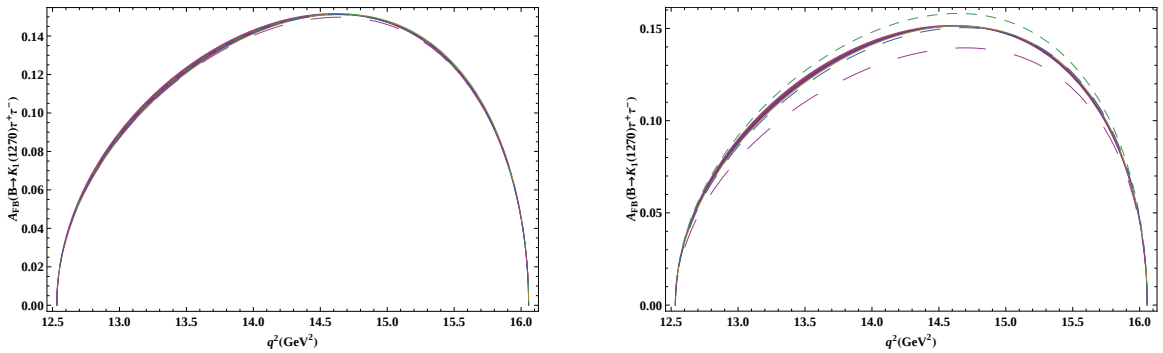

Figure 3.10: The dependence of forward backward asymmetry of $B \to K_1(1270)\tau^+\tau^-$ on q^2 for different values of $m_{t'}$ and $|V^*_{t'b}V_{t's}|$. The legends and the values of fourth generation parameters are same as in Fig. 3.1.

(**a**) (**b**)

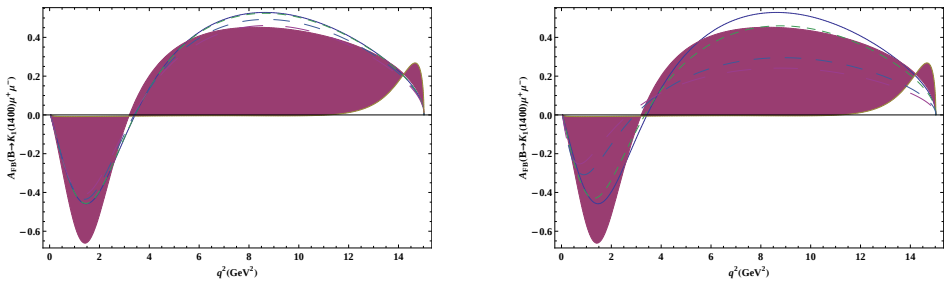

Figure 3.11: The dependence of forward backward asymmetry of $B \to K_1(1400)\mu^+\mu^-$ on q^2 for different values of $m_{t'}$ and $|V^*_{t'b}V_{t's}|$. The legends and the values of fourth generation parameters are same as in Fig. 3.1.

(**a**) (**b**)

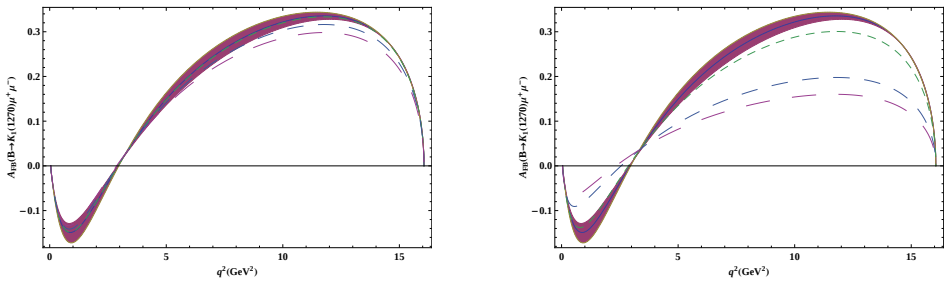

Figure 3.12: The dependence of forward backward asymmetry of $B \to K_1(1270)\mu^+\mu^-$ on q^2 for different values of $m_{t'}$ and $|V_{t'b}^* V_{t's}|$. The legends and the values of fourth generation parameters are same as in Fig. 3.5.

(**a**) (**b**)

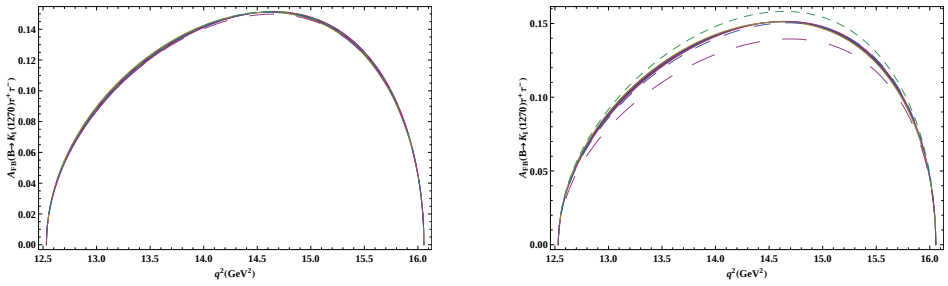

Figure 3.13: The dependence of forward backward asymmetry of $B \to K_1(1270)\tau^+\tau^-$ on q^2 for different values of $m_{t'}$ and $|V_{t'b}^* V_{t's}|$. The legends and the values of fourth generation parameters are same as in Fig. 3.5.

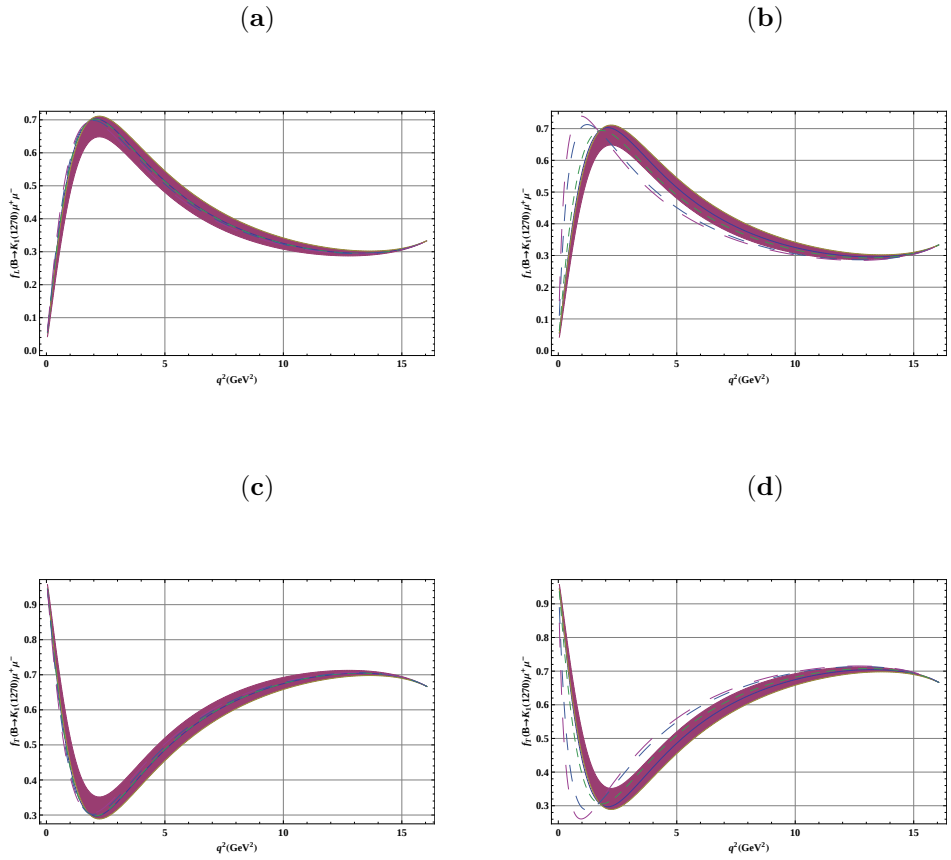

Figure 3.14: The dependence the probabilities of the longitudinal ($a,\ b$) and transverse ($c,\ d$) helicity fractions, $f_{L,T}$, of K_1 in $B \to K_1(1270)\mu^+\mu^-$ decays on q^2 for different values of $m_{t'}$ and $|V^*_{t'b}V_{t's}|$. In all the graphs, the solid line corresponds to the SM, small dashed , medium dashed, long dashed correspond, $m_{t'} = 300$ GeV, 500 GeV and 600 GeV respectively. $|V^*_{t'b}V_{t's}|$ has the value 0.003 and 0.015 in (a, c) and (b, d) respectively.

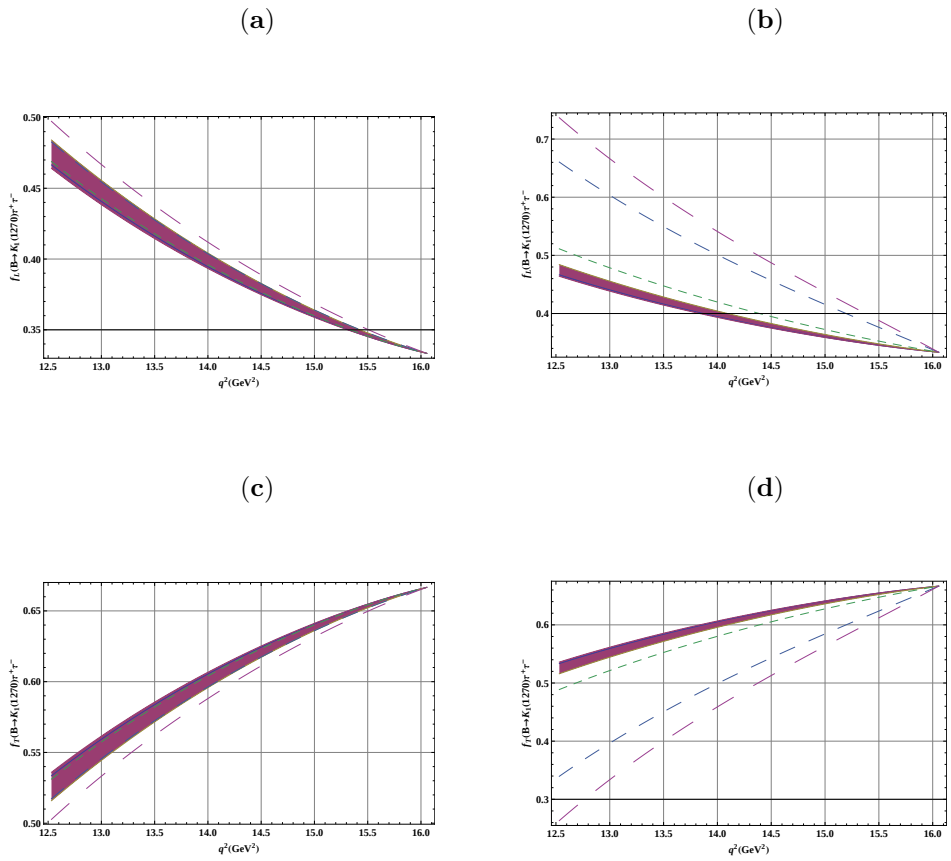

Figure 3.15: The dependence the probabilities of the longitudinal ($a,\ b$) and transverse ($c,\ d$) helicity fractions, $f_{L,T}$, of K_1 in $B \to K_1(1270)\tau^+\tau^-$ decays on q^2 for different values of $m_{t'}$ and $|V^*_{t'b}V_{t's}|$. The legends and the values of fourth generation parameters are same as in Fig. 3.14.

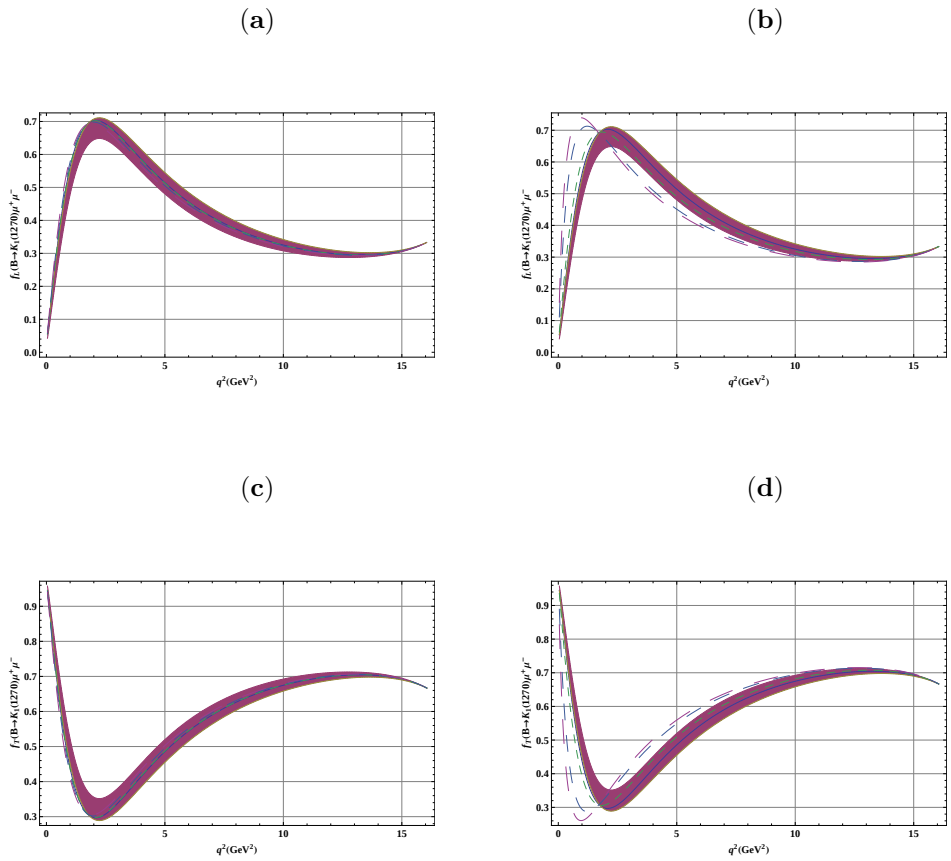

Figure 3.16: The dependence the probabilities of the longitudinal ($a,\ b$) and transverse ($c,\ d$) helicity fractions, $f_{L,T}$, of K_1 in $B \to K_1(1270)\mu^+\mu^-$ decays on q^2 for different values of $m_{t'}$ and $|V^*_{t'b}V_{t's}|$. The legends are the same as that of Fig.3.5.

(**a**) (**b**)

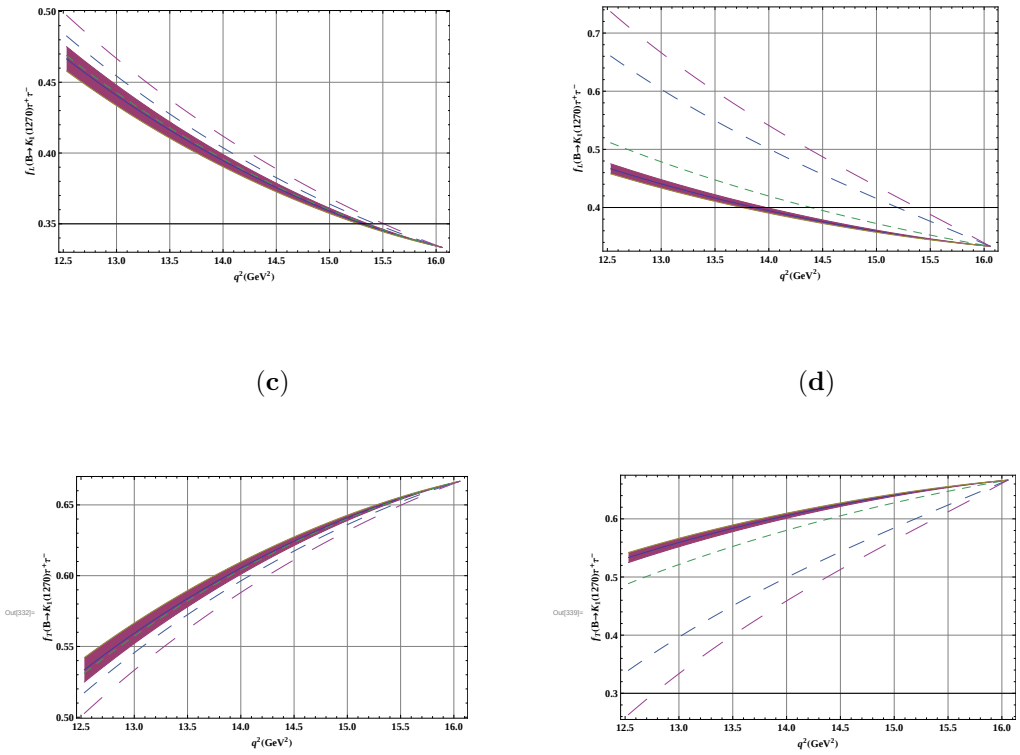

(**c**) (**d**)

Figure 3.17: The dependence the probabilities of the longitudinal ($a,\ b$) and transverse ($c,\ d$) helicity fractions, $f_{L,T}$, of K_1 in $B \to K_1(1270)\tau^+\tau^-$ decays on q^2 for different values of $m_{t'}$ and $|V^*_{t'b}V_{t's}|$. The legends are the same as that of Fig.3.5.

Chapter 4

Exclusive semileptonic $B \to K_1(1270, 1400)\ell^+\ell^-$ in single universal extra dimension model

4.1 Introduction

There are various extensions of SM, but the models with extra dimensions are of viable interest as they provide a unified framework for gravity and other interactions. In this way they give some hints of the hierarchy problem and a connection with string theory. Among different models of extra dimensions, which differ from one another depending on the number of extra dimensions, the most interesting ones are the scenarios with universal extra dimensions. In these UED models all the SM fields are allowed to propagate in the extra dimensions and compactification of an extra dimension leads to the appearance of KaluzaKlein (KK) partners of the SM fields in the four-dimensional description of higher dimensional theory. The Appelquist, Cheng and Dobrescu (ACD) model [49] with one universal extra dimension is very attractive, because it has only one free parameter with respect to the SM and that is the inverse of the compactification radius R [50].

By analyzing the signature of the extra dimensions in different processes, one can get bounds on the size of the extra dimensions, which are different in different models. These bounds are accessible for the processes already known at the particle accelerators or within the reach of planned future facilities. In the case of UED these bounds are more severe, and constraints from Tevatron run I allow one to put the bound $1/R \geq 300$ GeV [50].

Rare B decays can also be used to constrain the ACD scenario, and in this regard Buras and collaborators have already done some work [51, 52]. In addition to the effective Hamiltonian they have

calculated for bs decays and also investigated the impact of UED on B^0- $\bar{B}^0$ mixing as well as on the CKM unitarity triangle . Due to availability of precise data on the decays $B \to K(K^*)\ell^+\ell^-$, Colangelo et al. studied these decays in ACD model by calculating the branching ratio and forward backward asymmetry [50]. In this chapter we study the semileptonic decays of $B \to K_1(1270, 1400)\ell^+\ell^-$ in ACD model. The theoretical understanding of exclusive decays is complicated mainly due to long-distance non-perturbative quantities, which are modeled by form factors. One way of doing so is to use Ward identities which relate various form factors in a model independent way. This enables us to make a clear separation between non-pole and pole type contributions;the $q^2 \to 0$ behavior of the former is known in terms of a universal function $\xi_\perp(0) \equiv g_+(0)$ introduced in the large energy effective theory (LEET) of heavy (B) to light (K_1) form factors [86]. The residue of the pole is then determined in a self-consistent way in terms of $g_+(0)$ or $\xi_\perp(0)$, which will give information on the couplings of $B^*(1^-)$ and $B_A^*(1^+)$ with BK_1 channel. The form factors are then determined in terms of known parameters like $g_+(0)$ and the masses of the particles involved, which are then used to calculate the physical observables such as branching ratio and forward-backward asymmetry for the above mentioned decays both in the SM and in ACD model.

We compare the results for the forwardbackward asymmetry for $B \to K^*\ell^+\ell^-$ using the double pole parametrization of the form factors with the recent results obtained at LHCb [89] and is shown in fig 4.3. These decays may provide us a step forward towards the study of the existence of new physics beyond the SM and therefore deserve serious attention, both theoretically and experimentally.

4.2 Matrix Elements and Ward identities

The exclusive decay $B \to K_1(1270, 1400)\ell^+\ell^-$ involves the hadronic matrix elements and the parametrization in terms of form factors are given in Eqs.(3.2-3.6). The various form factors appearing in Eqs.(3.2-3.6) can be related by the Ward identities as follows

$$\langle K_1(k,\varepsilon)\,|\bar{s}i\sigma_{\mu\nu}q^\nu b|\,B(p)\rangle = -(m_b+m_s)\,\langle K_1(k,\varepsilon)\,|\bar{s}\gamma_\mu b|\,B(p)\rangle \tag{4.1}$$

$$\begin{aligned}\left\langle K_1(k,\varepsilon)\left|\bar{s}i\sigma_{\mu\nu}q^\nu\gamma^5 b\right|B(p)\right\rangle &= (m_b-m_s)\,\langle K_1(k,\varepsilon)\,|\bar{s}\gamma_\mu\gamma_5 b|\,B(p)\rangle \\ &\quad +(p+k)_\mu\,\langle K_1(k,\varepsilon)\,|\bar{s}\gamma_5 b|\,B(p)\rangle\end{aligned} \tag{4.2}$$

By putting Eq.(3.2)-(3.6) in Eq.(4.1) and (4.2)and comparing the coefficients of ε_μ^* and q_μ on both sides, one can get the following relations between the form factors:

$$F_1(q^2) = \frac{(m_b+m_s)}{M_B+M_{K_1}}A(q^2) \tag{4.3}$$

$$F_2(q^2) = \frac{m_b-m_s}{M_B-M_{K_1}}V_1(q^2) \tag{4.4}$$

$$F_3(q^2) \;=\; -(m_b - m_s)\frac{2M_{K_1}}{q^2}\left[V_3(q^2) - V_0(q^2)\right] \tag{4.5}$$

These are the model independent results and are derived by using Ward identities. The universal normalization of the above form factors at $q^2 = 0$ is obtained by defining

$$\begin{aligned}\left\langle K_1(k,\varepsilon)\left|\bar{s}i\sigma_{\alpha\beta}\gamma^5 b\right|B(p)\right\rangle &= -i\epsilon_{\alpha\beta\rho\sigma}\varepsilon^{*\rho}\left[(p+k)^\sigma g_+ + q^\sigma g_-\right] - (\varepsilon^*\cdot q)\epsilon_{\alpha\beta\rho\sigma}(p+k)^\rho q^\sigma h \\ &\quad -i\left[(p+k)_\alpha\varepsilon_{\beta\rho\sigma\tau}\varepsilon^{*\rho}(p+k)^\sigma q^\tau - \alpha\leftrightarrow\beta\right]h_1\end{aligned} \tag{4.6}$$

Using the Dirac identity

$$\sigma^{\mu\nu}\gamma^5 = -\frac{i}{2}\epsilon^{\mu\nu\alpha\beta}\sigma_{\alpha\beta} \tag{4.7}$$

in Eq.(4.6), one can write

$$\begin{aligned}\langle K_1(k,\varepsilon)\left|\bar{s}i\sigma_{\mu\nu}q^\nu b\right|B(p)\rangle &= \varepsilon^*_\mu\left[(M_B^2 - M_{K_1}^2)g_+ + q^2 g_-\right] \\ &\quad -q\cdot\varepsilon^*\left[q^2(p+k)_\mu g_+ - q_\mu g_-\right] \\ &\quad +q\cdot\varepsilon^*\left[q^2(p+k)_\mu - (M_B^2 - M_{K_1}^2)q_\mu\right]h\end{aligned} \tag{4.8}$$

Comparing the coefficients of q_μ, ε^*_μ and $\epsilon_{\mu\nu\alpha\beta}$ from (3.5),(3.6),(4.6) and (4.8), we get

$$F_1(q^2) \;=\; \left[g_+(q^2) - q^2 h_1(q^2)\right] \tag{4.9}$$

$$F_2(q^2) \;=\; g_+(q^2) + \frac{q^2}{M_B^2 - M_{K_1}^2}g_-(q^2) \tag{4.10}$$

$$F_3(q^2) \;=\; -g_-(q^2) - (M_B^2 - M_{K_1}^2)h(q^2) \tag{4.11}$$

The above results ensure that $F_1(0) = F_2(0)$. In terms of $g_+(0)$,$g_-(0)$ and h, the form factors $A(q^2)$,$V_1(q^2)$ and $V_2(q^2)$ become

$$A(q^2) \;=\; \frac{M_B + M_{K_1}}{m_b + m_s}\left[g_+(q^2) - q^2 h_1(q^2)\right] \tag{4.12}$$

$$V_1(q^2) \;=\; -\left(\frac{M_B + M_{K_1}}{m_b - m_s}\right)\left[g_+(q^2) + \frac{q^2}{M_B^2 - M_{K_1}^2}g_-(q^2)\right] \tag{4.13}$$

$$V_2(q^2) \;=\; -\left(\frac{M_B + M_{K_1}}{m_b - m_s}\right)\left[g_+(q^2) - q^2 h(q^2)\right] - \frac{2M_{K_1}}{M_B - M_{K_1}}V_0(q^2) \tag{4.14}$$

By looking at the above expressions one can see that the normalization of the form factors A and V_1 at $q^2 = 0$ is determined by the single constant $g_+(0)$, whereas that of V_2 is determined by $g_+(0)$ and $V_0(q^2)$.

4.3 Pole contribution

The pole contribution for B to ρ has been studied in detail by Gilani etal.[85]. This remains the same for the B to K_1 transition except that the role of vector and axial vector is interchanged and again only h_1, g_-, h and V_0 get contributions from $B_s^*(1^-)$, $B_A^*(1^+)$ and $B_s(0^-)$ mesons which can be parameterized as

$$h_1|_{pole} = -\frac{1}{2}\frac{g_{B_s^*BK_1}}{M^2_{B_s^*}}\frac{f_T^{B^*}}{1-q^2/M^2_{B^*}} = \frac{R_V}{M^2_{B_s^*}}\frac{1}{1-q^2/M^2_{B_s^*}} \tag{4.15}$$

$$g_-|_{pole} = -\frac{g_{B^*_{sA}BK_1}}{M^2_{B^*_{sA}}}\frac{f_T^{B^*_{sA}}}{1-q^2/M^2_{B^*_{sA}}} = \frac{R_A^S}{M^2_{B^*_{sA}}}\frac{1}{1-q^2/M^2_{B^*_{sA}}} \tag{4.16}$$

$$h|_{pole} = \frac{1}{2}\frac{f_{B^*_{SA}BK_1}}{M^2_{B^*_{sA}}}\frac{f_T^{B^*_{SA}}}{1-q^2/M^2_{B^*_{sA}}} = \frac{R_A^D}{M^2_{B^*_{sA}}}\frac{1}{1-q^2/M^2_{B^*_{sA}}} \tag{4.17}$$

$$V_0(q^2)|_{pole} = \frac{g_{B_s^*BK_1}}{M^2_{B_s^*}}f_{B_s}\frac{q^2/M^2_{B_s}}{1-q^2/M^2_{B_s}} = R_0\frac{q^2/M^2_{B_s}}{1-q^2/M^2_{B_s}} \tag{4.18}$$

where R_V , R_A^S , R_A^D and R_0 are related to the coupling constants $g_{B^*BK_1}$, $g_{B_A^*BK_1}$, $f_{B_A^*BK_1}$ and g_{BBK_1}, respectively. Thus one can write the form factors $A(q^2)$, $V_1(q^2)$ and $V_2(q^2)$ in terms of these quantities as

$$A(q^2) = \frac{M_B+M_{K_1}}{m_b+m_s}\left[g_+(q^2) - \frac{R_V}{M^2_{B_s^*}}\frac{q^2}{1-q^2/M^2_{B_s^*}}\right] \tag{4.19}$$

$$V_1(q^2) = -\left(\frac{M_B-M_{K_1}}{m_b-m_s}\right)\left[g_+(q^2) + \frac{q^2}{M_B^2-M_{K_1}^2}\tilde{g}_-(q^2) + \frac{R_A^S}{M^2_{B^*_{sA}}}\frac{q^2}{1-q^2/M^2_{B^*_{sA}}}\right] \tag{4.20}$$

$$V_2(q^2) = -\left(\frac{M_B+M_{K_1}}{m_b-m_s}\right)\left[g_+(q^2) - \frac{R_A^D}{M^2_{B^*_{As}}}\frac{q^2}{1-q^2/M^2_{B^*_{sA}}}\right] - \frac{2M_{K_1}}{M_B-M_{K_1}}V_0(q^2) \tag{4.21}$$

The behavior of $g_+(0)$, $\tilde{g}_-(q^2)$ and $V_0(q^2)$ near $q^2 \to 0$ is known from LEET and their form is given as

$$g_+(q^2) = \frac{\xi_\perp(0)}{(1-q^2/M_B^2)^2} = -\tilde{g}_-(q^2) \tag{4.22}$$

$$A_0(q^2) = \left(1-\frac{M_{K_1}^2}{M_B E_{K_1}}\right)\xi_\parallel(0) + \frac{M_{K_1}}{M_B}\xi_\perp(0) \tag{4.23}$$

$$E_{K_1} = \frac{M_B}{2}\left(1-\frac{q^2}{M_B^2}+\frac{M_{K_1}^2}{M_B^2}\right) \tag{4.24}$$

$$g_+(0) = \xi_\perp(0) \tag{4.25}$$

The pole term given in Eqs.(4.19)- (4.21) dominate near $q^2 = M^2_{B_s^*}$ and $q^2 = M^2_{B^*}$. One can make a remark here that the relations obtained from the Ward identities can not be expected to hold for the whole range of q^2. Therefore, near $q^2 = 0$ and that near the pole following parametrization is suggested [85].

$$F(q^2) = \frac{F(0)}{(1-q^2/M^2)\,(1-q^2/M'^2)} \tag{4.26}$$

where M^2 is $M^2_{B^*_s}$ or $M^2_{B^*_{sA}}$, and M' is the radial excitation of M. The parametrization given in Eq. (4.26) not only takes into account the corrections to single pole dominance suggested by the dispersion relation approach [87, 88] but also give the correction of off-mass shell-ness of the couplings of B^*_s and B^*_{sA} with the BK_1 channel.

Since $g_+(0)$ and $\tilde{g}_-(q^2)$ have no pole at $q^2 = M^2_{B^*_s}$, we get

$$A(q^2)(1 - \frac{q^2}{M^2_{B^*}})|_{q^2=M^2_{B^*}} = -R_V \left(\frac{M_B + M_{K_1}}{m_b - m_s} \right)$$

so that from Eq.(4.19)

$$R_V \equiv -\frac{1}{2} g_{B^*_s BK_1} f_{B^*_s} = -\frac{g_+(0)}{1 - M^2_{B^*}/M'^2_{B^*}} \tag{4.27}$$

and similarly

$$R^D_A \equiv \frac{1}{2} f_{B^*_{sA} BK_1} f_T^{B^*_{sA}} = -\frac{g_+(0)}{1 - M^2_{B^*_{sA}}/M'^2_{B^*_{sA}}} \tag{4.28}$$

We cannot use the parametrization given in Eq.(4.26) for the form factor $V_1(q^2)$, since near $q^2 = 0$, the behavior of $V_1(q^2)$ is $g_+(q^2)\left[1 - q^2/\left(M^2_B - M^2_{K_1}\right)\right]$, therefore we can write $V_1(q^2)$ as follows

$$V_1(q^2) = -\frac{g_+(0)}{\left(1 - q^2/M^2_{B^*_s}\right)\left(1 - q^2/M'^2_{B^*_s}\right)} \left(1 - \frac{q^2}{M^2_B - M^2_{K_1}}\right) \tag{4.29}$$

Until now we have expressed everything in terms of $g_+(0)$, which is the only unknown parameter in the calculation. The value of $g_+(0)$ was calculated in Light cone sum rules (LCSR) with mixing angle $\theta_K = -34^\circ$ for the decay $B \to K_1(1270)\gamma$ and $B \to K_1(1400)\gamma$ by H. Hatanka and K.C.Yang[78] and are given below

$$\begin{aligned} g_+^{K_1(1270)}(0) &= -(0.38^{+0.06+0.08+0.02}_{-0.04-0.07-0.04}) \\ g_+^{K_1(1400)}(0) &= \left(0.12^{+0.03+0.02+0.08}_{-0.02-0.00-0.09}\right) \end{aligned}$$

Using the value of decay constant $f_B = 180$ MeV we have a prediction from Eq.(4.27) that

$$g_{B^*_s BK_1(1270)} = 17.5 \text{ GeV}^{-1} \tag{4.30}$$

$$g_{B^*_s BK_1(1400)} = 5.55 \text{ GeV}^{-1} \tag{4.31}$$

The parametrization of the form factors for the decay $B \to K_1$ in terms of the mixing angle θ_K was given in Eqs. (3.7), (3.8) and (3.9). As already mentioned above that the only unknown parameter in the calculations of form factors for the said decay are $g_+(0)$ and θ_K, since final state meson $K_1(1270)$ and $K_1(1400)$ are mixed states of the K_{1A} and K_{1B} with mixing angle θ_K given in Eqs. (3.1a) and

Table 4.1: Values of the form factors at $q^2 = 0$.

$A^{K_{1A}}(0)$	$A^{K_{1B}}(0)$	$V_1^{K_{1A}}(0)$	$V_1^{K_{1B}}(0)$	$\tilde{V}_2^{K_{1A}}(0)$	$\tilde{V}_2^{K_{1B}}(0)$
0.44	-0.35	-0.26	0.21	-0.42	0.33

(3.1b).Using the value of θ_K = -34°, the value of unknown parameter $g_+(0)$ is found to be $g_+^{K_{1A}}(0) = 0.31$ and $g_+^{K_{1B}}(0) = -0.25$ [78].

The final expressions of the form factors which we will use for our numerical work are

$$A^{\chi}(q^2) = \frac{A^{\chi}(0)}{\left(1 - q^2/M^2_{B^*_{sA}}\right)\left(1 - q^2/M'^2_{B^*_{sA}}\right)} \tag{4.32}$$

$$V_1^{\chi}(q^2) = -\frac{V_1^{\chi}(0)}{\left(1 - q^2/M^2_{B^*_s}\right)\left(1 - q^2/M'^2_{B^*_s}\right)}\left(1 - \frac{q^2}{M_B^2 - M^2_{K_1}}\right) \tag{4.33}$$

$$V_2^{\chi}(q^2) = -\frac{\tilde{V}_2^{\chi}(0)}{\left(1 - q^2/M^2_{B^*_s}\right)\left(1 - q^2/M'^2_{B^*_s}\right)} - \frac{2M_{\chi}}{M_B - M_{\chi}}\frac{V_0(0)}{(1 - q^2/M_B^2)\,(1 - q^2/M'^2_B)} \tag{4.34}$$

where

$$A^{\chi}(0) = \left(\frac{M_B + M_{\chi}}{m_b - m_s}\right) g_+^{\chi}(0) \tag{4.35}$$

$$V_1^{\chi}(0) = -\left(\frac{M_B - M_{\chi}}{m_b - m_s}\right) g_+^{\chi}(0) \tag{4.36}$$

$$V_2^{\chi}(0) = -\left(\frac{M_B + M_{\chi}}{m_b - m_s}\right) g_+^{\chi}(0) - \frac{2M_{\chi}}{M_B - M_{\chi}} V_0(0) \tag{4.37}$$

and $\chi = K_{1A}$ and K_{1B}. The values of form factors for the decay $B \to K_1(1270, 1400)$ at $q^2 = 0$ were given in Table 4.1

4.4 Branching ratio and forward-backward asymmetry for the decay $B \to K_1(1270, 1400)\ell^+\ell^-$

In this section we will discuss the physical observables such as branching ratio ($\mathcal{BR}$) and forward backward asymmetry ($\mathcal{A}_{FB}$) for the above mentioned decay both in the SM and in ACD model. The detailed expressions for both these observables were given in section 3.3. It has already been mentioned in chapter 2 that the Wilson coefficient C_9^{eff}, contains the long distance contribution resulting from the $c\bar{c}$ resonances such as J/ψ and its excited states.

We first discuss the ($\mathcal{BR}$) of $B \to K_1(1270, 1400)\ell^+\ell^-$ with (ℓ=μ,τ) decays presented in fig 4.1 both in SM and in ACD model. Figs 4.1a and 4.1b show the branching ratio of $B \to K_1(1270, 1400)\mu^+\mu^-$ and figs 4.1c and 4.1d represent the same final state hadrons but the final state leptons are tauons.

Table 4.2: The values of branching ratio without long distance effects for decays $B \to K_1(1270, 1400)\ell^+\ell^-$ with ℓ=μ, τ for different values of $1/R$.

$Br(B \to K_1(1270)\ell^+\ell^-)$	$Br(B \to K_1(1270)\mu^+\mu^-) \times 10^{-6}$	$Br(B \to K_1(1270)\tau^+\tau^-) \times 10^{-8}$
SM value	2.12	4.34
$1/R$ =300 GeV	2.35	5.00
$1/R$ =500 GeV	2.14	4.56
$Br(B \to K_1(1400)\ell^+\ell^-)$	$Br(B \to K_1(1400)\mu^+\mu^-) \times 10^{-7}$	$Br(B \to K_1(1400)\tau^+\tau^-) \times 10^{-9}$
SM value	1.53	1.82
$1/R$ =300 GeV	1.73	2.09
$1/R$ =500 GeV	1.56	1.91

Table 4.3: The values of branching ratio with long distance effects for decays $B \to K_1(1270, 1400)\ell^+\ell^-$ with ℓ=μ, τ for different values of $1/R$.

$Br(B \to K_1(1270)\ell^+\ell^-)$	$Br(B \to K_1(1270)\mu^+\mu^-) \times 10^{-5}$	$Br(B \to K_1(1270)\tau^+\tau^-) \times 10^{-6}$
SM value	2.99	7.68
$1/R$ =300 GeV	3.01	7.69
$1/R$ =500 GeV	2.97	7.66
$Br(B \to K_1(1400)\ell^+\ell^-)$	$Br(B \to K_1(1400)\mu^+\mu^-) \times 10^{-6}$	$Br(B \to K_1(1400)\tau^+\tau^-) \times 10^{-7}$
SM value	1.65	5.22
$1/R$ =300 GeV	1.67	5.23
$1/R$ =500 GeV	1.66	5.22

From the figs of branching ratios one can see that there is a significant enhancement in the ($\mathcal{BR}$) due to KK-contribution for $1/R = 300$ GeV, whereas this value is shifted towards the SM at large values of $1/R$. The enhancement is more prominent in the low value of q^2 region, for the case of muon as a final state lepton. However for the case of taun as a final state lepton the NP effects are negligibly small. It is also important to point out the NP effects in the branching ratios are usually masked up by the uncertainties involved in different input parameters where form factors are the major contributors. However, there exists some other observables which have weak dependence on the choice of form factors. Among this the zero position of the forward-backward asymmetry which is almost free from hadronic uncertainties, in particular at low value of q^2 region, and hence serve as a handy tool to investigate NP. The numerical values of the ($\mathcal{BR}$) for the decay $B \to K_1(1270, 1400)\ell^+\ell^-$ in the SM as well as in ACD model with and without long distance contributions are given in table 4.2 and 4.3 respectively.

Figs 4.2(a) and 4.2(b) describe the behavior of the forward-backward asymmetry of $B \to K_1(1270, 1400)\mu^+\mu^-$ with q^2. Here one can see that the value of the forward-backward asymmetry passes from its zero position at a particular value of q^2 both in SM as well as in ACD model. This is because of the destructive interference between the photon penguin (C_7^{eff}) and the Z-penguin (C_9^{eff}). As one can see from the expression of $\mathcal{A}_{\mathcal{FB}}$ which is given in Eq.(3.37) that the $\mathcal{A}_{\mathcal{FB}}$ depends on the Wilson coefficients which

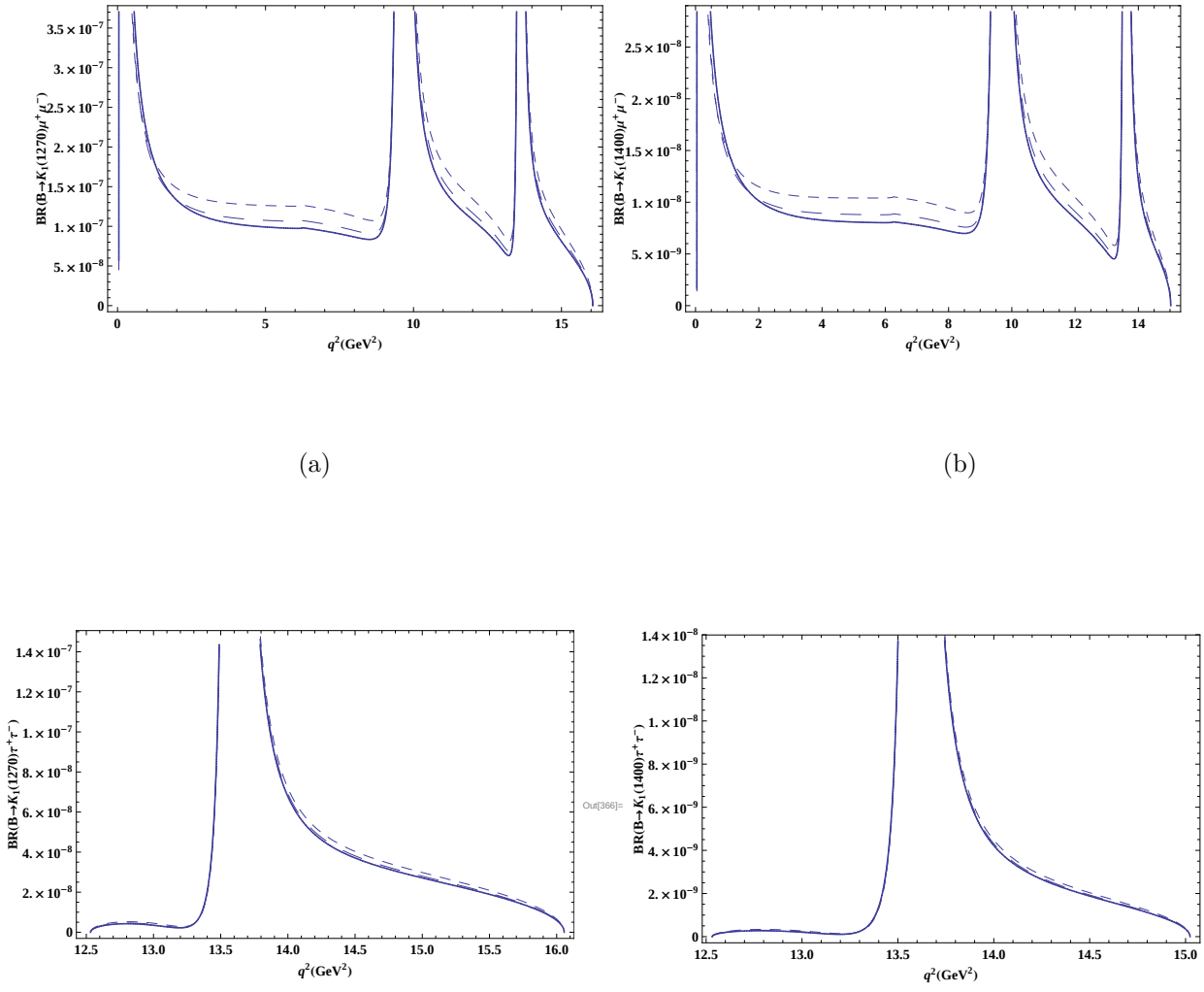

(a) (b)

(c) (d)

Figure 4.1: Branching ratio for the $B \to K_1(1270)\ell^+\ell^-$ decays with ($\ell = \mu, \tau$) using the form factors given in Eqs.(3.48)-(3.50). Solid line corresponding to SM value, the dashed line is for $1/R = 300$ GeV, and the long dashed lines are for $1/R = 500$ GeV.

in turn contain the effects of extra dimensions. Thus one expects that the zero crossing of the $\mathcal{A}_{\mathcal{FB}}$ will be different from the SM. This fact is illustrated in figs.(4.2a) and (4.2b) for $K_1(1270)$ and $K_1(1400)$ respectively. We can also see that the value of $\mathcal{A}_{\mathcal{FB}}$ shifts significantly towards left from the SM value when we set $1/R$= 300 GeV. However this value approaches the SM value at large value of $1/R$.

Now for $B \to K_1(1270, 1400)\tau^+\tau^-$ decays the $\mathcal{A}_{\mathcal{FB}}$ is presented in fig.4.2(c) and 4.2(d). In this case the zero crossing of the $\mathcal{A}_{FB}$ is absent both in SM and in ACD model, however there is a deviation in the magnitude of $\mathcal{A}_{\mathcal{FB}}$ for $1/R$ =300 GeV particularly for the case of $B \to K_1(1270)\tau^+\tau^-$. Moreover for the case of $B \to K_1(1400)\tau^+\tau^-$ the deviation in the magnitude of $\mathcal{A}_{FB}$ is not very large from its SM value. Since the analysis showed that the magnitude of $\mathcal{A}_{FB}$ is also an important tool to establish the NP, therefore, the experimental study of this observable will be helpful to investigate the status of extra dimension. Recently the LHCb collaboration has collected over 300 events for $B \to K^*\mu^+\mu^-$, with signal to background ratio above three which is the largest data sample in the world, and also cleaner than the sample used by the other B factories [89]. The collaboration found that the distribution of $\mathcal{A}_{FB}$ vs q^2 is in good agreement with the SM, but still the LHCb collaboration said that they will continue to collect more data and try to see possible deviation in the data if there is any signal to NP. We have plotted the $\mathcal{A}_{FB}$ with LHCb data points shown in fig 4.3. for the decay $B \to K^*\mu^+\mu^-$ by using the form factors calculated in the framework of Ward identities.

4.5 Conclusion

This chapter deals with the study of semileptonic decay $B \to K_1(1270, 1400)\ell^+\ell^-$ in ACD model with single universal extra dimension which is strong contender to study physics beyond SM and has received a lot of interest in the literature. We have studied the dependence of the physical observables such as decay rate and zero position of forward-backward asymmetry($\mathcal{A}_{FB}$) on the inverse of compactification radius $1/R$. The value of the branching ratio is found larger than the corresponding SM value. It is also found that the zero position of the $\mathcal{A}_{FB}$ is sensitive to $1/R$ for the decays $B \to K_1(1270, 1400)\mu^+\mu^-$ and it is seen that the zero position of $\mathcal{A}_{FB}$ shifts significantly towards left of the SM value. The shift in the zero position of $\mathcal{A}_{FB}$ is large at $1/R = 300$ GeV and when we increase the value of $1/R$ it approaches towards SM value. Therefore the measurement of these observables for $B \to K_1(1270, 1400)\ell^+\ell^-$ at current experiments such as LHCb where more data will be available in future, will put stringent constraints on the compactification radius so as to indicate the possible existence of extra dimensions.

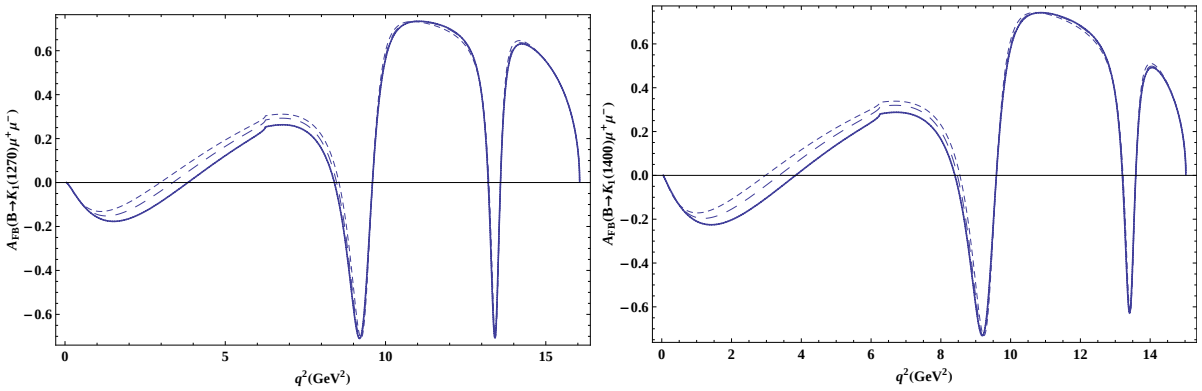

(a) (b)

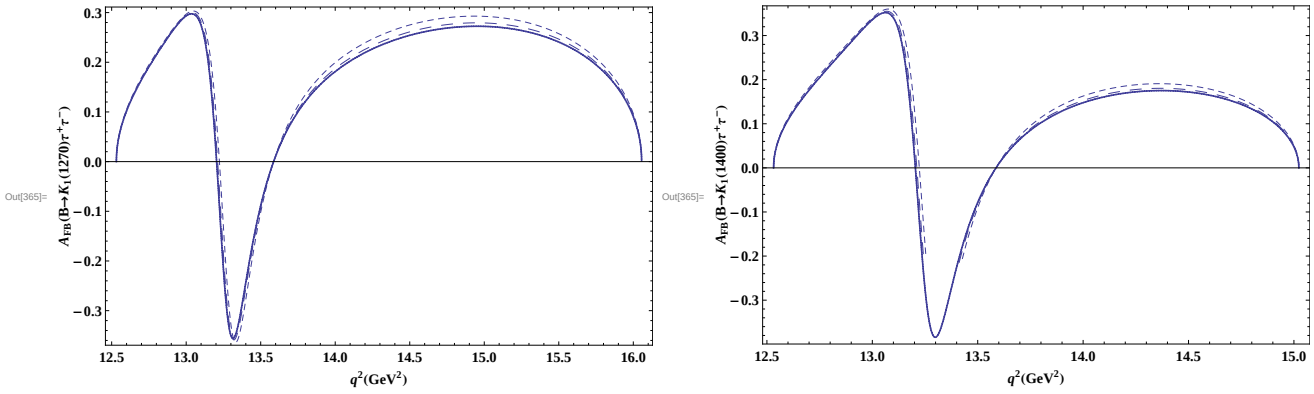

(c) (d)

Figure 4.2: The forward-backward asymmetry for the decay $B \to K_1(1270, 1400)\ell^+\ell^-$ with $(\ell = \mu, \tau)$ as a function of q^2 is plotted using the form factors as a function of q^2 given in Eqs.(3.48)-(3.50). Solid line corresponding to SM value, the dashed line is for $1/R = 300$ GeV, and the long dashed lines are for $1/R = 500$ GeV.

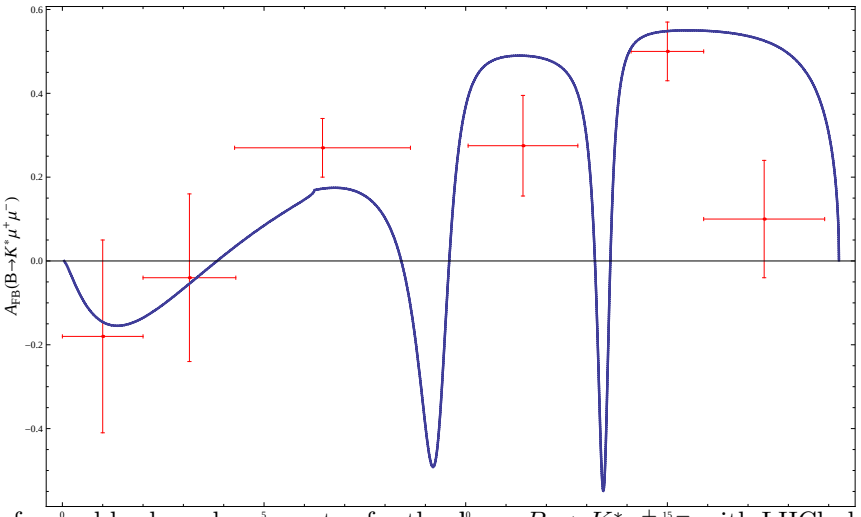

Figure 4.3: The forward-backward asymmetry for the decay $B \to K^*\mu^+\mu^-$ with LHCb data points as a function of q^2 is plotted using the form factors calculated in the framework of Ward identities.

Chapter 5

Exclusive charm B meson decays in universal extra dimensions

5.1 Introduction

The charmed B_c meson is a bound state of two heavy quarks, bottom b and charm c, and was first observed in 1998 at Tevatron in Fermilab [90]. Because of two heavy quarks, the B_c mesons are rich in phenomenology compared to the other B mesons. At the Large Hadron Collider (LHC) the expected number of events for the production of the B_c meson are about $10^8 - 10^{10}$ per year [91, 92] which is a reasonable number to work on the phenomenology of the B_c meson. It also provides a frame work to study physics in and beyond the SM. In the literature, some of the possible radiative and semileptonic exclusive decays of B_c mesons like $B_c \to (\rho, K^*, D_s^*, B_u^*)\,\gamma, B_c \to \ell\nu\gamma$, $B_c \to B_u^*\ell^+\ell^-, B_c \to D_1^0\ell\nu, B_c \to D_{s0}^*\ell^+\ell^-$ and $B_c \to D_{s,d}^*\ell^+\ell^-$ have been studied using the frame work of relativistic constituent quark model [93], QCD Sum Rules and the Light Cone Sum Rules [13]. In this chapter we will focus on the $B_c \to D_s^*\ell^+\ell^-$ decay.

Theoretically, what makes the $B_c \to D_s^*\ell^+\ell^-$ more important compared to the other B meson decays such as $B^0 \to (K^*, K_1, \rho, \pi)l^+l^-$ is that this decay can occur in two different ways i.e. through FCNC transitions and due to Weak Annihilations (WA). In ordinary B meson decays the WA contributions are very small and can be ignored. However, for the B_c meson the WA contributions are proportional to the CKM matrix elements $V_{cb}V_{cs}^*$ and hence can not be ignored. While working on the exclusive B-meson decays, the main job is to calculate the form factors which are the non perturbative quantities and are scalar functions of the momentum transfer squared. In the literature the form factors for $B_c \to D_s^*\ell^+\ell^-$ decay were calculated using different approaches, such as light front constituent quark models, a relativistic quark model and the QCD sum rules [93, 94]. In this work we calculate the form

factors for the above mentioned decay through Ward identities, which was earlier applied to $B \to \rho, \gamma$ [85, 95] and $B \to K_1$ decays [76]. This approach enables us to make a clear separation between the pole and non pole type contributions, the former is known in terms of a universal function $\xi_\perp(q^2) \equiv g_+(q^2)$. The residue of the pole is then determined in a self consistent way in terms of $g_+(0)$ which will give information about the couplings of $B_s^*(1^-)$ and $B_{sA}^*(1^+)$ in $B_c D_s^*$ channel. The above mentioned coupling arises at lower pole masses because the higher pole masses of B_c meson do not contribute to the decay $B_c \to D_s^* \ell^+ \ell^-$. The form factors are then determined in terms of a known parameter $g_+(0)$ and the pole masses of the particles involved, which will then be used to calculate different physical observables like the branching ratios and the helicity fractions of final state meson (D_s^*) for these decays.

In this chapter we will analyze the branching ratio and helicity fractions of D_s^* meson for $B_c \to D_s^* \ell^+ \ell^-$ decay both in the SM and ACD model. The chapter is organized as follows. In Sec. 5.2 we present the theoretical framework for the decay $B_c \to D_s^* \ell^+ \ell^-$ as well as the weak annihilation amplitude. Section 5.3 provides the definitions as well as the detailed calculation of the form factors using Ward Identities. Here we compare the dependence of our form factors on q^2 with the ones calculated using QCD sum rules [97]. In Sec. 5.4 we present the basic formulas for physical observables like decay rate and helicity fractions of D_s^* meson where as the numerical analysis of these observables will be given in Section 5.5. Section 5.6 gives the summary of the results.

5.2 Theoretical framework for $B_c \to D_s^* \ell^+ \ell^-$ decays

5.2.1 Weak Annihilation Amplitude

The weak annihilation amplitude (WA) for the decay $B_c \to D_s^* \ell^+ \ell^-$ can be written in analogy of $B_c \to D_s^* \gamma$ [98, 99].

$$\mathcal{M}^{\rm WA} = \frac{G_F \alpha}{2\sqrt{2}\pi} \frac{f_{D_s^*} f_{B_c}}{q^2} V_{cb} V_{cs}^* \left[-i\epsilon_{\mu\nu\alpha\beta} \varepsilon^{*\nu} p^\alpha q^\beta F_V^{D_s^*}(q^2) + (\varepsilon \cdot q p_\mu + p \cdot q \varepsilon_\mu) F_A^{D_s^*}(q^2) \right] \bar{l} \gamma^\mu l \tag{5.1}$$

where f_{B_c} and $f_{D_s^*}$ are the decay constants of B_c and D_s^* mesons, respectively. The functions $F_V^{D_s^*}(q^2)$ and $F_A^{D_s^*}(q^2)$ are the weak annihilation form factors which are calculated in QCD Sum Rules and can be parameterized as [97]:

$$F_{V,A}^{D_s^*}(q^2) = \frac{F_{V,A}^{D_s^*}(0)}{1 + \alpha \hat{q} + \beta \hat{q}^2} \tag{5.2}$$

where $\hat{q} = q^2/M_{B_c}^2$. In the present study we have also parameterized the form factors in terms of double poles as follows

$$F_V^{D_s^*}(q^2) = \frac{(m_b + m_s)}{M_{B_c^-} + M_{D_s^{*-}}} \frac{F_V^{D_s^*}(0)}{(1 - q^2/M_{B_s^*}^2)(1 - q^2/M_{B_s^*}'^2)} \tag{5.3}$$

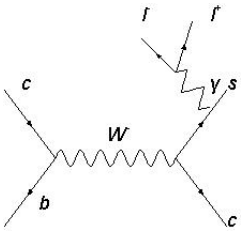

Figure 5.1: Weak annihilation diagram for the decay $B_c \to D_s^* \ell^+ \ell^-$

$$F_A^{D_s^*}(q^2) = \frac{m_b - m_s}{M_{B_c^-} - M_{D_s^{*-}}} \frac{F_A^{D_s^*}(0)}{(1 - q^2/M_{B_{sA}^*}^2)(1 - q^2/M_{B_{sA}^*}'^2)} \left(1 - \frac{q^2}{M_{B_c^-}^2 - M_{D_s^*}^2}\right) \tag{5.4}$$

The values of the form factors at $q^2 = 0$ are determined by using QCD sum rules [100]. The two set of form factors given in Eq.(5.2) and Eqs.(5.3-5.4) give the branching ratios 2.20×10^{-6} and By using the form factors given in Eq.(5.2) it is found that the branching ratio for $B_c \to D_s^* \mu^+ \mu^-$ is 2.82×10^{-6} respectively. It follows that the branching ratios are independent on the choice of form factors. These values of the branching ratios are almost five times larger than the penguin one which is given in table 5.2, therefore, one cannot ignore the weak annihilation contribution for the process under consideration.

At quark level the semileptonic decay $B_c \to D_s^* \ell^+ \ell^-$ is governed by the FCNC transition $b \to s \ell^+ \ell^-$ which effective Hamiltonian is given in Eq.(2.1). The ACD model is the most economical one because it has only one additional parameter R i.e. the radius of the compactification, leaving the same operators basis as that of the SM. At the low values of $1/R$ the KK states couples with the low energy theory and modified the Wilson coefficients which are now become the functions of the compactification radius R. The explicit form of these modified Wilson coefficients C_7^{eff} , C_9^{eff} and C_{10}^{eff} were given in Chapter 2. However, at large values of $1/R$ the new states become more and more massive, and will be decoupled from the low-energy theory,therefore one can recover the SM phenomenology.

5.3 Matrix Elements and Form Factors

The exclusive $B_c \to D_s^* \ell^+ \ell^-$ decay involves the hadronic matrix elements which can be obtained by sandwiching the quark level operators give in Eq. (2.17) between initial state B_c meson and final state D_s^* meson. These can be parameterized in terms of form factors which are the scalar functions of the square of the four momentum transfer($q^2 = (p-k)^2$). The non vanishing matrix elements for the process $B_c \to D_s^*$ can be parameterized exactly in the same fashion as that of $B \to K_1$ decay in chapter 3. The form factors for the decay $B_c \to D_s^*$ can be related through Ward identities[85] as

$$\langle D_s^*(k,\varepsilon) | \bar{s} i \sigma_{\mu\nu} q^\nu b | B_c(p) \rangle = -(m_b + m_s) \langle D_s^*(k,\varepsilon) | \bar{s} \gamma_\mu b | B_c(p) \rangle \tag{5.5}$$

$$\begin{aligned} \left\langle D_s^*(k,\varepsilon) \left| \bar{s} i \sigma_{\mu\nu} q^\nu \gamma^5 b \right| B_c(p) \right\rangle &= (m_b - m_s) \langle D_s^*(k,\varepsilon) | \bar{s} \gamma_\mu \gamma_5 b | B_c(p) \rangle \\ &\quad + (p+k)_\mu \langle D_s^*(k,\varepsilon) | \bar{s} \gamma_5 b | B_c(p) \rangle \end{aligned} \tag{5.6}$$

By using the parametrization of form factors in Eq.(5.5) and (5.6) and comparing the coefficients of ε_μ^* and q_μ on both sides, one can get the following relations between the form factors:

$$F_1(q^2) = \frac{(m_b+m_s)}{M_{B_c^-}+M_{D_s^{*-}}}V(q^2) \tag{5.7}$$

$$F_2(q^2) = \frac{m_b-m_s}{M_{B_c^-}-M_{D_s^{*-}}}A_1(q^2) \tag{5.8}$$

$$F_3(q^2) = -(m_b-m_s)\frac{2M_{D_s^{*-}}}{q^2}\left[A_3(q^2)-A_0(q^2)\right] \tag{5.9}$$

The results given in Eqs. (5.7, 5.8, 5.9) are derived by using Ward identities and therefore are the model independent.

The universal normalization of the above form factors at $q^2=0$ is obtained by defining [85]

$$\begin{aligned}\langle D_s^*(k,\varepsilon)\left|\bar{s}i\sigma_{\alpha\beta}b\right|B_c(p)\rangle &= -i\epsilon_{\alpha\beta\rho\sigma}\varepsilon^{*\rho}\left[(p+k)^\sigma g_+ + q^\sigma g_-\right] - (\varepsilon^*\cdot q)\epsilon_{\alpha\beta\rho\sigma}(p+k)^\rho q^\sigma h \\ &\quad -i\left[(p+k)_\alpha\varepsilon_{\beta\rho\sigma\tau}\varepsilon^{*\rho}(p+k)^\sigma q^\tau - \alpha\leftrightarrow\beta\right]h_1\end{aligned} \tag{5.10}$$

Making use of the Dirac identity

$$\sigma^{\mu\nu}\gamma^5 = -\frac{i}{2}\epsilon^{\mu\nu\alpha\beta}\sigma_{\alpha\beta} \tag{5.11}$$

in Eq.(5.10), we get

$$\begin{aligned}\left\langle D_s^*(k,\varepsilon)\left|\bar{s}i\sigma_{\mu\nu}q^\nu\gamma^5 b\right|B_c(p)\right\rangle &= \varepsilon_\mu^*\left[(M_{B_c^-}^2-M_{D_s^{*-}}^2)g_+ + q^2 g_-\right] \\ &\quad -q\cdot\varepsilon^*\left[q^2(p+k)_\mu g_+ - q_\mu g_-\right] \\ &\quad +q\cdot\varepsilon^*\left[q^2(p+k)_\mu - (M_{B_c^-}^2-M_{D_s^{*-}}^2)q_\mu\right]h\end{aligned} \tag{5.12}$$

On comparing coefficients of q_μ, ε_μ^* and $\epsilon_{\mu\nu\alpha\beta}$ from the parametrization of the form factors, we have

$$F_1(q^2) = \left[g_+(q^2) - q^2 h_1(q^2)\right] \tag{5.13}$$

$$F_2(q^2) = g_+(q^2) + \frac{q^2}{M_{B_c^-}^2-M_{D_s^{*-}}^2}g_-(q^2) \tag{5.14}$$

$$F_3(q^2) = -g_-(q^2) - (M_{B_c^-}^2-M_{D_s^{*-}}^2)h(q^2) \tag{5.15}$$

One can see from Eqs. (5.13, 5.14) that at $q^2=0$, $F_1(0)=F_2(0)$. The form factors $V(q^2), A_1(q^2)$ and $A_2(q^2)$ can be written in terms of g_+, g_- and h as

$$V(q^2) = \frac{M_{B_c^-}+M_{D_s^{*-}}}{m_b+m_s}\left[g_+(q^2) - q^2 h_1(q^2)\right] \tag{5.16}$$

$$A_1(q^2) = \frac{M_{B_c^-}+M_{D_s^{*-}}}{m_b-m_s}\left[g_+(q^2) + \frac{q^2}{M_{B_c^-}^2-M_{D_s^{*-}}^2}g_-(q^2)\right] \tag{5.17}$$

$$A_2(q^2) = \frac{M_{B_c^-} + M_{D_s^{*-}}}{m_b - m_s}\left[g_+(q^2) - q^2 h(q^2)\right] - \frac{2M_{D_s^{*-}}}{M_{B_c^-} - M_{D_s^{*-}}} A_0(q^2) \tag{5.18}$$

By looking at Eq. (5.16) and Eq. (5.17) it is clear that the normalization of the form factors V and A_1 at $q^2 = 0$ is determined by a single constant $g_+(0)$, where as from Eq. (5.18) the form factor A_2 at $q^2 = 0$ is determined by two constants i.e. $g_+(0)$ and $A_0(0)$.

5.3.1 Pole Contribution

In $B_c \to D_s^* \ell^+ \ell^-$ decay, there will be a pole contribution to h_1, g_-, h and A_0 from $B_s^*(1^-), B_{sA}^*(1^+)$ and $B_s(0^-)$ mesons which can be parameterized as

$$h_1|_{pole} = -\frac{1}{2}\frac{g_{B_s^* B_c D_s^*}}{M^2_{B_s^*}} \frac{f_T^{B^*}}{1 - q^2/M^2_{B^*}} = \frac{R_V}{M^2_{B_s^*}} \frac{1}{1 - q^2/M^2_{B_s^*}} \tag{5.19}$$

$$g_-|_{pole} = -\frac{g_{B_{sA}^* B_c D_s^*}}{M^2_{B_{sA}^*}} \frac{f_T^{B_{sA}^*}}{1 - q^2/M^2_{B_{sA}^*}} = \frac{R_A^S}{M^2_{B_{sA}^*}} \frac{1}{1 - q^2/M^2_{B_{sA}^*}} \tag{5.20}$$

$$h|_{pole} = \frac{1}{2}\frac{f_{B_{SA}^* B_c D_s^*}}{M^2_{B_{sA}^*}} \frac{f_T^{B_{SA}^*}}{1 - q^2/M^2_{B_{sA}^*}} = \frac{R_A^D}{M^2_{B_{sA}^*}} \frac{1}{1 - q^2/M^2_{B_{sA}^*}} \tag{5.21}$$

$$A_0(q^2)|_{pole} = \frac{g_{B_s^* B_c D_s^*}}{M^2_{B_s^*}} f_{B_s} \frac{q^2/M_B^2}{1 - q^2/M_B^2} = R_0 \frac{q^2/M^2_{B_s}}{1 - q^2/M^2_{B_s}} \tag{5.22}$$

where the quantities R_V, R_A^S, R_A^D and R_0 are related to the coupling constants $g_{B_s^* B_c D_s^*}, g_{B_{sA}^* B_c D_s^*}$ and $g_{B_{sA}^* B_c D_s^*}$, respectively. Here we would like to mention that the above mentioned couplings arises as the lower pole mass, because the higher pole masses of B_c meson do not contribute for the $B_c \to D_s^* \ell^+ \ell^-$ decay. The form factors $A_1(q^2), A_2(q^2)$ and $V(q^2)$ can be written in terms of these quantities as

$$V(q^2) = \frac{M_{B_c^-} + M_{D_s^*}}{m_b + m_s}\left[g_+(q^2) - \frac{R_V}{M^2_{B_s^*}} \frac{q^2}{1 - q^2/M^2_{B_s^*}}\right] \tag{5.23}$$

$$A_1(q^2) = \frac{M_{B_c^-} - M_{D_s^{*-}}}{m_b - m_s}\left[g_+(q^2) + \frac{q^2}{M^2_{B_c^-} - M^2_{D_s^{*-}}}\tilde{g}_-(q^2) + \frac{R_A^S}{M^2_{B_{sA}^*}} \frac{q^2}{1 - q^2/M^2_{B_{sA}^*}}\right] \tag{5.24}$$

$$A_2(q^2) = \frac{M_{B_c^-} + M_{D_s^{*-}}}{m_b - m_s}\left[g_+(q^2) - \frac{R_A^D}{M^2_{B_{As}^*}} \frac{q^2}{1 - q^2/M^2_{B_{sA}^*}}\right] - \frac{2M_{D_s^{*-}}}{M_{B_c} - M_{D_s^{*-}}} A_0(q^2) \tag{5.25}$$

Now, the behavior of $g_+(q^2), \tilde{g}_-(q^2)$ and $A_0(q^2)$ is known from LEET and their form is [85]

$$g_+(q^2) = \frac{\xi_\perp(0)}{(1 - q^2/M_B^2)^2} = -\tilde{g}_-(q^2) \tag{5.26}$$

$$A_0(q^2) = \left(1 - \frac{M^2_{D_s^{*-}}}{M_{B_c} E_{D_s^{*-}}}\right)\xi_\parallel(0) + \frac{M_{D_s^{*-}}}{M_{B_c}}\xi_\perp(0) \tag{5.27}$$

$$E_{D_s^*} = \frac{M_{B_c}}{2}\left(1 - \frac{q^2}{M^2_{B_c}} + \frac{M^2_{D_s^*}}{M^2_{B_c}}\right) \tag{5.28}$$

$$g_+(0) = \xi_\perp(0) \tag{5.29}$$

The pole terms given in Eqs.(5.23-5.25) dominate near $q^2 = M^2_{B^*_s}$ and $q^2 = M^2_{B^*_{sA}}$. Just to make a remark that relations obtained from the Ward identities can not be expected to hold for the whole q^2. Therefore, near $q^2 = 0$ and near the pole following parametrization is suggested [85]

$$F(q^2) = \frac{F(0)}{(1 - q^2/M^2)\,(1 - q^2/M'^2)} \tag{5.30}$$

where M^2 is $M^2_{B^*_s}$ or $M^2_{B^*_{sA}}$, and M' is the radial excitation of M. The parametrization given in Eq. (5.30) not only takes into account the corrections to single pole dominance suggested by the dispersion relation approach [87, 88] but also give the correction of off-mass shell-ness of the couplings of B^*_s and B^*_{sA} with the $B_c D^*_s$ channel.

Since $g_+(0)$ and $\tilde{g}_-(q^2)$ have no pole at $q^2 = M^2_{B^*_s}$, we get

$$V(q^2)(1 - \frac{q^2}{M^2_{B^*}})|_{q^2=M^2_{B^*}} = -R_V \left(\frac{M_{B_c} + M_{D^*_s}}{m_b - m_s}\right)$$

This becomes

$$R_V \equiv -\frac{1}{2} g_{B^*_s B_c D^*_s} f_{B^*_s} = -\frac{g_+(0)}{1 - M^2_{B^*}/M'^2_{B^*}} \tag{5.31}$$

and similarly

$$R^D_A \equiv \frac{1}{2} f_{B^*_{sA} B_c D^*_s} f_T^{B^*_{sA}} = -\frac{g_+(0)}{1 - M^2_{B^*_{sA}}/M'^2_{B^*_{sA}}} \tag{5.32}$$

We cannot use the parametrization given in Eq.(5.30) for the form factor $A_1(q^2)$, since near $q^2 = 0$, the behavior of $A_1(q^2)$ is $g_+(q^2)\left[1 - q^2/\left(M^2_{B_c^-} - M^2_{D_s^{*-}}\right)\right]$, therefore we can write $A_1(q^2)$ as follows

$$A_1(q^2) = \frac{g_+(0)}{\left(1 - q^2/M^2_{B^*_{sA}}\right)\left(1 - q^2/M'^2_{B^*_{sA}}\right)} \left(1 - \frac{q^2}{M^2_{B_c^-} - M^2_{D^*_s}}\right) \tag{5.33}$$

The only unknown parameter in the above form factors calculation is $g_+(0)$ and its value can be extracted by using the central value of branching ratio for the decay $B_c^- \to D_s^{*-}\gamma$ [100]. From the formula of decay rate

$$\Gamma\left(B_c \to D^*_s \gamma\right) = \frac{G_F^2 \alpha}{32\pi^4} \left|V_{tb} V^*_{ts}\right|^2 m_b^2 M^3_{B_c} \times \left(1 - \frac{M^2_{D^*_s}}{M_{B_c}}^2\right)^3 \left|C_7^{eff}\right|^2 |g_+(0)|^2 \tag{5.34}$$

From Eq.(5.34), the value of unknown parameter $g_+(0)$ is found to be $g_+(0) = 0.42$. Using $f_{B_c} = 0.35$ GeV we have prediction from Eq.(5.31) that

$$g_{B^*_s B_c D^*_s} = 10.38 GeV^{-1}. \tag{5.35}$$

Similarly the ratio of S and D wave couplings are found to be

$$\frac{g_{B^*_{sA}B_cD^*_s}}{f_{B^*_{sA}B_cD^*_s}} = -0.42GeV^2 \tag{5.36}$$

The different values of the $F(0)$ are

$$\begin{aligned} V(0) &= \frac{M_{B_c^-} + M_{D_s^{*-}}}{m_b + m_s} g_+(0) && (5.37)\\ A_1(0) &= \frac{M_{B_c^-} - M_{D_s^{*-}}}{m_b - m_s} g_+(0) && (5.38)\\ A_2(0) &= \frac{M_{B_c^-} + M_{D_s^{*-}}}{m_b - m_s} g_+(0) - \frac{2M_{D_s^{*-}}}{M_{B_c^-} - M_{D_s^{*-}}} A_0(0) && (5.39) \end{aligned}$$

The calculation of the numerical values of $V(0)$ and $A_1(0)$ is quite trivial but for the value of $A_2(0)$, the value of $A_0(0)$ has to be known. Although LEET does not give any relationship between $\xi_{||}(0)$ and $\xi_\perp(0)$, but in LCSR $\xi_{||}(0)$ and $\xi_\perp(0)$ are related due to numerical coincidence [96]

$$\xi_{||}(0) \simeq \xi_\perp(0) = g_+(0) \tag{5.40}$$

Thus from Eq. (5.27) we have

$$A_0(0) = 1.12 g_+(0)$$

For the other values of q^2 the form factors can be extrapolated as follows:

$$\begin{aligned} V(q^2) &= \frac{V(0)}{(1 - q^2/M^2_{B^*_s})(1 - q^2/M'^2_{B^*_s})} && (5.41)\\ A_1(q^2) &= \frac{A_1(0)}{(1 - q^2/M^2_{B^*_{sA}})(1 - q^2/M'^2_{B^*_{sA}})} \left(1 - \frac{q^2}{M^2_{B_c^-} - M^2_{D^*_s}}\right) && (5.42)\\ A_2(q^2) &= \frac{\tilde{A}_2(0)}{(1 - q^2/M^2_{B^*_{sA}})(1 - q^2/M'^2_{B^*_{sA}})} \\ &\quad - \frac{2M_{D_s^{*-}}}{M_{B_c^-} - M_{D_s^{*-}}} \frac{A_0(0)}{(1 - q^2/M^2_{B_s})(1 - q^2/M'^2_{B_s})} && (5.43) \end{aligned}$$

The behavior of the form factors $V(q^2)$, $A_1(q^2)$ and $A_2(q^2)$ which are given in Eqs.(5.41-5.43) are plotted as a function of q^2 shown in Fig.5.1. One can see that the value of the form factors increases with increasing q^2 except for $A_2(q^2)$ where the second term starts dominating at large q^2. This behavior of form factors also differs from the one calculated using three point QCD sum rules shown in Fig.5.2. The form factors obtained by QCD sum rules for the decay $B_c \to D_s^* \ell^+ \ell^-$[97] are given in Table 5.1

Table 5.1: The values of form factors at $q^2 = 0$ obtained by three point QCD sum rules [97]

	$B_c \to D_s^* l^+ l^-$
$A_V(0)$	0.54 ± 0.018
$A_0(0)$	0.30 ± 0.017
$A_+(0)$	0.36 ± 0.013
$A_-(0)$	-0.57 ± 0.04
$F_1(0)$	0.31 ± 0.017
$F_2(0)$	0.33 ± 0.016
$F_3(0)$	0.29 ± 0.034

(a) (b) (c)

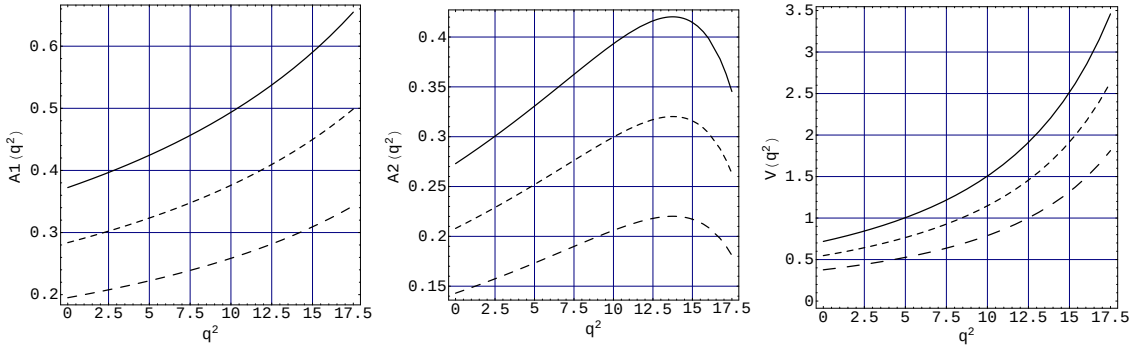

Figure 5.2: Form factors are plotted as a function of q^2. Solid line, dashed line and long-dashed line correspond to $g_+(0)$ equal to 0.42, 0.32 and 0.22 respectively.

5.4 Physical Observables for $B_c \to D_s^* \ell^+ \ell^-$

In this section we will present the calculations of the physical observables like the decay rates and the helicity fractions of D_s^* meson using the weak annihilation (WA) and the penguin amplitude that corresponds to the FCNC. From Eq. (2.17) it is straightforward to write the penguin amplitude

$$\mathcal{M}^{\rm PENG} = -\frac{G_F \alpha}{2\sqrt{2}\pi} V_{tb} V_{ts}^* \left[T_\mu^1 (\bar{l}\gamma^\mu l) + T_\mu^2 \left(\bar{l}\gamma^\mu \gamma^5 l\right)\right]$$

where

$$T_\mu^1 = f_1(q^2)\epsilon_{\mu\nu\alpha\beta}\varepsilon^{*\nu} p^\alpha k^\beta - i f_2(q^2)\varepsilon_\mu^* + i f_3(q^2)(\varepsilon^* \cdot q) P_\mu \quad (5.44)$$

$$T_\mu^2 = f_4(q^2)\epsilon_{\mu\nu\alpha\beta}\varepsilon^{*\nu} p^\alpha k^\beta - i f_5(q^2)\varepsilon_\mu^* + i f_6(q^2)(\varepsilon^* \cdot q) P_\mu \quad (5.45)$$

The functions f_1 to f_6 in Eq.(5.44) and Eq. (5.45) are known as auxiliary functions, which contain both long distance (form factors) and short distance (Wilson coefficients) effects and these can be written

(a) (b) (c)

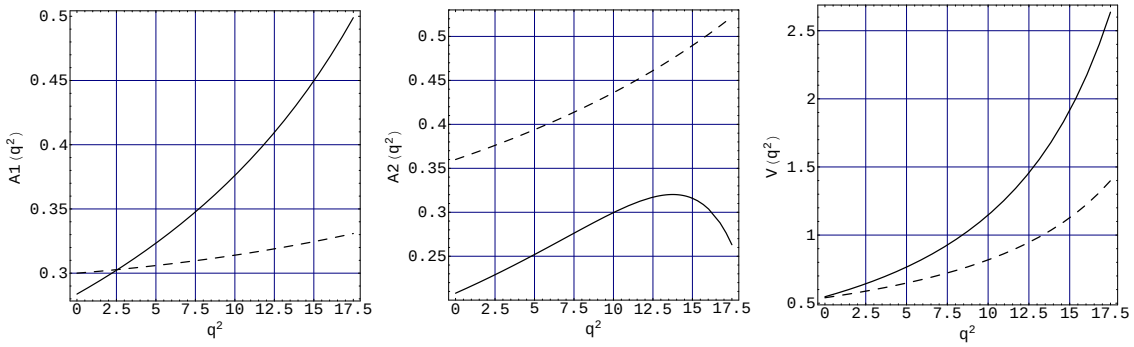

Figure 5.3: Form factors are plotted as a function of q^2. Solid line is drawn by using Ward Identities (our case) and dashed line is drawn by using 3 point QCD sum rules. In both cases we took the central value of the form factors.

as

$$
\begin{aligned}
f_1(q^2) &= 4(m_b+m_s)\frac{C_7^{eff}}{q^2}F_1(q^2)+2C_9^{eff}\frac{V(q^2)}{M_{B_c}+M_{D_s^*}} \\
f_2(q^2) &= \frac{C_7^{eff}}{q^2}2(m_b-m_s)F_2(q^2)\left(M_{B_c}^2-M_{D_s^*}^2\right)+C_9^{eff}A_1(q^2)\left(M_{B_c}+M_{D^*}\right) \\
f_3(q^2) &= \left[4\frac{C_7^{eff}}{q^2}(m_b-m_s)\left(F_2(q^2)+q^2\frac{F_3(q^2)}{\left(M_{B_c}^2-M_{D_s^*}^2\right)}\right)+C_9^{eff}\frac{A_2(q^2)}{M_{B_c}+M_{D_s^*}}\right] \\
f_4(q^2) &= C_{10}\frac{2V(q^2)}{M_{B_c}+M_{D_s^*}} \\
f_5(q^2) &= C_{10}A_1(q^2)\left(M_{B_c}+M_{D_s^*}\right) \\
f_6(q^2) &= C_{10}\frac{A_2(q^2)}{M_{B_c}+M_{D_s^*}} \\
f_0(q^2) &= C_{10}A_0(q^2)
\end{aligned}
\tag{5.46}
$$

The next task is to calculate the decay rate and the helicity fractions of the D_s^* meson in terms of these auxiliary functions.

5.4.1 The Differential Decay Rate of $B_c \to D_s^*\ell^+\ell^-$

In the rest frame of B_c meson the differential decay width of $B_c \to D_s^*\ell^+\ell^-$ can be written as

$$
\frac{d\Gamma(B_c\to D_s^*\mu^+\mu^-)}{dq^2}=\frac{1}{(2\pi)^3}\frac{1}{32M_{B_c}^3}\int_{-u(q^2)}^{+u(q^2)}du\,|\mathcal{A}|^2 \tag{5.47}
$$

where

$$
\mathcal{A} = \mathcal{M}^{\rm WA}+\mathcal{M}^{\rm PENG} \tag{5.48}
$$

$$
q^2 = (p_{l^+}+p_{l^-})^2 \tag{5.49}
$$

$$u = (p - p_{l^-})^2 - (p - p_{l^+})^2 \tag{5.50}$$

Now the limits on q^2 and u are

$$4m_l^2 \leq q^2 \leq (M_{B_c} - M_{D_s^*})^2 \tag{5.51}$$

$$-u(q^2) \leq u \leq u(q^2) \tag{5.52}$$

with

$$u(q^2) = \sqrt{\lambda\left(1 - \frac{4m_l^2}{q^2}\right)} \tag{5.53}$$

and

$$\lambda \equiv \lambda(M_{B_c}^2, M_{D_s^*}^2, q^2) = M_{B_c}^4 + M_{D_s^*}^4 + q^4 - 2M_{B_c}^2 M_{D_s^*}^2 - 2M_{D_s^*}^2 q^2 - 2q^2 M_{B_c}^2$$

Here m_l corresponds to the mass of the lepton which for our case are the μ and τ. The total decay rate for the decay $B_c \to D_s^* \ell^+ \ell^-$ can be expressed in terms of WA, penguin amplitude and interference of these two which takes the form

$$\frac{d\Gamma}{dq^2} = \frac{d\Gamma^{\rm WA}}{dq^2} + \frac{d\Gamma^{\rm PENG}}{dq^2} + \frac{d\Gamma^{\rm WA\text{-}PENG}}{dq^2} \tag{5.54}$$

with

$$\frac{d\Gamma^{\rm WA}}{dq^2} = \frac{G_F^2 \left|V_{cb}V_{cs}^*\right|^2 \alpha^2}{2^{11}\pi^5 3 M_{B_c}^3 M_{D_s^*}^2 q^2} u(q^2) \times g\left(q^2\right) \tag{5.55}$$

$$\frac{d\Gamma^{\rm PENG}}{dq^2} = \frac{G_F^2 \left|V_{tb}V_{ts}^*\right|^2 \alpha^2}{2^{11}\pi^5 3 M_{B_c}^3 M_{D_s^*}^2 q^2} u(q^2) \times h\left(q^2\right) \tag{5.56}$$

$$\frac{d\Gamma^{\rm WA\text{-}PENG}}{dq^2} = \frac{G_F^2 \left|V_{cb}V_{cs}^*\right| \left|V_{tb}V_{ts}^*\right| \alpha^2}{2^{11}\pi^5 3 M_{B_c}^3 M_{D_s^*}^2 q^2} u(q^2) \times I\left(q^2\right). \tag{5.57}$$

The function $u(q^2)$ is defined in Eq. (5.53) and $g(q^2)$, $h(q^2)$ and $I(q^2)$ are

$$\begin{aligned}
g\left(q^2\right) &= \frac{1}{2}\left(2m_l^2 + q^2\right)\kappa^2\Bigg[8\lambda M_{D_s^*}^2 q^2 \left(F_V^{D_s^*}(q^2)\right)^2 + \left(F_A^{D_s^*}(q^2)\right)^2 [12 M_{D_s^*}^2 q^2(\lambda \\
&\quad + 4M_{B_c}^2 q^2) + \lambda^2 + \lambda(\lambda + 4q^2 M_{D_s^*}^2 + 4q^4)]\Bigg] \\
h(q^2) &= 24\left|f_0(q^2)\right|^2 m_l^2 M_{D_s^*}^2 \lambda + 8M_{D_s^*}^2 q^2 \lambda(2m_l^2 + q^2)\left|f_1(q^2)\right|^2 - (4m_l^2 - q^2)\left|f_4(q^2)\right|^2] \\
&\quad + \lambda(2m_l^2 + q^2)\left|f_2(q^2) + (M_{B_c}^2 - M_{D_s^*}^2 - q^2) f_3(q^2)\right|^2 - (4m_l^2 - q^2)|f_5(q^2) \\
&\quad + (M_{B_c}^2 - M_{D_s^*}^2 - q^2) f_6(q^2)|^2] + 4M_{D_s^*}^2 q^2[(2m_l^2 + q^2)(3\left|f_2(q^2)\right|^2 - \lambda\left|f_3(q^2)\right|^2) \\
&\quad - (4m_l^2 - q^2)(3\left|f_5(q^2)\right|^2 - \lambda\left|f_6(q^2)\right|^2)] \\
I(q^2) &= 2\kappa[f_2(q^2) F_A^{D_s^*}(q^2) q^2 (2m_l^2 + q^2)(\lambda + 6M_{D_s^*}^2 (M_{B_c}^2 - M_{D_s^*}^2 + q^2)) \\
&\quad - (\lambda(2f_1(q^2) F_V^{D_s^*}(q^2) M_{D_s^*}^2 q^4 + f_3(q^2) F_A^{D_s^*}(q^2)(2m_l^2 + q^2)(\lambda + q^4 + 4M_{B_c} M_{D_s^*}))].
\end{aligned} \tag{5.58}$$

where

$$\kappa = \frac{8\pi^2 M_{D_s^*} f_{B_c} f_{D_s^*}}{(m_c^2 - m_s^2)\, q^2} \tag{5.59}$$

5.4.2 Helicity Fractions Of D_s^* In $B_c \to D_s^* \ell^+ \ell^-$

We now discuss the helicity fractions of D_s^* in $B_c \to D_s^* \ell^+ \ell^-$ which are interesting variables and as such are independent of the uncertainties arising due to form factors and other input parameters. The final state meson helicity fractions were already discussed in literature for $B \to K^* (K_1)\, \ell^+ \ell^-$ decays [50, 76]. Even for the K^* vector meson, the longitudinal helicity fraction f_L has been measured by Babar collaboration for the decay $B \to K^* l^+ l^- (l = e, \mu)$ in two bins of momentum transfer and the results are [83]

$$\begin{aligned} f_L &= 0.77^{+0.63}_{-0.30} \pm 0.07, \qquad 0.1 \leq q^2 \leq 8.41 GeV^2 \\ f_L &= 0.51^{+0.22}_{-0.25} \pm 0.08, \qquad q^2 \geq 10.24 GeV^2 \end{aligned} \tag{5.60}$$

while the average value of f_L in full q^2 range is

$$f_L = 0.63^{+0.18}_{-0.19} \pm 0.05, \quad q^2 \geq 0.1 GeV^2 \tag{5.61}$$

The explicit expression of the decay rate for $B_c^- \to D_s^{*-} l^+ l^-$ decay can be written in terms of longitudinal Γ_L and transverse components Γ_T as

$$\frac{d\Gamma_L(q^2)}{dq^2} = \frac{d\Gamma_L^{\rm WA}(q^2)}{dq^2} + \frac{d\Gamma_L^{\rm PENG}(q^2)}{dq^2} + \frac{d\Gamma_L^{\text{WA-PENG}}(q^2)}{dq^2} \tag{5.62}$$

$$\frac{d\Gamma_\pm(q^2)}{dq^2} = \frac{d\Gamma_\pm^{\rm WA}(q^2)}{dq^2} + \frac{d\Gamma_\pm^{\rm PENG}(q^2)}{dq^2} + \frac{d\Gamma_\pm^{\text{WA-PENG}}(q^2)}{dq^2} \tag{5.63}$$

$$\frac{d\Gamma_T(q^2)}{dq^2} = \frac{d\Gamma_+(q^2)}{dq^2} + \frac{d\Gamma_-(q^2)}{dq^2}. \tag{5.64}$$

where

$$\frac{d\Gamma_L^{\rm WA}(q^2)}{dq^2} = \frac{G_F^2 \left|V_{cb} V_{cs}^*\right|^2 \alpha^2}{2^{11}\pi^5} \frac{u(q^2)}{M_{B_c}^3} \times \frac{1}{3} A_L^{\rm WA} \tag{5.65}$$

$$\frac{d\Gamma_L^{\rm PENG}(q^2)}{dq^2} = \frac{G_F^2 \left|V_{tb} V_{ts}^*\right|^2 \alpha^2}{2^{11}\pi^5} \frac{u(q^2)}{M_{B_c}^3} \times \frac{1}{3} A_L^{\rm PENG} \tag{5.66}$$

$$\frac{d\Gamma_L^{\text{WA-PENG}}(q^2)}{dq^2} = \frac{G_F^2 \left|V_{cb} V_{cs}^*\right| \left|V_{tb} V_{ts}^*\right| \alpha^2}{2^{11}\pi^5} \frac{u(q^2)}{M_{B_c}^3} \times \frac{1}{3} A_L^{\text{WA-PENG}} \tag{5.67}$$

$$\frac{d\Gamma_\pm^{\rm WA}(q^2)}{dq^2} = \frac{G_F^2 \left|V_{cb} V_{cs}^*\right|^2 \alpha^2}{2^{11}\pi^5} \frac{u(q^2)}{M_{B_c}^3} \times \frac{2}{3} A_\pm^{\rm WA} \tag{5.68}$$

$$\tag{5.69}$$

$$\frac{d\Gamma_{\pm}^{\rm PENG}(q^2)}{dq^2} = \frac{G_F^2\,|V_{tb}V_{ts}^*|^2\,\alpha^2}{2^{11}\pi^5}\frac{u(q^2)}{M_{B_c}^3}\times\frac{4}{3}A_{\pm}^{\rm PENG} \tag{5.70}$$

$$\frac{d\Gamma_{\pm}^{\text{WA-PENG}}(q^2)}{dq^2} = \frac{G_F^2\,|V_{cb}V_{cs}^*|\,|V_{tb}V_{ts}^*|\,\alpha^2}{2^{11}\pi^5}\frac{u(q^2)}{M_{B_c}^3}\times\frac{2}{3}A_{\pm}^{\text{WA-EP}}. \tag{5.71}$$

The different functions appearing in above equation can be expressed in terms of auxiliary functions (c.f. Eq. (5.46)) as

$$\begin{aligned}
A_L^{\rm WA} &= \frac{\kappa^2}{4q^2M_{D_s^*}^2}\Bigg[\left(F_V^{D_s^*}(q^2)\right)^2\Big\{q^2\lambda(\lambda+4q^2M_{D_s^*}^2)-4M^2\lambda(2\lambda+8q^2M_{D_s^*}^2)\\
&\quad-q^2\left(M_{B_c}^2-M_{D_s^*}^2-q^2\right)^2\left(\lambda-2u^2(q^2)\right)\Big\}+\left(F_A^{D_s^*}(q^2)\right)^2\Big\{12\lambda q^2((M_{B_c}^2-M_{D_s^*}^2)^2-M_{D_s^*}^2)\\
&\quad-\lambda^2(q^2-4m_l^2)+q^2(8q^2M_{D_s^*}^2-\lambda)(M_{B_c}^2-M_{D_s^*}^2+q^2)^2\\
&\quad-2u^2(q^2)q^2((M_{B_c}^2-M_{D_s^*}^2)^2+q^4)+4m_l^2((M_{B_c}^2-M_{D_s^*}^2)^2-q^4)^2\Big\}\Bigg]\\
A_L^{\rm PENG} &= \frac{1}{2M_{D_s^*}^2q^2}[24\left|f_0(q^2)\right|^2m_l^2M_{D_s^*}^2\lambda+(2m_l^2+q^2)\left|(M_{B_c}^2-M_{D_s^*}^2-q^2)f_2(q^2)+\lambda f_3(q^2)\right|^2\\
&\quad+(q^2-4m_l^2)\left|(M_{B_c}^2-M_{D_s^*}^2-q^2)f_5(q^2)+\lambda f_6(q^2)\right|^2]\\
A_L^{\text{WA-PENG}} &= \frac{\kappa}{q^2M_{D_s^*}^2}\Bigg[\Re(f_1\left(q^2\right)F_V^{D_s^*}(q^2))\left\{(\lambda+4M_{D_s^*}^2q^2)\left(8m_l^2\sqrt{\lambda}+q^2(2u(q^2)-\sqrt{\lambda})\right)-4M_{D_s^*}^2q^2\lambda\right\}\\
&\quad+\Re(f_2\left(q^2\right)F_A^{D_s^*}(q^2))\Big\{q^2u^2(q^2)(M_{B_c}^2-M_{D_s^*}^2-q^2)+6q^2\lambda(M_{D_s^*}^2-M_{B_c}^2)\\
&\quad+q^2(\lambda-8q^2M_{D_s^*}^2)(M_{B_c}^2-M_{D_s^*}^2+q^2)-4m_l^2q^2(4q^2M_{D_s^*}^2+\lambda)\Big\}\\
&\quad+\Re(f_3\left(q^2\right)F_A^{D_s^*}(q^2))\Big\{\lambda^2(4m_l^2-q^2)+q^4(q^2u(q^2)\sqrt{\lambda}\\
&\quad-6\lambda(M_{B_c}^2+M_{D_s^*}^2))+q^2(M_{B_c}^2-M_{D_s^*}^2)(6\lambda-u^2(q^2))\Big\}\Bigg]\\
A_{\pm}^{\rm WA} &= \kappa^2\left[\left(2m_l^2+q^2\right)\left[\lambda\left(F_V^{D_s^*}(q^2)\right)^2+\left(F_A^{D_s^*}(q^2)\right)^2\left(\lambda+4M_{D_s^*}^2q^2\right)\right]\right]\\
A_{\pm}^{\rm PENG} &= (q^2-4m_l^2)\left|f_5(q^2)\mp\sqrt{\lambda}f_4(q^2)\right|^2+\left(q^2+2m_l^2\right)\left|f_2(q^2)\pm\sqrt{\lambda}f_1(q^2)\right|^2\\
A_{\pm}^{\text{WA -PENG}} &= -\kappa\Big\{2\sqrt{\lambda}(q^2-4m_l^2)\Re(f_2\left(q^2\right)F_V^{D_s^*}(q^2))+4\lambda(q^2+2m_l^2)\Re(f_1\left(q^2\right)F_V^{D_s^*}(q^2))\\
&\quad\pm2(q^2+2m_l^2)(M_{B_c}^2-M_{D_s^*}^2+q^2)[2\Re[(f_1\left(q^2\right)F_A^{D_s^*}(q^2))]\sqrt{\lambda}\mp2\Re(f_2\left(q^2\right)F_V^{D_s^*}(q^2))]\Big\}
\end{aligned} \tag{5.72}$$

Finally the longitudinal and transverse helicity amplitude becomes

$$\begin{aligned}
f_L(q^2) &= \frac{d\Gamma_L(q^2)/dq^2}{d\Gamma(q^2)/dq^2}\\
f_{\pm}(q^2) &= \frac{d\Gamma_{\pm}(q^2)/dq^2}{d\Gamma(q^2)/dq^2}\\
f_T(q^2) &= f_+(q^2)+f_-(q^2)
\end{aligned} \tag{5.73}$$

so that the sum of the longitudinal and transverse helicity amplitudes is equal to one i.e. $f_L(q^2) + f_T(q^2) = 1$ for each value of q^2.

5.5 Numerical Analysis.

In this section we present the numerical analysis of the branching ratio and helicity fractions of D_s^* meson both in the SM and in ACD model. Among the different input parameters the important one are the form factors which are the major source of uncertainties. To study the above mentioned physical observables we use two different form factors, in one where we parameterized the form factors in terms of double pole and then relate them through the Ward identities which are given in Section 5.3, the other one obtained by three point QCD sum rules given in Table 5.1 . The differences in the results obtained in physical observables using two different approaches of form factors represents an indication of the error related to the hadronic uncertainty. We have used next-to-leading order approximation for the Wilson Coefficients at the renormalization scale $\mu = m_b$. It has already been mentioned that besides the contribution in the C_9^{eff}, there are long distance contributions resulting from the $c\bar{c}$ resonances like J/ψ and its excited states. For the present analysis we do not take into account these long distance effects. The numerical results for the branching ratio and helicity fractions of D_s^* for the decay mode $B_c \to D_s^* \ell^+ \ell^-$ using the form factors given in section 5.3 and QCD sum rules are depicted in Figs. 5.4-5.9, both in the SM and the ACD model. Figs. (5.4-5.5) represents the branching ratio of $B_c \to D_s^* \ell^+ \ell^-$ decay. One can clearly see from the Figs.(5.4) and (5.5) that the branching ratio is increased due to the increment in the inverse of the compactification radius R of the KK-contribution, while at the larger values of the inverse of the compactification radius R the branching ratio is shifted towards the SM. We have also displayed the numerical results of the branching ratio for the decay $B_c \to D_s^* \ell^+ \ell^-$ separately for penguin, WA and combination of both are given in Table 5.2.

Table 5.2: Branching ratio for $B_c \to D_s^* \mu^+ \mu^- (\tau^+ \tau^-)$ decay in the SM.

	Form factors defined in section 5.3	QCD Sum Rule
$BR^{(\text{PENG})}(B_c \to D_s^* \mu^+ \mu^- (\tau^+ \tau^-))$	$4.17 \times 10^{-7} (2.22 \times 10^{-8})$	$2.57 \times 10^{-7} \left(1.13 \times 10^{-8}\right)$
$BR^{(\text{WA})}(B_c \to D_s^* \mu^+ \mu^- (\tau^+ \tau^-))$	$2.82 \times 10^{-6} \left(0.92 \times 10^{-9}\right)$	$2.20 \times 10^{-6} \left(0.35 \times 10^{-9}\right)$
$BR^{(\text{Total})}(B_c \to D_s^* \mu^+ \mu^- (\tau^+ \tau^-))$	$3.24 \times 10^{-6} \left(3.03 \times 10^{-8}\right)$	$2.46 \times 10^{-6} \left(1.49 \times 10^{-8}\right)$

From table 5.2 one can also see that the branching ratio for the decay $B_c \to D_s^* \mu^+ \mu^-$ obtained from the WA is about 5 times larger than the corresponding penguin one. It is therefore expected that these WA contributions will reduce the new physics effects in helicity fractions of the final state meson.

In general the sensitivity of NP on the branching ratio is effected by the uncertainties which arises due to the number of different input parameters. Among them the major one lies in the numerical analysis of $B_c \to D_s^* \ell^+ \ell^-$ decay originated from the $B_c \to D_s^*$ transition form factors. The large uncertainties

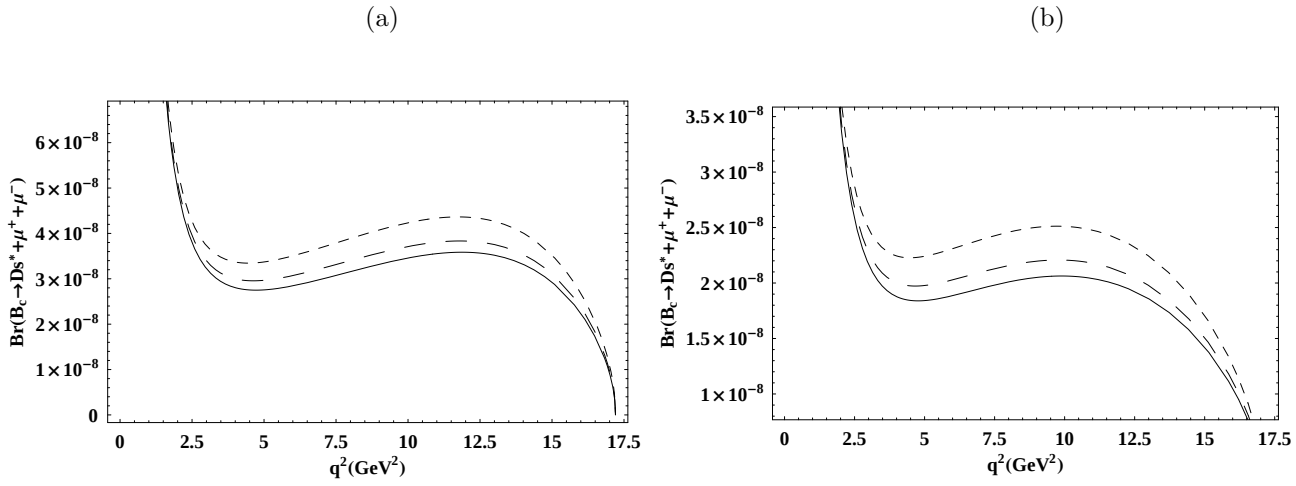

Figure 5.4: (a)Branching ratio using double pole parametrization and (b) using three point QCD sum rules for the $B \to D_s^* \mu^+ \mu^-$ decay as functions of q^2 for different values of $1/R$. Solid line correspond to SM value,dashed line is for $1/R = 300$, long dashed is for $1/R = 500$.

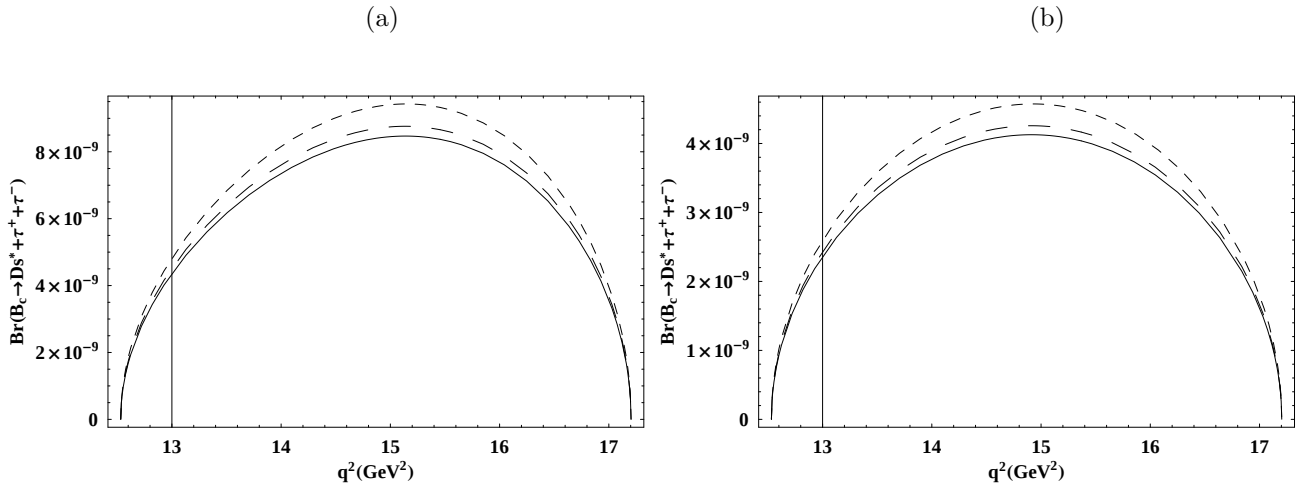

Figure 5.5: Branching ratio for the decay $B_c \to D_s^* \tau^+ \tau^-$. The legends are same as that of Fig.5.4

involved in the form factors are mainly from the variations of the decay constant of B_c meson and also there are some uncertainties from the strange quark mass m_s. The latter are expected to be tiny on account of the negligible role of m_s suppressed by the much larger energy scale of m_b. Moreover, the uncertainties of the charm quark and bottom quark mass are at the 1% level, which will not play significant role in the numerical analysis and can be dropped out safely. It also needs to be stressed that these hadronic uncertainties almost have no influence on the various asymmetries including the polarization asymmetries of final state meson on account of the cancelation among different polarization states and this make them as one of the best tools to look for physics beyond the SM.

Figs. 5.6 (a, b, c, d) and 5.7(a, b, c, d) show the longitudinal and transverse helicity fractions of D_s^* for the decay $B_c \to D_s^* \mu^+ \mu^-$ as a function of q^2, where we have used the form factors calculated in

Section 5.3. Choosing the different values of the compactification radius $1/R$, one can see from these figures that the effect of extra dimensions are visible at low q^2 region. In this case these effects interfere constructively to the SM value for the case of transverse helicity fraction and destructive for the case of longitudinal helicity fraction. Just to see their dependence on the choice of the form factors we have plotted these longitudinal and transverse helicity fractions of D_s^* in Figs. 6 (a, b) using three point QCD sum rules form factors (c.f. Table 5.1). Here we want to emphasize that the behavior of longitudinal and transverse helicity fraction changes when we consider WA (c.f. Figs. 5.6(b,d) and 5.7(b,d)) contribution in addition to the penguin one (c.f. Figs. 5.6(a,c) and 5.7(a,c)). This is due to the large contribution of WA amplitude in the decay rate of $B_c \to D_s^* \mu^+ \mu^-$.

Figs. 5.8(a, b, c, d) and 5.9(a, b, c, d) show the longitudinal and transverse helicity fractions of D_s^* for the decay $B_c \to D_s^* \tau^+ \tau^-$ decay as a function of q^2 for the form factors given in section 5.3 and three point QCD sum rules. Here one can see that the shift from the SM value is very mild for both choices of form factors as well as due to the WA contribution.

Here one can see that the helicity fractions of the final state meson have mild dependence on the choice of form factors and NP effects are quite significant in the lower q^2 region. Moreover from Figs. 5.6-5.9 it is clear that for each value of the momentum transfer q^2 the sum of the longitudinal and transverse helicity fractions are equal to one, i.e. $f_L(q^2) + f_T(q^2) = 1$.

5.6 Conclusion:

We have investigated the semileptonic decay $B_c \to D_s^* \ell^+ \ell^-$ by including both the penguin and WA contributions. In particular we found that branching ratio obtained from WA amplitude is 6.7 times large as compared to penguin amplitude for $B_c \to D_s^* \ell^+ \ell^-$ decay. In order to calculate the WA form factors $F_V^{D_s^*}(q^2)$ and $F_A^{D_s^*}(q^2)$, we use Eqs. (5.2, 5.3, 5.4), where the value of the form factors at $q^2 = 0$ can be obtained from QCD sum rules [100]. However for the penguin amplitude the form factors for the above mentioned decay are calculated using the framework of Ward identities which is discussed in Section-5.3. Here we have also compared the values of our form factors with the ones calculated using three point QCD sum rules [97].

The form factors contributing to the penguin amplitudes were calculated in the framework of Ward identities which can be expressed in terms of a single universal constant $g_+(0)$. The value of $g_+(0) = (0.42)$ is obtained from the decay $B_c \to D_s^* \gamma$ [100]. Considering the radial excitation at lower pole masses M (where $M = M_{B_s^*}$ and $M_{B_{sA}^*}$) one can predict the coupling of B_s^* with $B_c D_s^*$ channel as indicated in Eq.(5.35) which is $g_{B_s^* B_c D_s^*} = 10.38$ GeV^{-1}. Also we predicted the ratio of S and D wave couplings $\frac{g_{B_{sA}^* B_c D_s^*}}{f_{B_{sA}^* B_c D_s^*}} = -0.42\ GeV^2$ given in Eq.(5.36). We have studied the physical observables such as the branching ratio and the helicity fraction of D_s^* in the decay $B_c \to D_s^* \ell^+ \ell^-$ both in SM and in the

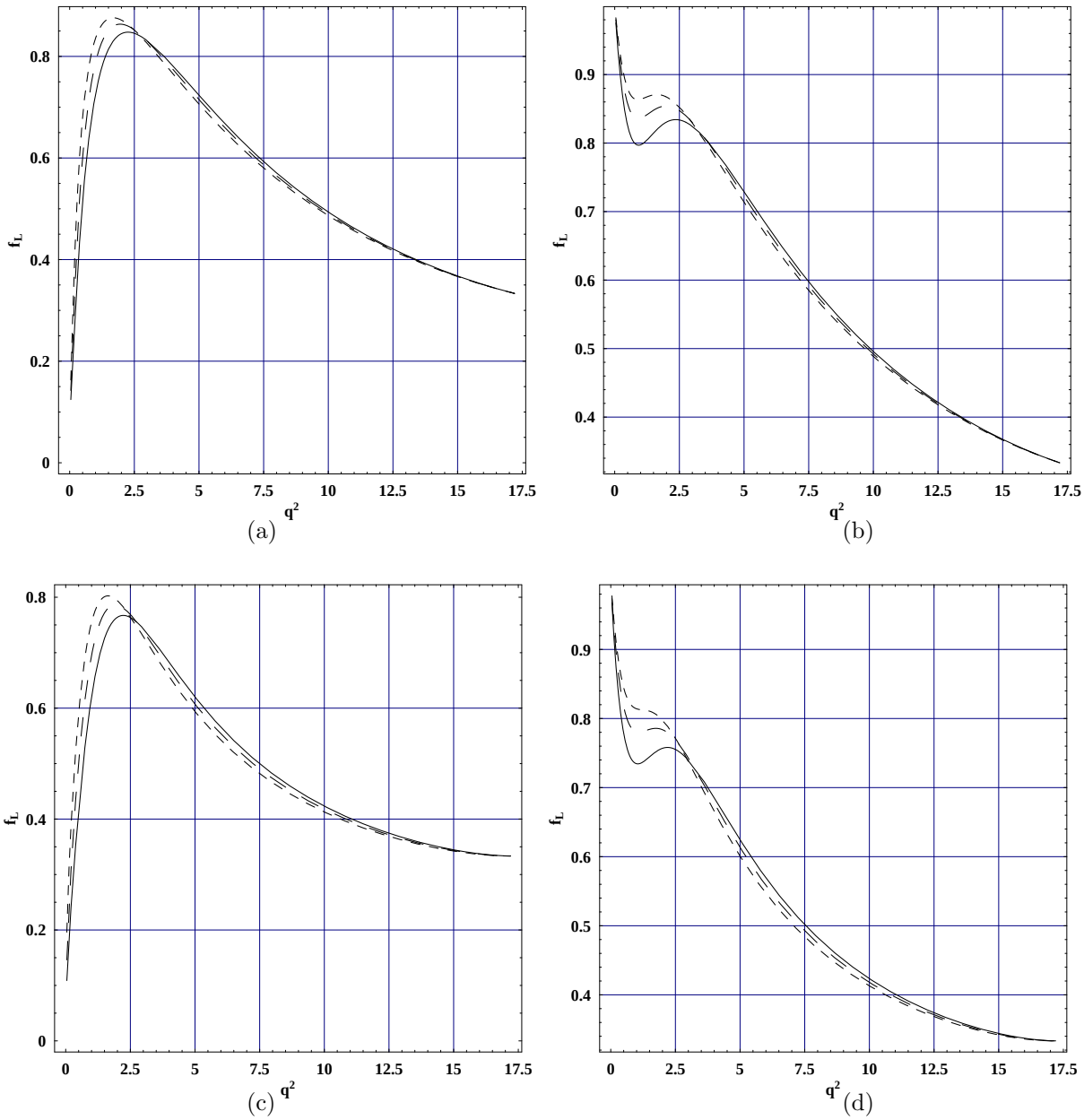

Figure 5.6: Longitudinal helicity fraction for the $B \to D_s^* \mu^+ \mu^-$ as a function of q^2 for different values of $1/R$.The legends are same as that of Fig 5.4.

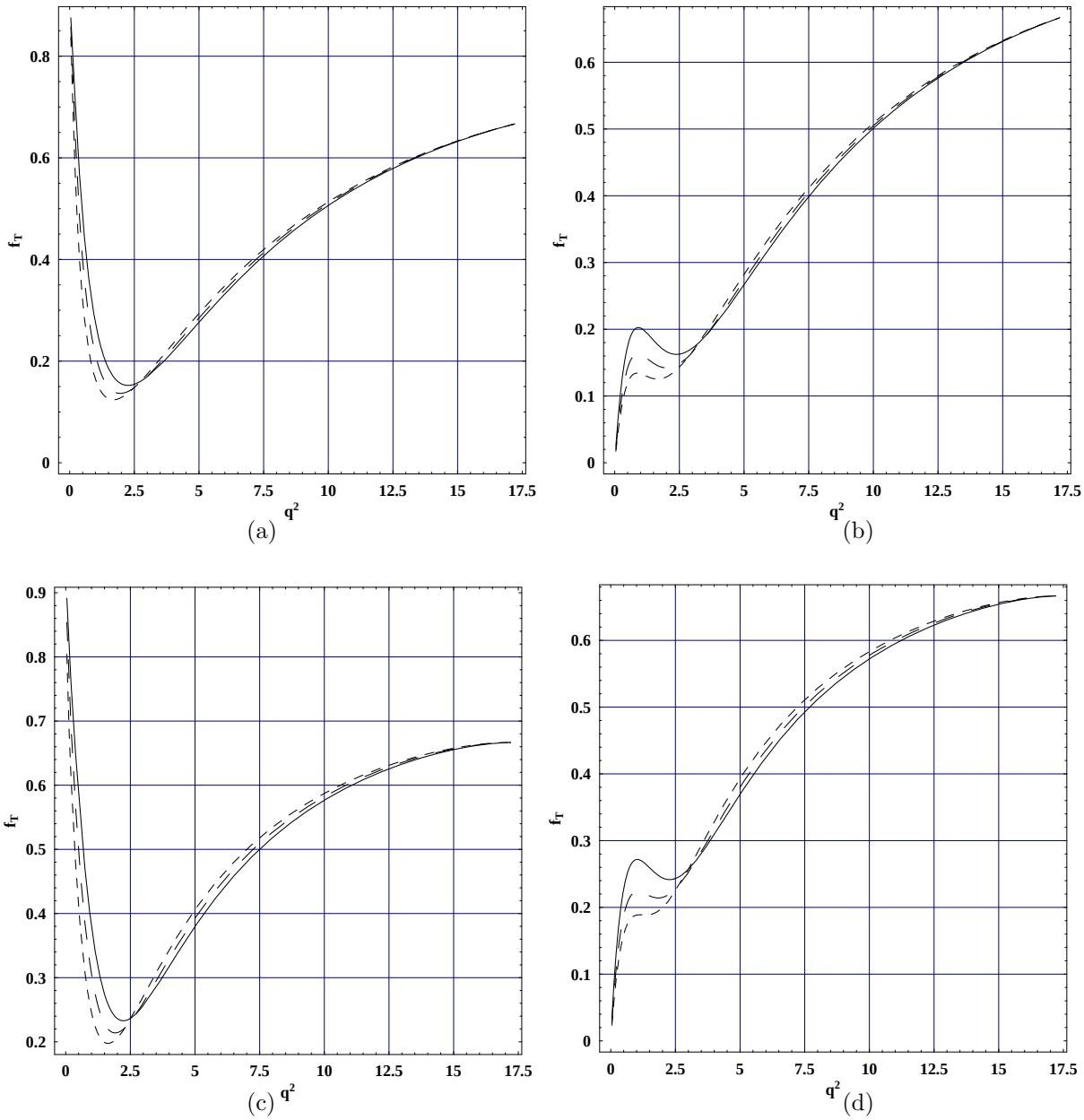

Figure 5.7: Transverse helicity fraction for the $B \to D_s^* \mu^+ \mu^-$ as a function of q^2 for different values of $1/R$.The legends are same as that of Fig 5.4.

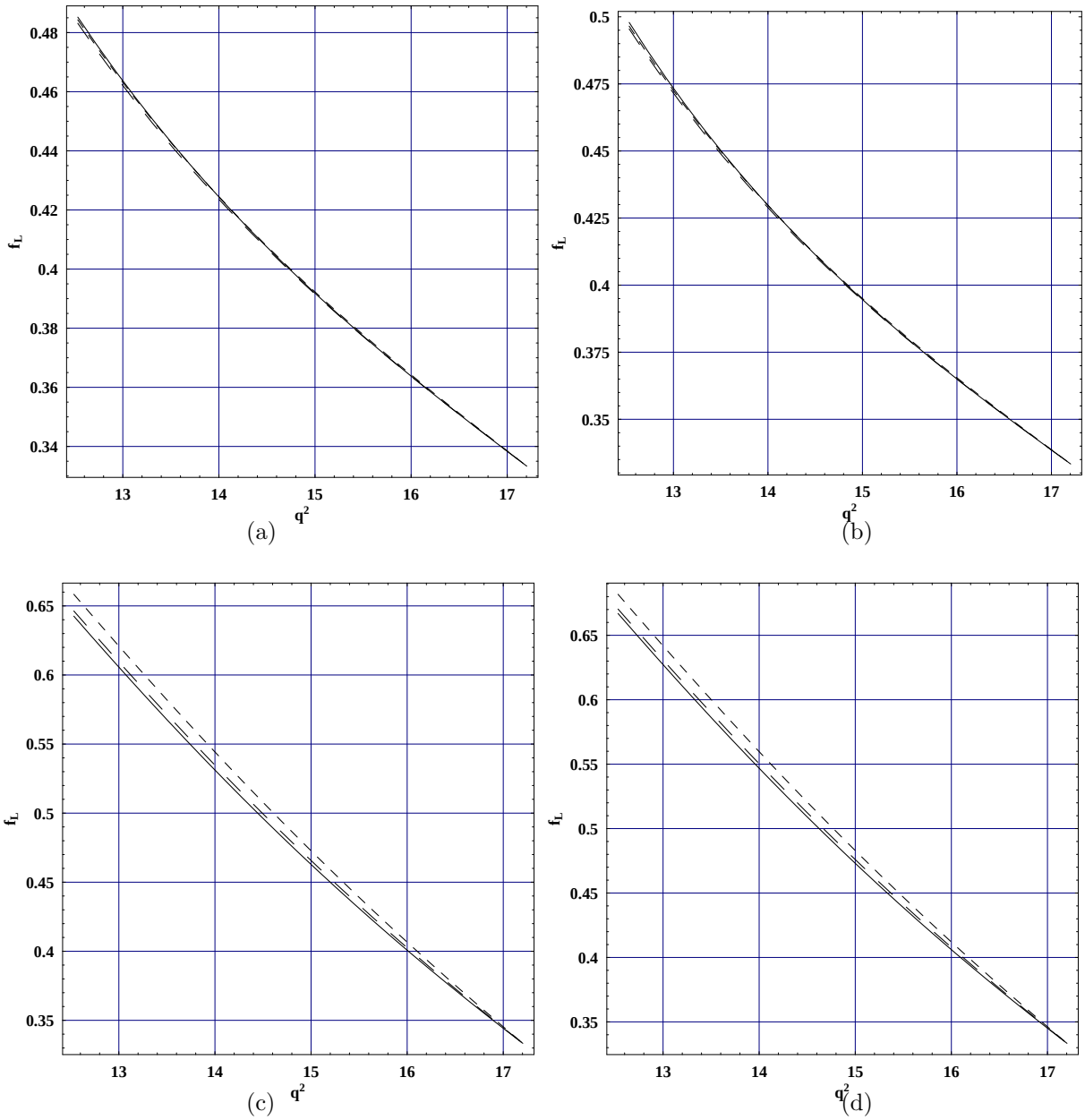

Figure 5.8: Longitudinal helicity fraction for the $B \to D_s^* \tau^+ \tau^-$ as a function of q^2 for different values of $1/R$.The legends are same as that of Fig 5.4.

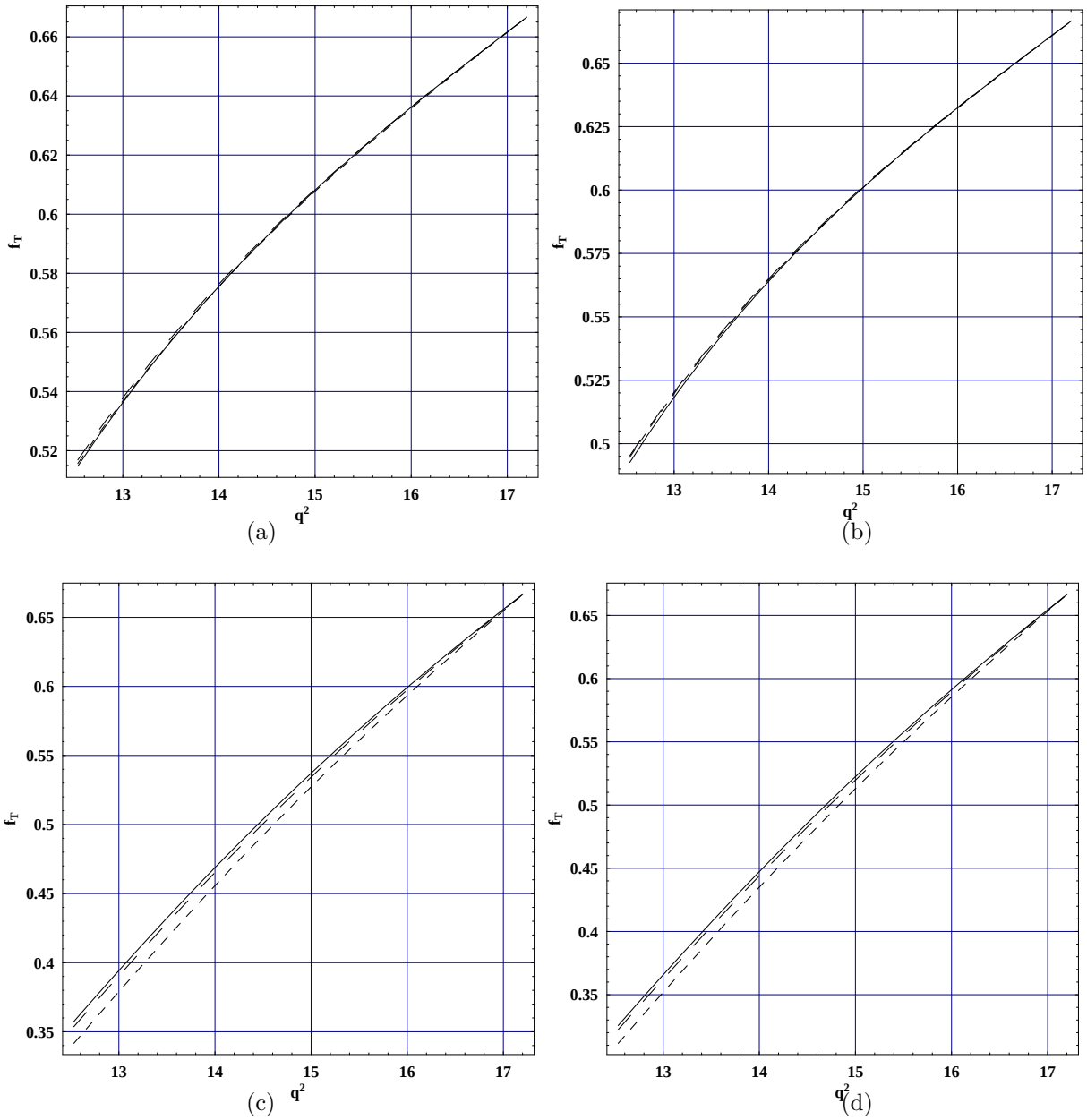

Figure 5.9: Transverse helicity fraction for the $B \to D_s^* \tau^+ \tau^-$ as a function of q^2 for different values of $1/R$. The legends are same as that of Fig 5.4.

ACD model. We have seen that the effects of ACD model in the helicity fractions of D_s^* meson for the decay $B_c \to D_s^* \mu^+ \mu^-$ are quite significant at low q^2 region. Furthermore to see the sensitivity of the said physical observables on the choice of form factors against q^2 using the three point QCD sum rules form factors. We have shown that the helicity fractions of the final state meson have weak dependence on the choice of form factors which make them good tool to look for NP which we hope to be seen at LHC.

In short, the experimental measurements of the extra dimensions effects in the above mentioned observables at LHC will be a useful tool to describe the status of physics beyond the SM. Further we are hopeful that when more data will be collected at LHC, it will not only test the SM but also puts some stringent constraints on the compactification radius $1/R$.

Bibliography

[1] S. W. Herb et al., Phys. Rev. Lett. **39** (1977) 252.

[2] P. F. Harrison and H. R. Quinn [BABAR Collaboration], The BaBar physics book: Physics at an asymmetric B factory, SLAC-R-0504 Papers from Workshop on Physics at an Asymmetric B Factory (BaBar Collaboration Meeting), Rome, Italy, 11-14 Nov 1996, Princeton, NJ, 17-20 Mar 1997, Orsay, France, 16-19 Jun 1997 and Pasadena, CA, 22-24 Sep 1997.

[3] S. Mori et al. [BELLE Collaboration], Nucl. Instrum. Meth. A **479** (2002) 117.

[4] Y. Kubota et al. [CLEO Collaboration], Nucl. Instrum. Meth. A **320** (1992) 66.

[5] D. Abbaneo et al. [ALEPH Collaboration], Combined results on b-hadron production rates, lifetimes, oscillations and semileptonic decays, arXiv:hep-ex/0009052.

[6] F. Abe et al. [CDF Collaboration], Nucl. Instrum. Meth. A **271** (1988) 387; S. Abachi et al. [D0 Collaboration], Nucl. Instrum. Meth. A **338** (1994) 185.

[7] S. L. Glashow, J. Iliopoulos, and L. Maiani, Phys. Rev. **D2**, 1285 (1970).

[8] M. S. Alam et al. Phys. Rev. Lett. **74**, 2885 (1995).

[9] R. Ammar et al., Phys. Rev. Lett. **71**, 674 (1993); CLEO CONF 96-05 (1996).

[10] S.R. Choudhury, N. Gaur, N. Mahajan, Phys. Rev. D 66, 054 003 (2002) [arXiv:hep-ph/0203041]; S.R. Choudhury, N. Gaur, arXiv:hep-ph/0205076; S.R. Choudhury, N. Gaur, arXiv:hep-ph/0207353.

[11] U.O. Yilmaz, B.B. Sirvanli, G. Turan, Nucl. Phys. 692, 249 (2004) [arXiv:hep-ph/0407006]; U.O. Yilmaz, B.B. Sirvanli, G. Turan, Eur. Phys. J. C 30, 197 (2003) [arXiv:hep-ph/0304100].

[12] A. Ali, P. Ball, L.T. Handoko, G. Hiller, Phys. Rev. D 61, 074 024 (2000) [arXiv:hep-ph/9910221]; A. Ali, E. Lunghi, C. Greub, G. Hiller, Phys. Rev. D 66, 034 002 (2002) [arXiv:hep-ph/0112300].

[13] T.M. Aliev, M.K. Cakmak, M. Savci, Nucl. Phys. B 607, 305 (2001) [arXiv:hep-ph/0009133]; T.M. Aliev, A. Ozpineci, M. Savci, C. Yuce, Phys. Rev. D 66, 115 006 (2002) [arXiv:hep-ph/0208128]; T.M. Aliev, A. Ozpineci, M. Savci, Phys. Lett. B 511, 49 (2001) [arXiv:hep-ph/0103261]; T.M.

Aliev, M. Savci, Phys. Lett. B 481, 275 (2000) [arXiv:hep-ph/0003188];T.M. Aliev, D.A. Demir, M. Savci, Phys. Rev. D 62, 074 016 (2000) [arXiv:hep-ph/9912525]; T.M. Aliev, C.S. Kim, Y.G. Kim, Phys. Rev. D 62, 014 026 (2000) [arXiv:hep-ph/9910501]; T.M. Aliev, E.O. Iltan, Phys. Lett. B 451, 175 (1999) [arXiv:hep-ph/9804458]; T.M. Aliev, V. Bashiry, M. Savci, JHEP 0405, 037 (2004) [arXiv:hep-ph/0403282]; T.M. Aliev, V. Bashiry, M. Savci, Phys. Rev. D 71, 035 013 (2005) [arXiv:hep-ph/0411327]; T.M.Aliev, M.Savci, Eur. Phys. J. C 50, 91 (2007)

[14] C.H. Chen, C.Q. Geng, Phys. Rev. D 66, 034 006 (2002) [arXiv:hep-ph/0207038]; C.H. Chen, C.Q. Geng, Phys. Rev. D 66, 014 007 (2002) [arXiv:hep-ph/0205306].

[15] G. Erkol, G. Turan, Nucl. Phys. B 635, 286 (2002) [arXiv:hep-ph/0204219]; E.O. Iltan, G. Turan, I. Turan, J. Phys. G 28, 307 (2002) [arXiv:hep-ph/0106136].

[16] W.J. Li, Y.B. Dai, C.S. Huang, arXiv:hep-ph/0410317.

[17] Q.S. Yan, C.S. Huang, W. Liao, S.H. Zhu, Phys. Rev. D 62, 094 023 (2000) [arXiv:hep-ph/0004262].

[18] S.R. Choudhury, N. Gaur, A.S. Cornell, G.C. Joshi, Phys. Rev. D 68, 054 016 (2003) [arXiv:hep-ph/0304084]; S.R. Choudhury, A.S. Cornell, N. Gaur, G.C. Joshi, Phys. Rev. D 69, 054 018 (2004) [arXiv:hep-ph/0307276].

[19] F. Kruger, E. Lunghi, Phys. Rev. D 63, 014 013 (2001) [arXiv:hep-ph/0008210].

[20] R. Mohanta, A.K. Giri, arXiv:hep-ph/0611068.

[21] C.S. Kim et al., Phys. Lett. B 218 (1989) 343; X. G. He et al., Phys. Rev. D 38 (1988) 814; B. Grinstein et al., Nucl. Phys. B 319 (1989) 271; N. G. Deshpande et al., Phys. Rev. D 39 (1989) 1461; P. J. ODonnell and H. K. K. Tung, Phys. Rev. D 43 (1991) 2067; N. Paver and Riazuddin, Phys. Rev. D 45 (1992) 978; J. L. Hewett, Phys. Rev. D 53, 4964 (1996); T. M. Aliev, V. Bashiry, and M. Savci, Eur. Phys. J. C 35, 197 (2004); T. M. Aliev, V. Bashiry, and M. Savci, Phys. Rev. D 72, 034031 (2005); T. M. Aliev, V. Bashiry, and M. Savci, J. High Energy Phys. 05 (2004) 037; T. M. Aliev, V. Bashiry, and M. Savci, Phys. Rev. D 73, 034013 (2006); T. M. Aliev, V. Bashiry, and M. Savci, Eur. Phys. J. C 40, 505 (2005); F. Kruger and L. M. Sehgal Phys. Lett. B 380, 199 (1996); Y. G. Kim, P. Ko, and J. S. Lee,Nucl. Phys. B544, 64 (1999); Chuan-Hung Chen and C. Q. Geng, Phys. Lett. B 516, 327 (2001); V. Bashiry, Chin. Phys. Lett. 22, 2201 (2005); W.S. Hou, A. Soni and H. Steger, Phys. Lett. B 192, 441 (1987); W.S. Hou, R.S. Willey and A. Soni, Phys. Rev. Lett. 58, 1608 (1987) [Erratum-ibid. 60, 2337 (1987)]; T. Hattori, T. Hasuike and S. Wakaizumi, Phys. Rev. D 60, 113008 (1999); T.M. Aliev, D.A. Demir and N.K. Pak, Phys. Lett. B 389, 83 (1996); Y. Dincer, Phys. Lett. B 505, 89 (2001) and references therin; C.S. Huang, W.J. Huo and Y.L. Wu, Mod. Phys. Lett. A 14, 2453 (1999); C.S. Huang, W.J. Huo and Y.L. Wu, Phys. Rev. D 64, 016009 (2001).

[22] A. Ali, T. Mannel and T. Morosumi, Phys. Lett. B 273, 505 (1991).

[23] T. Goto *et al.*, Phys. Rev. D **55** (1997) 4273; T.Goto *et al.*, Phys. Rev. D **58** (1998) 094006; S.Bertolini *et al.*, Nucl. Phys. B **353** (1991) 591.

[24] Andrzej J. Buras and Robert Fleischer, Adv.Ser.Direct.HighEnergyPhys.15:65-238,1998.

[25] C.S. Kim et al., Phys. Lett. B 218 (1989) 343; X. G. He et al., Phys. Rev. D 38 (1988) 814; B. Grinstein et al., Nucl. Phys. B 319 (1989) 271; N. G. Deshpande et al., Phys. Rev. D 39 (1989) 1461; P. J. ODonnell and H. K. K. Tung, Phys. Rev. D 43 (1991) 2067; N. Paver and Riazuddin, Phys. Rev. D 45 (1992) 978; J. L. Hewett, Phys. Rev. D 53, 4964 (1996); T. M. Aliev, V. Bashiry, and M. Savci, Eur. Phys. J. C 35, 197 (2004); T. M. Aliev, V. Bashiry, and M. Savci, Phys. Rev. D 72, 034031 (2005); T. M. Aliev, V. Bashiry, and M. Savci, J. High Energy Phys. 05 (2004) 037; T. M. Aliev, V. Bashiry, and M. Savci, Phys. Rev. D 73, 034013 (2006); T. M. Aliev, V. Bashiry, and M. Savci, Eur. Phys. J. C 40, 505 (2005); F. Kruger and L. M. Sehgal Phys. Lett. B 380, 199 (1996); Y. G. Kim, P. Ko, and J. S. Lee,Nucl. Phys. B544, 64 (1999); Chuan-Hung Chen and C. Q. Geng, Phys. Lett. B 516, 327 (2001); V. Bashiry, Chin. Phys. Lett. 22, 2201 (2005); W.S. Hou, A. Soni and H. Steger, Phys. Lett. B 192, 441 (1987); W.S. Hou, R.S. Willey and A. Soni, Phys. Rev. Lett. 58, 1608 (1987) [Erratum-ibid. 60, 2337 (1987)]; T. Hattori, T. Hasuike and S. Wakaizumi, Phys. Rev. D 60, 113008 (1999); T.M. Aliev, D.A. Demir and N.K. Pak, Phys. Lett. B 389, 83 (1996); Y. Dincer, Phys. Lett. B 505, 89 (2001) and references therin; C.S. Huang, W.J. Huo and Y.L. Wu, Mod. Phys. Lett. A 14, 2453 (1999); C.S. Huang, W.J. Huo and Y.L. Wu, Phys. Rev. D 64, 016009 (2001).

[26] D. Melikhov et al., Phys. Lett. B 430, 332 (1998); J.M. Soares, Nucl. Phys. B367, 575 (1991); G.M. Asatrian and A. Ioannisian, Phys. Rev. D 54, 5642 (1996); J.M. Soares, Phys. Rev. D 53, 241 (1996).

[27] C. H. Chen and C. Q. Geng, Phys. Rev. D 64, 074001 (2001).

[28] Erin De Pree, G. Marshall and Marc Sher, The Fourth Generation t-prime in Extensions of the Standard Model, arXiv: 0906.4500 [hep-ph].

[29] C. Amsler et al. [Particle Data Group], Phys. Lett. B667 (2008) 1.

[30] M. Maltoni, V. A. Novikov, L. B. Okun, A. N. Rozanov and M. I. Vysotsky, Phys. Lett. B476 (2000) 107 [arXiv:hepph/ 9911535]; H. J. He, N. Polon- sky and S. f. Su, Phys. Rev. D64 (2001) 053004 [arXiv:hep-ph/0102144]; B. Holdom, Phys. Rev. D54 (1996) 721 [arXiv:hep-ph/9602248].

[31] G. D. Kribs, T. Plehn, M. Spannowsky, and T. M. P. Tait, Phys. Rev. D 76, 075016 (2007).

[32] W. S. Hou and C. Y. Ma, Phys. Rev. D82 (2010) 036002.

[33] S. Bar-Shalom, D. Oaknin and A. Soni, Phys. Rev. D80 (2009) 015011.

[34] A. J. Buras, B. Duling, T. Feldmann, T. Heidsieck, C. Promberger and S. Recksiegel, JHEP 1009 (2010) 106.

[35] A. Soni, A. K. Alok, A. Giri, R. Mohanta and S. Nandi, Phys. Lett. B683 (20100 302; A. Soni, A. K. Alok, A. Giri, R. Mohanta and S. Nandi, Phys. Rev. D82 (2010) 033009; A. K. Alok, A. Dighe and D. London, Phys. Rev. D83 (2011) 073008.

[36] O. Eberhardt, A. Lenz and J. Rohrwild, Phys. Rev. D82 (2010) 095006.

[37] B. Holdom, Phys. Rev. Lett. 57 (1986) 2496 [Erratum-ibid. 58 (1987) 177].

[38] C. T. Hill, M. A. Luty and E. A. Paschos, Phys. Rev. D43 (1991) 3011.

[39] T. Elliott and S. F. King, Phys. Lett. B283 (1992) 371.

[40] P.Q. Hung and C. Xiong, Nucl. Phys. B848 (2011) 288.

[41] B. Holdom, JHEP 0608 (2006) 076;B. Holdom, W. S. Hou, T. Hurth, M. L. Mangano, S. Sultansoy and G. Unel, PMC Phys. A3 (2009) 4.

[42] P. Q. Hung and M. Sher, Phys. Rev. D77 (2008) 037302; P. Q. Hung, C. Xiong, Phys. Lett. B694 (2011) 430; P. Q. Hung and C. Xiong, Nucl. Phys. B847 (2011) 160.

[43] O. Cakir, A. Senol and A. T. Tasci, Europhys. Lett. 88 (2009) 11002.

[44] A. Lister (for the CDF collaboration), pre-sented at ICHEP 2008, arXiv:0810.3349 [hep-ex]; J. Conway et al., CDF public conference note CDF/PUB/TOP/PUBLIC/10110.

[45] L. Scodellaro (for the CDF collaboration) presented at ICHEP 2010. D. Whiteson et al., CDF public conference note CDF/PUB/TOP/PUBLIC/10243.

[46] G.D. Kribs, T. Plehn, M. Spannowsky, T.M.P. Tait, Phys. Rev. D76 (2007) 075016; ibid. Nucl. Phys. Proc. Suppl. 177- 178 (2008) 241-245; M.S. Chanowitz, Phys. Rev. D79 (2009) 113008; V.A. Novikov, A.N. Rozanov and M.I. Vysotsky, arXiv:0904.4570 [hep-ph] and refer-ences therein; J. Erler and P. Langacker, arXiv:1003.3211 [hep-ph].

[47] M. Hashimoto, arXiv:1001.4335 [hep-ph].

[48] C. J. Flacco, D. Whiteson, M. Kelly, arXiv:1101.4976 [hep-ph].

[49] T. Appelquist, H. C. Cheng and B. A. Dobrescu, Phys. Rev. **D64**, 035002 (2001).

[50] P. Colangelo, F. De Fazio, R. Ferrandes, T.N. Pham, Phys.Rev. **D73**, 115006 (2006); P. Colangelo, F. De Fazio, P. Santorelli, E. Scrimieri, Phys. Rev. D 53, 3672 (1996);P. Colangelo, Phys. Rev. D 57, 3186 (1998), Erratum; A. Saddique *et al.*, Eur. Phys. J. **C 56** (2008) 267; Yu-Ming Wang, M.Jamil Aslam, Cai-Dian-Lu, Eur.Phys.J.**C 59** (2009) 847.

[51] A.J. Buras, M. Spranger, A.Weiler, Nucl. Phys. B 660, 225 (2003).

[52] A.J. Buras, A. Poschenrieder, M. Spranger, A. Weiler, Nucl. Phys. B 678, 455 (2004).

[53] A.J. Buras, M. Misiak, M. Munz, S. Pokorski, Nucl. Phys. B 424, 374 (1994).

[54] A.J. Buras et al., Nucl. Phys. B 424, 374 (1994).

[55] P. Frampton et al., Phys. Rep. 330, 263 (2000); P.Q. Hung and M. Sher, Phys. Rev. D 77, 037302 (2008); Y. Kikukawa et al., Prog. Theor. Phys. 122, 401 (2009); D. Atwood et al., arXiv:1104.3874.

[56] A. Soni, A. Alok, A. Giri, R. Mohanti, and S. Nandi, arXiv:0807.1871; A. Soni, A. Kumar Alok, A. Giri, Rukmani Mohanta, and S. Nandi, Phys. Lett. B 683, 302 2010.

[57] Possible role of the fourth family in B-decays has also been emphasized in, W. S. Hou, M. Nagashima, G. Raz, and A. Soddu, J. High Energy Phys. 09 (2006) 012; W.S. Hou, M. Nagashima, and A. Soddu, Phys. Rev. Lett. 95, 141601 (2005); W. S. Hou, H. Nan Li, S. Mishima, and Nagashima, Phys. Rev. Lett. 98, 131801 (2007); Phys. Rev. D 76, 016004 (2007).

[58] W. S. Hou, arXiv:0803.1234; C. Jarlskog and R. Stora, Phys. Lett. B 208, 268 (1988); F. del Aguila and J. A. Aguilar-Saavdra, Phys. Lett. B 386, 241 (1996); F. del Aguila, J. A. Aguilar-Saavedra, and G. C. Branco, Nucl. Phys. B510, 39 1998; R. Fok and G. D. Kribs, arXiv:0803.4207.

[59] B. Holdom, Phys. Rev. Lett. 57, 2496 (1986); C. T. Hill, M. A. Luty, and E. A. Paschos, Phys. Rev. D 43, 3011 (1991); S. F. king, Phys. Lett. B 234, 108 (1990); G. Burdman and L. Da Rold, J. High Energy Phys. 12 (2007) 086; P.Q. Hung and C. Xiong, Nucl. Phys. B847,160 (2011); , Phys. Lett. B 694, 430 (2011);B. Holdom, Phys. Lett. B 686, 146 (2010).

[60] J. Alwall et al., Eur. Phys. J. C 49, 791 (2006); M.S. Chanowitz, Phys. Rev. D 79, 113008 (2009); V.A. Novikov, A. N. Rozanov, and M. I. Vysotsky, Phys. At. Nucl. 73, 636 (2010).

[61] H.-J. He, N. Polonsky, and S.-f. Su, Phys. Rev. D 64, 053004 (2001).

[62] H.-J. He, N. Polonsky, and S.-f. Su, Phys. Rev. D 64, 053004 (2001).

[63] G. D. Kribs, T. Plehn, M. Spannowsky, and T. M. P. Tait, Phys. Rev. D 76, 075016 (2007).

[64] M. Hashimoto, Phys. Rev. D 81, 075023 (2010).

[65] P. Q. Hung, Phys. Rev. Lett. 80, 3000 (1998).

[66] W.-S. Hou, Chin. J. Phys. 47, 134 (2009); Y. Kikukawa, M. Kohda, and J. Yasuda, Prog. Theor. Phys. 122, 401 (2009); R. Fok and G. D. Kribs, Phys. Rev. D 78, 075023 (2008).

[67] W.-S. Hou, M. Nagashima, and A. Spddu, Phys. Rev. D 72, 115007 (2005); 76, 016004 (2007); A. Soni, A. K. Alok, A. Giri, R. Mohanta, and S. Nandi, Phys. Lett. B 683, 302 (2010).

[68] Heavy Flavor Averaging Group, arXiv:hep-ex/0603003.

[69] M. Beneke, G. Buchalla, M. Neubert, and C. T. Sachrajda, Phys. Rev. Lett. 83, 1914 (1999); Nucl. Phys. B591, 313 (2000); B606, 245 (2001); Y.Y. Keum, H-n. Li, and A. I. Sanda, Phys. Lett. B 504, 6 (2001); Phys. Rev. D 63, 054008 (2001); C.W. Bauer, I. Z. Rothstein, and I.W. Stewart, Phys. Rev. D 74, 034010 (2006); 59, 057501 (1999).

[70] Plenary talk by M. Yamauchi (Belle Collaboration) at ICHEP 2002; B. Aubert et al. (BABAR Collaboration), arXiv:hep-ex/0207070, at ICHEP 2002.

[71] M. Ciuchini, G. Degrassi, P. Gambino and G.F. Giudice, Nucl. Phys. **B 527**, 21 (1998); F.M. Borzumati and C. Greub, Phys.

[72] M. Beneke *et al.*, Nucl. Phys. **B 612** (2001) 25 [hep-ph/0106067]; A. Ali *et al.*, Phys. Rev. **D 66** (2002) 034002 [hep-ph/0112300]; T. Feldmann and J. Matias, JHEP 0301 (2003) 074 [hep-ph/0212158]; F. Kruger and J. Matias, Phys. Rev. **D 71** (2005) 094009 [hep-ph/0502060]; C. Bobeth *et al.*, JHEP **0807** (2008) 106 [arXiv:0805.2525]; U. Egede *et al.*, JHEP **0811** (2008) 032 [arXiv:0807.2589]; C. H. Chen *et al.*, Phys. Lett. **B 670** (2009) 374 [arXiv:0808.0127]; A. K. Alok *et al.*, JHEP **1002**, 053 (2010) [arXiv:0912.1382]; A. K. Alok *et al.*, arXiv:1008.2367; A. K. Alok *et al.*, arXiv:1103.5344; W. Altmannshofer *et al.*, JHEP **0901**, 019 (2009).

[73] A.J. Buras and M. Munz, Phys. Rev. D52 (1995) 186; M. Misiak, Nucl. Phys. B393 (1993) 23; Err. ibid. B439 (1995) 461.

[74] M.S. Alam et.al. (CLEO Collaboration), Phys. Rev. Lett. 74 (1995) 2885; S. Ahmed et.al. (CLEO Collaboration), CLEO CONF 9910 (hepex/9908022); R. Barate et.al. (ALEPH Collaboration), Phys. Lett. B429 (1998) 169.

[75] S. Sultansoy, hep-ph/0004271.

[76] M. A. Paracha *et al.*, Eur. Phys. J. **C 52** (2007) 967 [arXiv:0707.0733]; I. Ahmed *et al.*, Eur. Phys. J. **C 54** (2008) 591 [arXiv:0802.0740]; I. Ahmed *et al.*, Eur. Phys. J. **C 71** (2011) 1521 [arXiv:1002.3860]; A. Saddique *et al.*, Eur. Phys. J. **C 56** (2008) 267 [arXiv:0803.0192]; M.Jamil Aslam and Riazuddin, Phys. Rev. **D 66** (2002) 096005 [hep-ph/0209106]; V. Bashiry, K. Azizi, JHEP 1001:033, (2010) [arXiv:0903.1505].

[77] M. Suzuki, Phys. Rev. D **47**, 1252 (1993); L. Burakovsky and J. T. Goldman, Phys. Rev. D **57**, 2879 (1998) [hep-ph/9703271]; H. Y. Cheng, Phys. Rev. D **67**, 094007 (2003) [hep-ph/0301198]

[78] H. Hatanaka and K. C. Yang, Phys. Rev. D **77**, 094023 (2003) [arXiv:0804.3198]; H. Hatanaka and K. C. Yang, Phys. Rev. **D 78** (2008) 074007 [arXiv:0808.3731[hep-ph]].

[79] Ying Li, Juan Hua and Kwei-Chou Yang, EPJC 71, 1775, 2011.

[80] A. Ali et al., Phys. Rev. D 61, 074024 (2000); G. Burdman, Phys. Rev. D 57, 4254 (1998).

[81] K. Nakamura et al. (Particle Data Group), J. Phys. G 37, 075021 (2010).

[82] V. Bashiry and F. Falahati, arXiv:0707.3242 (2007).

[83] B. Aubert *et al.* [BABAR Collaboration], Phys. Rev. **D 73**, 092001 (2006) [arXiv:hep-ex/0604007].

[84] Ashutosh Kumar Alok *et al.* JHEP 1111,122 (2011).

[85] A.H.S. Gilani, Riazuddin, T.A. Al-Aithan, JHEP 09, 065 (2003).

[86] M. Jamil Aslam, Riazuddin, Phys. Rev. D 72, 094 019 (2005) [arXiv:hep-ph/0509082]; M. Jamil Aslam, Eur. Phys. J. C 49, 651 (2007) [hepph/ 0604025]:M.Jamil Aslam, Phys.Rev.D 83,035017; Ishtiaq Ahmed et al. JHEP 2012,2012:45; M.Junaid, M.Jamil Aslam and Ishtiaq Ahmed, IJMPA 27, 1250149 (2012).

[87] C. A. Dominguez, N. Paver, Riazuddin, Z. Phys. **C48** (1990) 55; C. A. Dominguez, N. Paver, Riazuddin, Phys. Lett. **B214** (1988) 459.

[88] C. A. Dominguez, N. Paver, Z. Phys. **C41** (1988) 217.

[89] CERN Courier, page 14, September 2011.

[90] F. Abe et al. (CDF Collaboration) Phys. Rev. D 58, 112004 (1998).

[91] D. S. Du and Z.Wang, Phys. Rev. D 39, 1342 (1989); C.H. Chang and Y. Q. Chen, ibid. 48, 4086 (1993); K. Cheung, Phys. Rev. Lett. 71, 3413 (1993); E. Braaten, K. Cheung, and T. Yuan, Phys. Rev. D 48, R5049 (1993).

[92] Sheldon Stone, arXiv:hep-ph/9709500.

[93] A. Faessler, Th. Gutsche, M. A. Ivanov, J.G. Korner, and V. E. Lyubovitskij, Eur. Phys. J. direct C 4, 1 (2002).

[94] C. Q. Geng, C.W. Hwang, and C. C. Liu, Phys. Rev. D 65, 094037 (2002).

[95] M. S. Khan, M. J. Aslam, A. H. S. Gilani, and Riazuddin, Eur. Phys. J. C 49, 665 (2006).

[96] J. Charles, A. Le Yaouanc, L. Oliver, O. Pene, and J. C. Raynal, Phys. Rev. D 60, 014001 (1999); M. Jamil Aslam and Riazuddin, Phys. Rev. D 72, 094019 (2005); M. Jamil Aslam, Eur. Phys. J. C 49, 651 (2006).

[97] K. Azizi, F. Falahati,V. Bashiry, and S. M.Zebarjad, Phys. Rev. D 77, 114024 (2008).

[98] H.Y. Cheng et al., Phys. Rev. D 51, 1199 (1995).

[99] D. Du, X. Li, and Y. Yang, Phys. Lett. B 380, 193 (1996).

[100] K. Azizi and V. Bashiry, Phys. Rev. D 76, 114007 (2007).